ASSESSMENT OF CLIMATE AND LAND USE CHANGE IMPACTS ON FLOOD INUNDATION IN A HUMID TROPICAL RIVER BASIN: A CASE STUDY OF SUMATRA ISLAND IN INDONESIA

KODAI YAMAMOTO

2021

ASSESSMENT OF CLIMATE AND LAND USE CHANGE IMPACTS ON FLOOD INUNDATION IN A HUMID TROPICAL RIVER BASIN: A CASE STUDY OF SUMATRA ISLAND IN INDONESIA

（気候変動と土地利用変化が湿潤熱帯流域の洪水氾濫に及ぼす影響評価:　インドネシア国スマトラ島における事例研究）

by

KODAI YAMAMOTO

A dissertation

Submitted in partial fulfillment of the requirements for the
Degree of Doctor of Engineering

Department of Civil and Earth Resources Engineering
Kyoto University, Japan

March 2021

Acknowledgements

The completion of the dissertation entitled "Assessment of *climate and land use change impacts on flood inundation in a humid tropical river basin: a case study of Sumatra Island in Indonesia*" was carried out in Innovative Disaster Prevention Technology and Policy Research Laboratory, Disaster Prevention Research Institute (DPRI), Kyoto University. This accomplishment was possible due to the helps and thoughts of many people.

I wish to extend my deepest gratitude to Associate Professor Takahiro Sayama for his supervision, guidance, and inspiring motivations so that this study can progressed steadily and completed in time. His dedication and deep interest for research always bring back my motivation to progress in my study. He always makes time for students to discuss results and solve challenges, not only for research but also for life matters. I wish also to extend my appreciation for support and advices to Professor Kaoru Takara. He opened a lot of opportunities and links for research both in Japan and internationally.

I also extend my gratitude to Professor Yasuto Tachikawa and Professor Shigenobu Tanaka for their valuable suggestions and motivations as my sub-supervisors in Department of Civil and Earth Resources Engineering, Kyoto University.

I also wish to thank Jr. Assoc. Prof. Florence Lahournat for her valuable insights and advises. Furthermore, I wish also to thank the work of Sayama laboratory staff members: Ms. Sono Inoue, Ms. Kaori Sadeira and Ms. Saori Hayakawa for all the helps during my study. Moreover, I wish to thank the lecturers, visiting professors, JSPS Fellows and researchers in Sayama laboratory during my study: Prof. Van-Thanh Van Nguyen, Dr. Emmanuel Akpabio, Ms. Wai Mi Myat, Dr. Netrananda Sahu, Dr. Apip, Mr. Arif Ma'arufi, Dr. Eva Mia Siska Yamamoto, Dr. Masafumi Yamada, and Ms. Zar Zar Thaung.

I would also like to acknowledge the GSS Program Faculty Members, who always gave me valuable insight and suggestions: Assoc. Prof. Masamitsu Onishi as my mentor for his valuable suggestions and motivations especially towards the

completion my GSS activities, Jr. Assoc. Prof. Florence Lahournat. Assoc. Prof. Kumiko Kondo, Assoc. Prof. Minako Yoshikawa, Assoc. Prof. Shinpei Kudo, Assoc. Prof. Nobuyuki Ito, Assoc. Prof. Masanori Katsuyama for their assistance during GSS activities. I also wish to acknowledge Ms. Maki Katsuyama, Ms. Saori Hayakawa, Mr. Takeuchi and all GSS staff members for providing help in GSS Program.

I also extend my gratitude for Indonesian counterparts, Research Center for Limnology LIPI and Meteorology, Climatology, and Geophysical Agency (BMKG), Jambi, as well as other institutions, which has helped me to complete this study: the Jambi Provincial Environmental Office, Jambi University, Warsim, WWF Jambi, and Indonesian Oil Palm Association (GAPKI). I wish to extend my deep appreciation for Dr. Apip for his continues support in providing both data and information, field experience and technical knowledge. I also wish to thank Mrs. Lindawati (Jambi Prov. Env. Office), Mr. Arif Ma'arufi (BMKG Jambi), Prof. Bambang (Univ. Jambi) and other counterparts.

I express my acknowledgment to all former laboratory members: Dr. Maochuan Hu, Dr. Bounhieng Vilaysane, Dr. Pham Hong Nga, Dr. Josko Troselj, Dr. Chong Khai Lin, Dr. Hendy Setiawan, Dr. Han Xue, Dr. Eva Mia Siska, Dr. Karlina, Dr. Shi Yongxue, Dr. Pham Van Tien, Dr. Nguyen Duc Ha, Mr. Toma Stoyanov, Mr. Adnan Arutyunov, Mr. Tsukasa Goto, Ms. Jamila Rajabi, Mr. Susuke Takahashi, Mr. Takuma Ushiro, Mr. Doan Huy Loi, Mr. Ryosuke Kobayashi, Mr. Shintaro Miyake, Mr. Koji Matsumoto, Ms. Saeka Togashi, Mr. Try Sophal, Mr. Sosuke Ichihashi; and all my laboratory colleagues: Mr. Yoshito Sugawara, Mr. Sohaib Baig, Mr. Steven Ly, Ms. Ryoko Araki, Mr. Eilif Djamres and Mr. Ayato Yamakita.

I wish to express my gratitude to institutions, which have extended financial support to allow me completing this research. This study was supported by the Global Survivability Studies (GSS) Leading Program of Kyoto University, Integrated Research Program for Advancing Climate Models (TOUGOU) Project (Theme D), JST Japan –ASEAN Science, Technology and Innovation Platform (JASTIP WP4), and KAKENHI Project.

There are no words I can extend to express my sincere gratitude to my family: my mother, my father, my sister, my wife, my daughter and my family's dog who always

there to support me. Especially, I would like to express my gratitude again to my wife who always support my research life as well as daily life.

Kyoto, 12 November 2020

Abstract

Most of low and lower-middle income countries are located in the tropical region where most of the world's remaining forests are located. It is inevitable that the decreasing rate of forest cover was very high in the region in the last decades where about 200 million hectares of the tropical forest was converted for economic activities. Changes in forest cover may change the water cycle in the region which may lead to the change in frequency and magnitude of water related disasters such as floods and droughts. In the future, the water related disasters may be exacerbated by the climate change. Particularly in the regions, areas where projected extreme rainfall increases, the exposure of population to floods will also increase.

Understanding the impacts of land use and climate change in this region is important to ensure the sustainable economic growth. However, the runoff process in humid tropics is poorly understood owing to lacks of observation and modeling studies. Runoff mechanism in humid tropical region is unique because of unique characteristic of soil. Thus, rainfall runoff model that is developed based on runoff mechanism in temperature region might not be suitable for humid tropical region. General Circulation Model (hereafter, GCM) has high uncertainties in Maritime Continent Indonesia due to coarse resolution of models and a lack of representation of local atmospheric condition. Regional Climate Model (hereafter, RCM) is capable of representing local weather condition and accurately project climate change effects. In addition, it is not clear whether climate change or land use change impacts are more on water related disasters. The above mentioned environmental change may have an impact on flood inundation that leads to impacts on agriculture and peatlands and thereby, it is important to assess the impact on peatland area.

The overall objective of this study is to understand the response of humid tropical region to land use and climate change and assess suitable adaptation measures. In order to achieve this objective, I set the following specific objectives:

1. To clarify the reasonable model structure for a humid tropical area and potential use for analyzing long-term rainfall runoff and inundation process with satellite

rainfall and potential evapotranspiration estimated by global data in data-scarce region in Sumatra island;

2. To assess the impact of climate change on flood inundation in a river basin in Sumatra Island. This study applied dynamically downscaled rainfall data by RCM as the input for the RRI model and identified appropriate bias correction methods for flood simulations;
3. To compare climate change and land use change impacts on flood inundation;
4. To assess sustainable adaptation measures for oil palm production.

The study area of this research is Batanghari river basin that is located in Sumatra Island and has the second largest area (42,960 km^2) in Indonesia. The Batanghari river originates in the Barisan Mountains before merging with the Tembesi River as it runs eastward towards the coast. Downstream, the river is diverted into the Kumpeh River and merged again. At Simpang, the river is diverged into the Berbak River. The topography of the area is comprised of mountains in the western part to and wetlands in the low-lying flat areas. The mountainous area, that is a source of rivers, is a part of Bukit Barisan range and range in height from 1,000 m to 3,700 m. The largest part of the basin consists of undulating hills covering 60% of the area with elevation between 10–100 m a.s.l. In the middle part of the basin close to Muara Tembesi station, the Batanghari River is merged with the Tembesi River and flows to the east through flat swamp land up to 200 km from the coast. Parallel with the coastline in the eastern province, peatland covers areas approximately 700,000 ha.

In the first part of this study, the aim is to clarify suitable rainfall-runoff model structure for humid tropics. This study investigated combinations of runoff process and parameter setting and discussed the suitable simulation condition of Rainfall-Runoff-Inundation (hereafter, RRI) model. The simulated discharge was improved when an evapotranspiration was used as an input for RRI model. In addition to this, parameter of soil was changed from 1m to 3m. The 3m-soil layer decreases surface flow and increases temporal storage. Consequently, the condition improved peaks of simulated discharge but could not reproduce discharge in dry season. Furthermore, the model was capable of reproducing discharge for long term including dry season by adding groundwater model to the updated simulation conditions. These results

and discussions indicate that a model is capable of performing for long-term discharge, given that a simulation considers characteristic of hydrology in humid tropics such as evapotranspiration input, thicker soil layer and groundwater process in a deep soil layer. In addition, the model was able to reproduce flood inundation extent, compared with flood extent estimated by Sentinel satellite imagery. The simulation showed that flooding occurs almost every year at downstream of the basin (14 out of 17 years simulation). In conclusion, this study suggests that the RRI model is applicable for a humid tropical river basin by taking account into characteristic of hydrology in humid tropics for analyzing long-term river discharge and inundation.

The second part of this study compared the two bias correction methods, i.e., the Quantile Mapping method (hereafter, QM) and a combination of the QM and Variance Scaling (hereafter, VS) methods, to examine how each method improves estimates of rainfall patterns, and subsequently, the simulated flood inundation by the RRI model in the Batanghari river basin, Indonesia. Originally, the dynamically downscaled NHRCM rainfall data showed higher spatial variation in the 15-day rainfall and annual rainfall compared to the reference data. While this does not markedly influence the simulated Flow Duration Curve (hereafter, FDC), it largely overestimated the extreme values, such as the annual maximum flood inundation volume. The combination of QM and VS methods successfully decreased the rainfall spatial variability and improved the estimations of the FDCs and the extreme values. Our analysis showed that annual maximum flood inundation volume corresponding to a 20-year return period would increase by 3.3 times in the future. In addition, the flood inundation extent would increase, particularly in the lowland areas of Sumatra Island. In conclusion, this study suggests the need to consider future climate change scenarios for river basin management, particularly to reduce the flood damage and to sustainably maintain the unique ecosystem of tropical peatlands.

The objective of third part of the study is to clarify whether climate change or land use change has more impacts on flooding. Specifically, this study compares the effects of climate change and land use change on river discharge and flood inundation. In addition, this study also compares these impacts estimated using the RRI model and the Soil Water Assessment Tools model that is widely used for land use impact assessment all over the world. According to estimated FDC and annual

maximum discharge, both SWAT model and RRI models suggest that climate change has more impacts than land use change. In addition, RRI model suggests that climate change has more impacts on annual maximum inundation volume than land use change. Specifically, due to climate change, inundation area increases by 1,812 km^2 and the maximum inundation depth increases by 1.1 m, while inundation area increases by 149 km^2 and the maximum inundation depth does not change, due to land use change. The above-mentioned results show that the estimated change of river flows and flooding using the RRI model is similar to those of the SWAT model. In conclusion, this study suggests that the effect of climate change on river flows and flooding is more significant than that of land use change in the study area.

The objective of fourth part of research is to assess the impact of flood inundation on young oil palm plantation in peatland to discuss sustainable adaptation measures for oil palm production. This study estimates mortality maps of oil palm within three years after planting at basin scale under present climate and future climate condition. Under future climate condition, inundation duration is projected to be longer and larger part of downstream area shows mortality exceeding 50%, compared with present climate. Moreover, peatland area, which consists of higher elevation called a peat dome, shows that mortality of oil palm within three years will be significantly higher in the future. These results suggest that prolonged inundation would increase groundwater level in peatland that gives a challenge to maintain oil palm production that requires drainage. Furthermore, this study implies that prolonged inundated area due to climate change may not be used for oil palm production, which leads to poor management of drainage and fire disaster during dry season. In conclusion, this study suggests that current oil palm plantation is not be sustainable, particularly in peatland under climate change condition and thereby, adaptation measures for climate change should be taken for sustainable oil palm management and environmental protection of peatland.

This study concluded that the RRI model is applicable to simulate discharge and inundation extent in the humid tropical river basin and can be used for land use and climate change impact studies. However, the application needs careful parameterization considering the deep soil layer in the region as well as effects of evapotranspiration especially for the long-term simulation. The results of this study

also showed that the use of RCM is better than GCM, particularly in the study area. Furthermore, the use of RCM should be bias corrected based on the needs of the study. In the case of this study, the combination of QM and VS was able to give better results in the simulation. After comparing the results of changes due to land use and climate change, this study concluded that the impact of climate change is much severe than land use change, particularly on the increase of inundation extent and maximum depth. Finally, this study suggested that the adaptation strategies to mitigate impacts of land use and climate change in the future should carefully consider the sensitive areas such as peatlands which are abundant in the region.

Table of Contents

List of Figures

List of Tables

Chapter 1 Introduction

1.1 Background

Based on data from FAO's Global Forest Resources Assessment (FAO, 2015), in 1990 the world's forest cover was 4,128 million ha and reduced to 3,999 million ha in 2015. In 1990, most of the forest area are located in the tropics (48%) while the forest in the temperate and sub-tropics covered less than 20% of the forest area. Based on Sachs (2001), the countries located in the tropics are mostly low income and lower-middle income countries based on the 1995 PPP adjusted GDP. Assuming that these countries are developing their economies, it is logical that the loss of forest area occurred largely in the region. In 2015, the tropics loss about 200 million ha of forest while the temperate region gained about 66 million ha of forest (Keenan *et al.*, 2015). The highest net forest loss in Asia between 2010 and 2015 occurred in Indonesia, one of the humid tropical regions.

There are a lot of concerns regarding the impact of deforestation. The alteration in the natural forest cover may have changde the water cycle, particularly runoff and evapotranspiration (Bruijnzeel, 2004, Costa and Foley, 1997, Panday *et al.*, 2015, Kleinhans and Gerold, 2004, Kuraji and Paul, 1994, Malmer, 1996) even though the magnitude varies from site to site. The change in water cycle may impact the human activities through increasing water related disasters such as floods and droughts (Sayama *et al.*, 2019). Furthermore, considering the diverse ecosystem and high biodiversity in humid tropics, the change of water cycle may impact its most sensitive ecosystems. In some southeast Asian countries, the coastal lowland areas are mostly covered with tropical peat soil. The land use change on peatland is lowering the groundwater level due to canalization for agricultural purposes. The lowering of groundwater level increases the CO_2 emission and further on results in the thinning of peat layer. Prolonged droughts, such as those caused by El-Nino, may increase the risk of fires in the peatland areas. In extreme cases such as in the year of 1997 and 2015, the El-Nino has caused severe fires and therefore haze problems over the southeast Asia region.

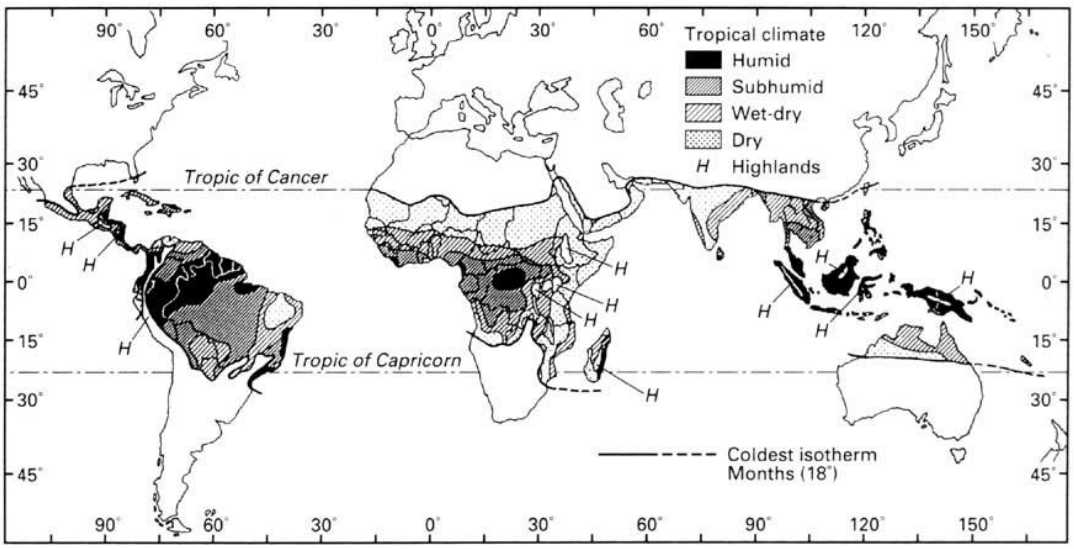

Figure 1-1 The world map showing distribution of humid tropic regions (Bonell et al., 1993).

The climatic classification which are commonly used are the Koppen and Thornthwaite but this study follows the definition of humid tropics adopted by UNESCO Intergovernmental Hydrological Programme (IHP) by Chang and Lau (1993) as regions with 9.5 to 12 'wet' months (monthly average rainfall above 100 mm) and temperature in the coldest month is more or equal to18° C (Figure 1-1). According to Bonell *et al.* (2005), in general the humid tropics has an order of magnitude higher rainfall than in the humid temperate region. Due to fast weathering under high rainfall and constant high temperature, the soil in the region is typically deeper. In addition to its depth, the rainforest in the region has high surface permeability (Nortcliff and Thornes, 1981) and unique soil properties. Compared to the temperate kaolinitic clayey soils, the tropical soils have 'unusual' properties such as low bulk density, high permeability and low available water capacity (Tomasella and Hodnett, 2004). The runoff process in humid tropics can be different to the temperate region due to its soil characteristics. Therefore, the impact of land use change can be also different.

A typical approach to analyze the impact of land use changes at a basin scale is by using hydrological model. However, the use hydrological model in assessing the impact should be chosen carefully and soil parameters should be set properly. This is particularly important since most of hydrological models were designed based on conditions in the temperate regions.

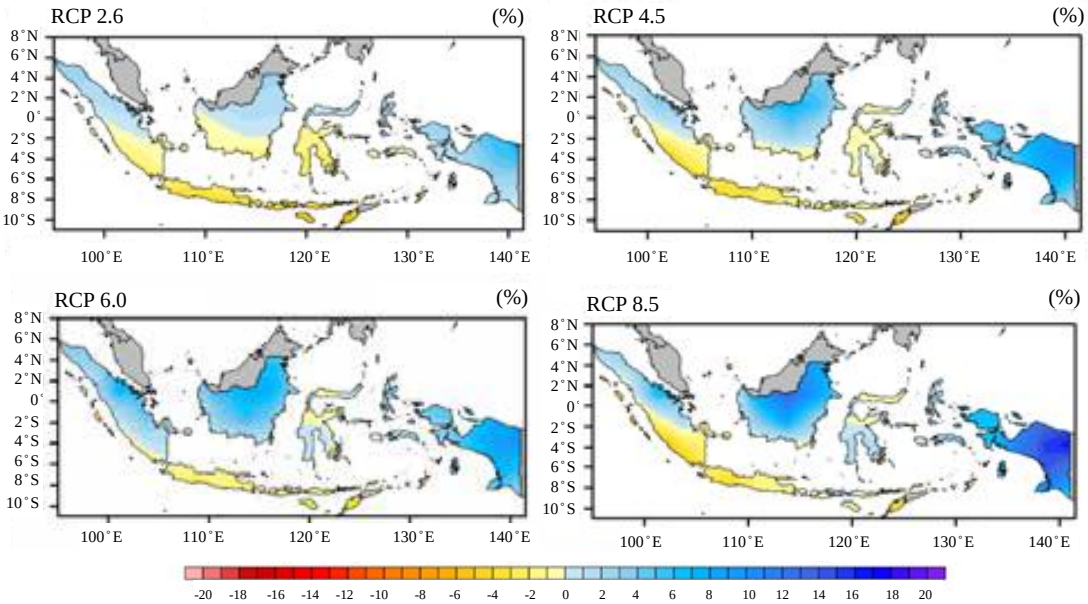

Figure 1-2 Changes (in %) of annual rainfall in Indonesia for 2076-2100 (multi-model ensemble mean of 24 CMIP GCMs) compare with 1981-2005 (CHIRPS v2.0 dataset) (Ministry of Environment and Forestry Republic of Indonesia, 2017).

In the future, the change in water cycle will be further exacerbated by the climate change. Figure 1-2, obtained from the Indonesia Third National Communication (Indonesia TNC) under UNFCCC Report, shows that changes in annual rainfall Indonesia, as one of humid tropical regions, will be higher in northern part of Indonesia in all scenarios. In the same report, it was mentioned that in general the dry season will be drier and the wet and transition seasons will be wetter. Hijioka *et al.* (2014) stated that in some areas, including area where Indonesia is located, extreme monsoon-related rainfall is projected to increase and Hirabayashi *et al.* (2013) stated that a larger proportion of population is expected to be exposed to floods. On the other hand, climate change can enhance drying peatlands and increase CO_2 emission. Climate model prediction under A1B scenarios suggests that there is a high probability of decreasing rainfall during dry season (July, August and September) in Indonesia over 21st century (2050-2099) compared with rainfall in 20th century (1950-1999) that results in surface dryness and decrease of groundwater in southern part of Indonesia (Li *et al.*, 2007). Drying the peatland by climate change or other human activities decreases ground water level, increasing CO_2 emission as

a result of its decomposition (Hirano *et al.*, 2012) and increasing the frequency of peatland fire (Takahashi *et al.*, 2003).

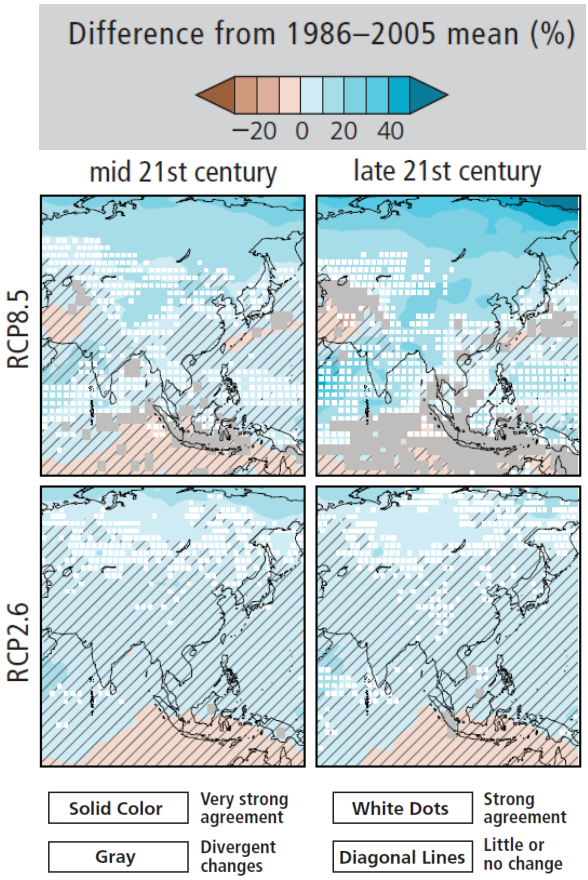

Figure 1-3 Projected changes in annual precipitation in Asia (Hijioka et al., 2014).

However, the climate change in humid tropical region, particularly in the South East Asia, was difficult to be projected due to local atmospheric cycle. The above-mentioned Indonesia TNC report stated that due to coarse resolution data of GCM, the future spatial changes of the annual and seasonal rainfall are not significant across Indonesia. The use of different statistical bias correction approach leads to different results among regions and thus the uncertainty of future rainfall also increases. However, the use of RCM (RegCM4) results in general consistencies for future rainfall, particularly over the land area. Figure 1-3 (Hijioka *et al.*, 2014) showed that over the southern part of Indonesia, particularly for RCM 8.5, the results of projected rainfall shows divergent changes where less than 66% of models have similar direction of change. The available General Circulation Models (GCMs) have

limitations in reproducing reasonable rainfall patterns which may be attributed to the imperfect parameterization of physical processes (e.g., convection, cloud generation, local land sea breeze circulation and regional variations in the diurnal cycle) (Gianotti *et al.*, 2012; Ulate *et al.*, 2014). The Regional Climate Models (RCMs) on the other hands have more potential to reproduce realistic rainfall events in the Maritime Continent (MC) where Indonesia is located.

As mentioned earlier, the tropical region mostly consisted of countries from low and lower-middle economies in 1995 (Sachs, 2001). Some of the countries were able to become upper-middle income countries in 2020 (World Bank, 2020) and most of them needs to maintain sustainable economic growth in the future. The land use and climate change impacts to water cycle, which may increase the water related disasters, such as floods and droughts, will impact on the economy in the future. A comprehensive understanding on how these changes may impact future economic activities is important to develop sound adaptation strategies to maintain the economic growth. Furthermore, attention should be placed to reduce further damage in unique ecosystems, such as peatland areas, due to the combination of anthropogenic activities and impact of climate change.

As the typical land use and climate change impact studies at basin scale use hydrological models, it is important to carefully choose and set up its parameters to fit with the soil conditions in the humid tropics. Most of hydrological models are developed based on assumptions of runoff generation processes in temperate region, such as quick subsurface flow in a shallow soil layer. As an example, the typical flood prediction models in Japan assumes that major source of runoff is the subsurface flow coming from saturated shallow soil layer. On the other hands, considering the high permeability and deep soil layer in the humid tropics, the rainfall may infiltrate vertically further into the soil and the runoff may be generated from deeper soil layer. Even though some of the rainfall-runoff models do not explicitly consider the runoff process in a deep soil layer, but the recent models can consider groundwater flow from bedrock layer. In addition, taking account into the high energy flux and tropical forest, it is important to consider the effect of evapotranspiration for both short or long-term rainfall-runoff simulation.

The Rainfall-Runoff-Inundation (RRI) model is one of distributed hydrological models which can consider groundwater flow from bedrock layer and can consider the effect of evapotranspiration. This study investigates the applicability of RRI model, as an example of distributed rainfall runoff model, to a humid tropical river basin. The RRI is capable of simulating rainfall-runoff process and flood inundation at the same time. In the previous research, there is not sufficient consideration of a deep soil layer for long-term rainfall runoff process in a humid tropical region. This research discusses the capacity of RRI for simulating long-term rainfall runoff and flood inundation in a tropical peatland area at the downstream. Specifically, this study clarifies the reasonable model structure for a humid tropical area and potential use for analyzing long-term rainfall runoff process and inundation process with satellite rainfall and potential evapotranspiration estimated by global data in data-scarce region in Sumatra island.

The use of RRI model to assess inundation extent in the humid tropical regions increases in the recent years, such as in Malaysia (Chong et al, 2017), in the Philippines (Juarez-Lucas *et al.*, 2016), in Indonesia (Nastiti *et al.*, 2015, Syarifuddin *et al.*, 2017) and a few studies even used the model to study impact of climate change such as in the Philippines (Ushiyama *et al.*, 2016) and in Indonesia (Kudo *et al.*, 2015). However, the applications did not consider deep soil layer and long-term simulation which considered to be important in improving simulation results in humid tropical region.

1.2 Objectives

The overall objective of this study is to understand the response of humid tropical river basin to land use and climate changes and assess suitable adaptation measures. In order to achieve this objective, I set the following specific objectives:

1. To clarify the reasonable model structure for a humid tropical area and potential use for analyzing long-term rainfall runoff process and inundation process with satellite rainfall and potential evapotranspiration estimated by global data in data-scarce region in Sumatra Island;
2. To assess the impact of climate change on flood inundation in a river basin on Sumatra Island. This study applied dynamically downscaled RCM rainfall data

as the input for the RRI model, and identified appropriate bias correction methods for flood simulations;

3. To assess the impact of land use change in humid tropical river basin and to compare it with impact of climate change; and
4. To assess sustainable adaptation measures for oil palm production.

1.3 Organization of the Dissertation

This dissertation consists of four chapters which are briefly explained as follows:

Chapter 1 consists of background, objectives of the study and organization of dissertation.

Chapter 2 explains about the study area such as the topography, climate, geological features, etc.

Chapter 3 describes the study on the applicability of the RRI model, as an example of distributed rainfall runoff model, to a humid tropical river basin. This chapter mainly discusses the capacity of RRI for simulating long-term rainfall runoff and flood inundation in a tropical peatland area at the downstream and clarifies the reasonable model structure for a humid tropical area and potential use for analyzing long-term rainfall runoff process and inundation process with satellite rainfall and potential evapotranspiration estimated by global data in data-scarce region in Sumatra island.

Chapter 4 describes the study on the applicability of Non-Hydrostatic Regional Climate Model (NHRCM) in projecting future river discharge and flood inundation extent using RRI model. This chapter mainly discusses the potential of NHRCM for future rainfall projection and suitable bias correction method to obtain reasonable estimates for river discharge and the extent of future flood inundation.

Chapter 5 compares results of land use change and climate change impacts in the future. In this chapter, the results are also compared with simulation using hydrological model that is widely used in the region such as the Soil Water Assessment Tools (SWAT) model.

Chapter 6 analyzes the impact future floods inundation extent to the economic activities, specifically oil palm plantations which were currently widely grown in the peat areas in the downstream of river basin. This chapter discusses how future floods

inundation impacts on the agricultural activities by calculating its mortality rates and suggests adaptation strategies to lower the loss due to floods.

Chapter 7 summarizes results from all chapters and highlighted the findings from this study.

References

Bonell M, Hufschmidt MM, Gladwell JS (1993) Hydrology and Water Management in the Humid Tropics: Hydrological research issues and strategies for water management. UNESCO, Cambridge: Cambridge University Press; 571–574.

Bonell M (2005) Runoff generation in tropical forests. In *Forest, Water and People in the Humid Tropics: Past, Present and Future Hydrological Research for Integrated Land and Water Management*, Bonell M, Bruijnzeel LA (eds). Cambrige University Press, Cambridge, UK; 314-406.

Bruijnzeel LA (2004) Hydrological functions of tropical forests: not seeing the soil for the trees?. *Agriculture Ecosystem and Environment* 104: 185-228. DOI: 10.1016/j.agee.2004.01.015.

Chang JH, Lau LS (1993) A definition of the humid tropics. In Bonell M, Hufschmidt MM, Gladwell JS (eds.), *Hydrology and Water Management in the Humid Tropics: Hydrological research issues and strategies for water management*, UNESCO, Cambridge: Cambridge University Press; 571–574.

Chong KL, Sayama T, Takara K, Abustan I (2017) Effects of diffusive wave and flood inundation on time of concentration. Journal of Japan Society of Civil Engineers, Ser. B1 73(4):I_151-6.

Costa MH, Foley JA (1997) Water balance of the Amazon Basin: Dependence on vegetation cover and canopy conductance. *Journal of Geophysical Research: Athmospheres* 102: 23973–23989. DOI: 10.1029/97JD01865.

FAO (2015) Global Forest Resources Assessment 2015: Desk Reference. http://www.fao.org/3/a-i4808e.pdf

Gianotti RL, Zhang D, Eltahir EAB (2012) Assessment of the regional climate model version 3 over the maritime continent using different cumulus parameterization and land surface schemes. J Climate 25:638-656. DOI:10.1175/JCLI-D-11-00025.1

Hijioka Y, Lin E, Pereira JJ, Corlett RT, Cui X, Insarov GE, Lasco R, Lindgren E, Surjan A (2014) Asia. In: Barros VR, Field CB, Dokken DJ, Mastrandrea MD, Mach KJ, Bilir TE, Chatterjee M, Ebi KL, Estrada YO, Genova RC, Girma B, Kissel ES, Levy AN, MacCracken S, Mastrandrea PR, White LL (eds.) Climate Change 2014: Impacts, Adaptation, and Vulnerability. Part B: Regional Aspects. Contribution of Working Group II to the Fifth Assessment Report of the Intergovernmental Panel on Climate Change. Cambridge University Press, Cambridge, United Kingdom and New York, NY, USA, pp 1327-1370

Hirabayashi Y, Mahendran R, Koirala S, Konoshima L, Yamazaki D, Watanabe S, Kim H, Kanae S (2013) Global flood risk under climate change. Nature Clim Change 3:816-821. DOI:10.1038/nclimate1911

Hirano T, Segah H, Kusin K, Limin S, Takahashi H, Osaki M (2012) Effects of disturbances on the carbon balance of tropical peat swamp forests. Glob Chang Biol 18(11):3410-3422. DOI: 10.1111/j.1365-2486.2012.02793.x

Juarez-Lucas AM, Kibler KM, Ohara M, Sayama T (2016) Benefits of flood-prone land use and the role of coping capacity, Candaba floodplains, Philippines. Natural Hazards 84:2243-2264. DOI 10.1007/s11069-016-2551-2

Keenan JR, Reams GA, Achard F, de Freitas JV, Grainger A, Lindquist E (2015) Dynamics of global forest area: Results from the FAO Global Forest

Resources Assessment 2015. *Forest Ecology and Management* **352:**9-20. DOI: 10.1016/j.foreco.2015.06.014.

Kleinhans A, Gerold G (2004) The Effects of Rainforest Conversion on Water Balance, Water Yield and Seasonal Flows in a Small Tropical Catchment in Central Sulawesi, Indonesia. In *Land Use, Nature Conservation and the Stability of Rainforest Margins in Southeast Asia. Environmental Science*, Gerold G, Fremerey M, Guhardja E (eds). Springer, Berlin, Heidelberg; 353-365. DOI: 10.1007/978-3-662-08237-9_20.

Kudo S, Sayama T, Hasegawa A, Iwami Y (2015) Assessment of climate change impact on flood discharge and inundation in the Solo river basin, Indonesia. Journal of Japan Society of Civil Engineers Ser B1 71(4): I_1321-6. DOI: 10.2208/jscejhe.71.I_1321

Kuraji K, Paul LL (1994) Effects of rainfall interception on water balance of two tropical rainforest catchments, Sabah, Malaysia. *Proceedings of the International Symposium of Forest Hydrology 291-298, 1994 Tokyo, Japan;672p.*

Li W, Dockinson RE, Fu R, Niu G-Y, Yang Z-L (2007) Future precipitation changes and their implications for tropical peatlands. *Geophys. Res. Lett.* 34, DOI:10.1029/2006GL028364.

Malmer A (1996) Observations on slope processes in a tropical rain forest environment before and after forest plantation establishment. In *Advances in hillslope processes*, Anderson MG, Brooks SM (eds), John Wiley & Sons, Chichester, UK; 961–973.

Ministry of Environment and Forestry Republic of Indonesia (2017) Indonesia Third National Communication under the United Nations Framework Convention on Climate Change. Directorate General of Climate Change,

Ministry of Environment and Forestry, Republic of Indonesia, Jakarta, Indonesia. 219p.

Nastiti KD, Kim Y, Jung K, An H (2015) The application of Rainfall-Runoff-Inundation (RRI) model for inundation case in upper Citarum Watershed, West Java-Indonesia. The 5th International Conference of Euro Asia Civil Engineering Forum (EACEF-5). Procedia Engineering. 125: 166-172. DOI: 10.1016/j.proeng.2015.11.024

Nortcliff S, Thornes JB (1981) Seasonal variations in the hydrology of a small forested catchment near Manaus, Amazonia, and the implications for its management. *In Tropical Agricultural Hydrology – Watershed Management and Land Use*. Lal R and Russell EW (eds.), Wiley, Chichester, UK. 37–57.

Panday PK, Coe MT, Macedo MN, Lefebvre P, Castanho ADDA (2015) Deforestation offsets water balance changes due to climate variability in the Xingu River in eastern Amazonia. *Journal of Hydrology* 523: 822-829. DOI: 10.1016/j.jhydrol.2015.02.018.

Sachs JD (2001) Tropical Underdevelopment. National Bureau of Economic Research (NBER) Working Paper 8119. 40p. https://www.nber.org/system/files/working_papers/w8119/w8119.pdf

Sayama T, Yamamoto K, Araki R, Apip, Siska EM, Takara K (2019) Impact of Climate Change on Hydrological Cycle in a Humid Tropical River Basin in Sumatra, Indonesia. *Proceedings of the 8th International Conference on Water Resources and Environment Research (ICWRER 2019)*. Easy Chair Preprint No. 1943.

Syarifuddin, M, Oishi S, Hapsari RI, Legono D (2017) Empirical model for remote monitoring of rain-triggered lahar at Mount Merapi. Journal of Japan Society of Civil Engineers Ser B1 62(4): I_1483-1488. DOI: 10.2208/jscejhe.74.I_1483.

Takahashi H, Usup A, Hayasaka H, Limin SH (2003) Estimation of ground water level in a peat swamp forest as an Index of peat/forest fire. In: Osaki M, Iwakuma T, Kohyama T, Hatano R, Yonebayashi K, Tachibana H, Takahashi H, Shinano T, Higashi S, Simbolon H, Tuah SJ, Wijaya H, Limin SH (eds) *Proceeding of the International Symposium of Land Management and Biodiversity in Southeast Asia, Bali, 2002*

Ulate M, Dudhia J, Zhang C (2014) Sensitivity of the water cycle over the Indian Ocean and Maritime Continent to parameterized physics in a regional model. J Adv Model Earth Syst 6(4):1095-1120. DOI:10.1002/2014MS000313

Ushiyama, T, Hasegawa, A, Miyamoto, M, Iwami, Y (2016) Dynamic downscaling and bias correction of rainfall in the Pampanga River Basin, Philippines, for investigating flood risk changes due to global warming. Hydrological Research Letters 10(3), 106–112 (2016). DOI: 10.3178/hrl.10.106

World Bank (2020) Country classification by income. https://datahelpdesk.worldbank.org/knowledgebase/articles/906519-world-bank-country-and-lending-groups

Tomasella J, Hodnett, M (2004) Pedotransfer functions for tropical soils. *Development in Soil Science* 30: 415-429. DOI: 10.1016/S0166-2481(04)30021-8.

Chapter 2 Study Area

2.1 The Batanghari River Basin

Figure 2-1 Maps of the study area (a) Indonesian Maritime Continent and (b) the Batanghari river basin in Sumatra Island (R.=River, WLS=Water level station).

The Batanghari river basin is located in the western part of Indonesia in Jambi and Western Sumatra Provinces and has the second largest area (42,960 km^2) in Indonesia. The Batanghari river originates in the Barisan Mountains and merges with the Tembesi River running eastward towards the coast. Downstream, the river is diverted into the Kumpeh River and merged again. At Simpang, the river is diverged

into the Berbak River (Figure 2-1). The topography of the area is comprised of mountains in the western part to and wetlands in the low-lying flat areas. The mountainous area, that is a source of rivers, is a part of Bukit Barisan range and range in height from 1,000 m to 3,700 m. The largest part of the basin consists of undulating hills covering 60% of the area with elevation between 10–100 m a.s.l. (Ministry of Public Works, 2003). In the middle part of the basin close to Muara Tembesi station, the Batanghari River is merged with the Tembesi River and flows to the east through flat swamp land up to 200 km from the coast (NASA and METI (National Aeronautics and Space Administration and Ministry of Economy Trade and Industry of Japan), 2017). Parallel with the coastline in the eastern province, peatland covers areas approximately 700,000 ha (Wahyunto and Subagjo, 2003).

2.2 Climate

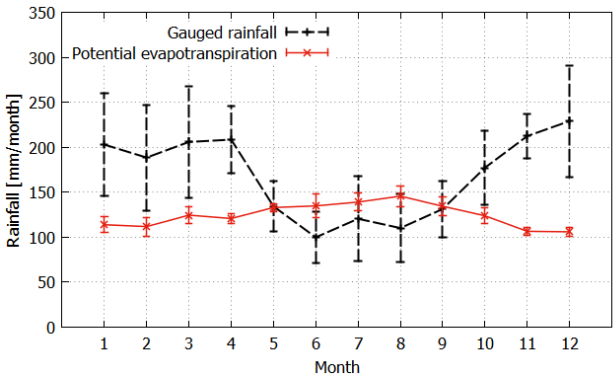

Figure 2-2 Basin averaged rainfall (23 stations) and potential evapotranspiration in Batanghari river basin (2001-2013).

The climate is classified as humid tropical and monthly rainfall typically exceeds 100 mm (Chang and Lau, 1993). The average air temperature is within the range of 22.2±0.2°C (upstream) and 26.8±0.2°C (downstream) based on climate stations maintained by the Indonesian Agency for Meteorological, Climatological and Geophysics (BMKG) from 2001 to 2013 (Yamamoto *et al.*, 2020). Despite high monthly rainfall, there is a distinct wet season and dry season that is strongly influenced by two monsoons (Figure 2-2). Based on Aldrian and Susanto (2003), the wet northwest monsoon originates in the northern hemisphere to the basin from November to March, and the dry southeast monsoon originates in the southern hemisphere to the basin from May to September. The wet monsoon has two clear

peaks; one in December and another in April (bimodal rainfall). In the wet season, river is flooding downstream area in the Batanghari river basin. In some extreme cases, these floods can affect Jambi city.

2.3 Land cover and land use change

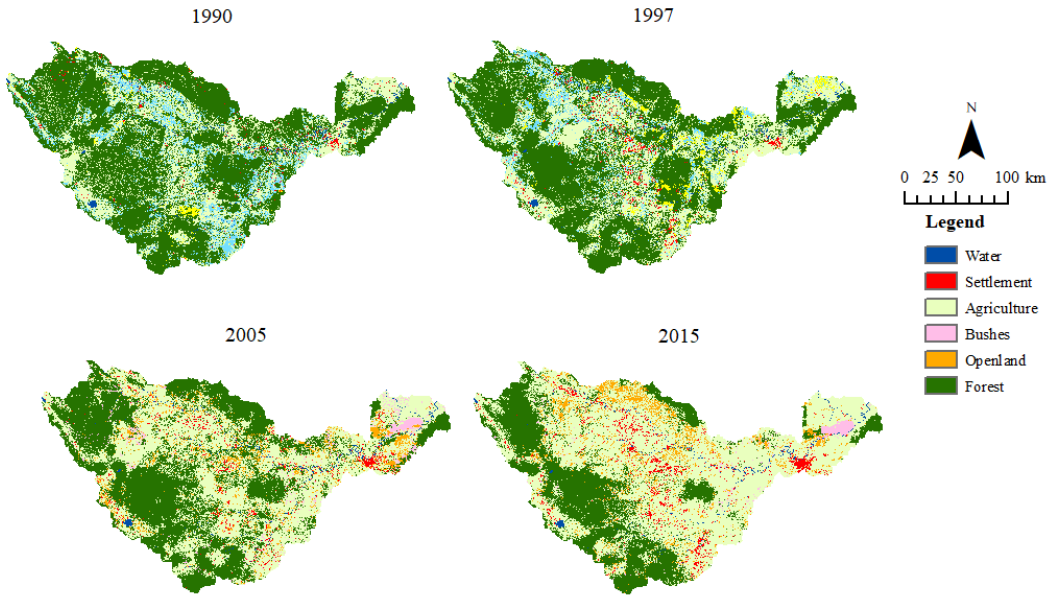

Figure 2-3 Land cover and land use maps in Batanghari river basin in 1990, 1997, 2005 and 2015.

The serious deforestation and rapid land cover and land use change occurred in the study area since 1990s. In Figure 2-3, the land cover maps by Utami *et al.* (2017) show that forest area is the largest (59% of the basin area) in the Batanghari river basin in 1990 that was dramatically decreased to 33% in 2015. Meanwhile, agricultural area increases from 28% of the basin in 1990 and becomes the largest (57% of the basin area) in 2015. The maps also show that about 49% of the forestry area in 1990 is converted into agricultural area in 2015. Downstream, forest has been also cleared in 2015. Since 1960s, the peatlands area has been deforested, drained and converted to agricultural area (Sumawijaya, 2006).

The forests in Jambi Province have been largely transformed into plantations (Drescher *et al.*, 2016). In Jambi province, oil palm is a major agricultural plantation in recent years. In early of 1990s, the oil palm covers relatively small area. Estimates using datasets of agriculture department in Jambi province (Figure 2-4) show that in 1994, a major agricultural product was rubber (approximately 290 thousand ha)

followed by coconuts (approximately 115 thousand ha) and oil palm (approximately 8.8 thousand ha). Since then, oil palm area gradually increases and replace rubber in 1999. In 2015, oil palm becomes a most major agricultural product in Jambi (approximately 1 million ha) followed by rubber (approximately 330 thousand ha). In Batanghari river basin, large parts of oil palm area in 2013 was previously forest or shrub (Tarigan, 2016). Since 2000, oil palms have been increasing in peatlands because mineral soils were scarce for expanding the plantation area (Afriyanti *et al.*, 2019).

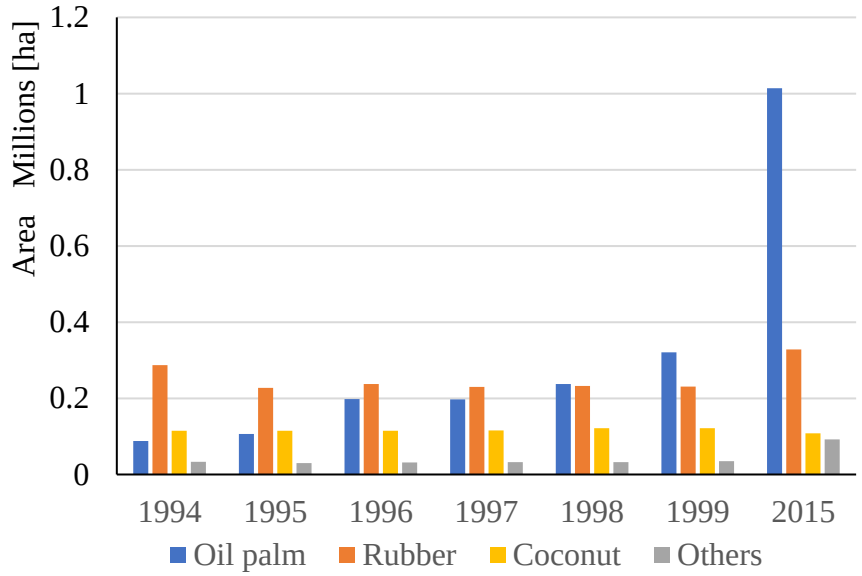

Figure 2-4 Change of agricultural area between 1994 and 2015 (Jambi Province Statistical Agency, 2015).

2.4 Soil properties and geological settings

The FAO (Food and Agriculture Organization)/UNESCO (The United Nations Educational, Scientific and Cultural Organization) soil map shows that the upper and middle river basin areas are dominated by Acrisols and Ferrasols and the downstream part of the basin, particularly along the river banks, is dominated by Fluvisols. In this study, we did field investigation on a forested hillslope in Sekancing township, which is located on the west side of a catchment (marked by orange star in Figure 2-1). As shown in Figure 2-5, the soil depth was measured at three locations (upslope, middle slope and downslope of a hill slope) in a natural forest at Sekancing. A simple penetration test using a cone penetrometer with a weight of 5±0.05 kg, and a fall

distance of 500±10 mm was conducted at this location. The Nc value, calculated as the number of blows required for a 100 mm penetration (Katsura *et al.*, 2014), is shown in Figure 2-5. Soil depth above bedrock is defined as a depth when Nc value exceeds 50 (Katsura *et al.*, 2014). The Nc value increased sharply to 50 at the depth of approximately 1.7 m at upslope and 2.7 m at middle slope. At downslope the Nc value does not reach 50 even though a depth reaches approximately 4.6 m.

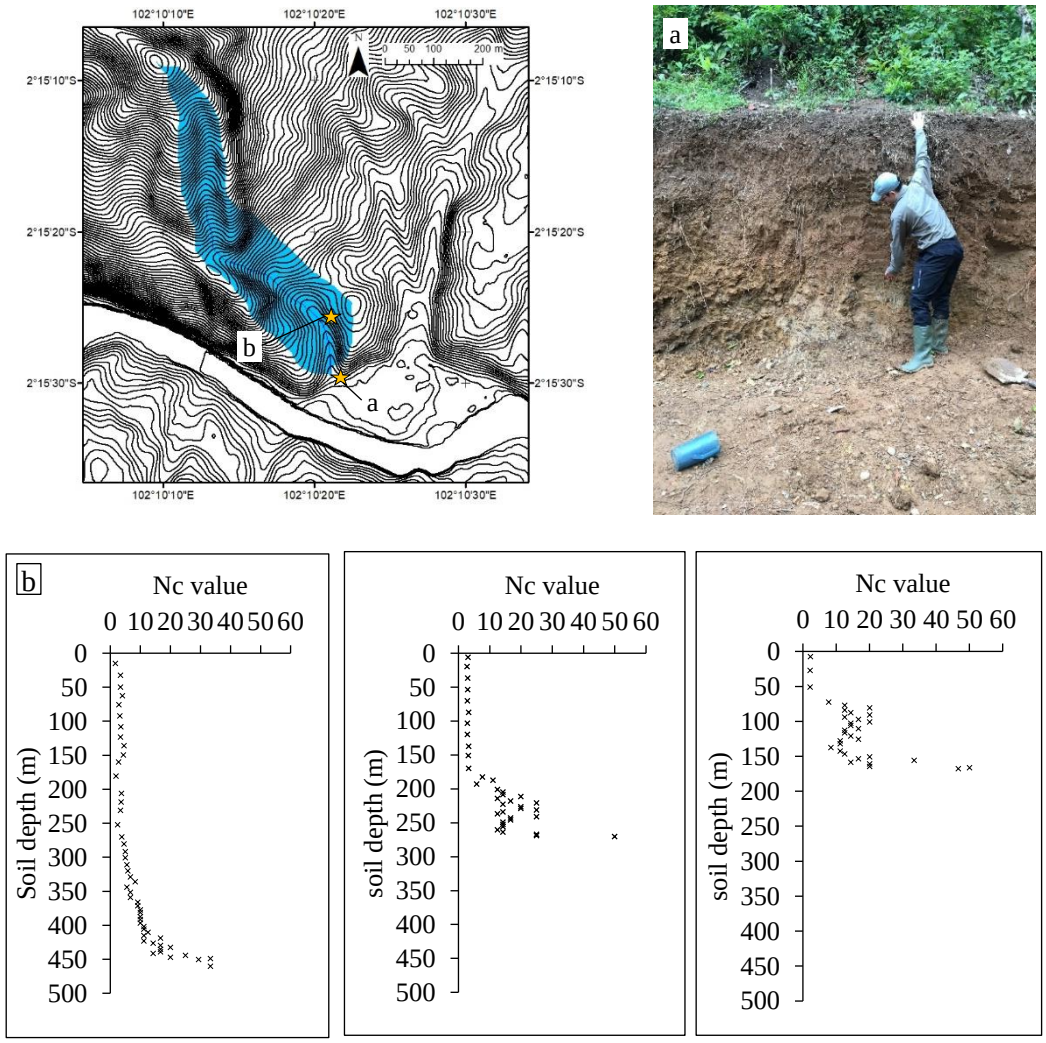

Figure 2-5 A photograph of the soil observed and profile of the Nc value in natural forest area at Sekancing site. Note that Nc profile at a) downslope, b) middle slope, c) upslope.

Prior studies on soil properties in the upstream area carried out by Araki (2019) at a hillslope scale and Susiwidiyaliza (2015) at a sub-catchment scale show thick soil layer ranging from 1.1 m to 4.5 m depth with high hydraulic conductivity up to

320 mm/h. Supiandi (1988) carried out soil sampling in the downstream area (east of Jambi to the coastline) and showed soil depths ranging from about 1.4 m to more than 3 m. Supiandi (1988) also measured peat depth and showed that peats are formed up to 6 m depth in eastern part of Jambi province (Supiandi,1988).

2.5 Peatland

In the Batanghari river basin, peatland is distributed in eastern part of Jambi province. Peat swamps in this area are mostly composed of dead body of woods, having acid reaction and a wide range from eutrophic to oligotrophic peats. These peat soils have been deposited since the terrestrial soils on the Pleistocene terrace were transformed into fluviatile swampy soils (Furukawa and Supiandi, 1985). The lowland area of the area can be divided into terrace and tidal zone. During the post-Glacial period, when the sea level rose, the terrace surface with terrestrial soils is supposed to have been transformed into fluviatile swampy lands. Ombrogenous peatlands were then developed on terrace, sometimes exceeding six meters (Supiandi and Furukawa, 1986). During the period before 1,500 years, coastal line moved back to the offing and peats start accumulating on tidal zone. Figure 2-6 below shows how peatland is generally formed. Initially, a river inundates a depression zone and makes wetlands. In wetlands, freshwater swamp forests were developed and the dead body of the trees were accumulated in water logged conditions. Floodwater has brought a mineral and peatlands at this stage has more or less nutrients. from rivers. Flood water contributes to formation of peat until a peat forms flat surface. Due to relatively high rainfall, a peat accumulates further and peat dome developed, which is a higher land than river water levels.

The human activity causes the CO_2 emission in tropical peatlands. As mentioned earlier, a previous study shows that a peat swamp forest has been deforested and converted into plantation. Drying peats due to dense canalization are decomposed, including oxidation and emits a large amount of CO_2. In dry season, drying peats can increase hydrological drought, and thereby increase fire risk (Taufik *et al.*, 2019). In particular, this is a primary concern in prolonged dry season due to El Niño because huge peatlands area can be burned. During the latest El Niño in 2015, about 67,000 ha of peatland was burned that accounts for more than 50% of total burned area,

including forest (estimates from burned area of Ministry of Environment and Forestry). One of the consequences was that Indonesia's daily carbon emissions in September–October 2015 were greater than the fossil fuel CO_2 release rate of the European Union (Huijnen *et al.*, 2016). About 81% of the total emissions in whole Indonesia, including emissions from fire on other land uses, were generated from peatland fire (Pribadi and Kurata, 2017).

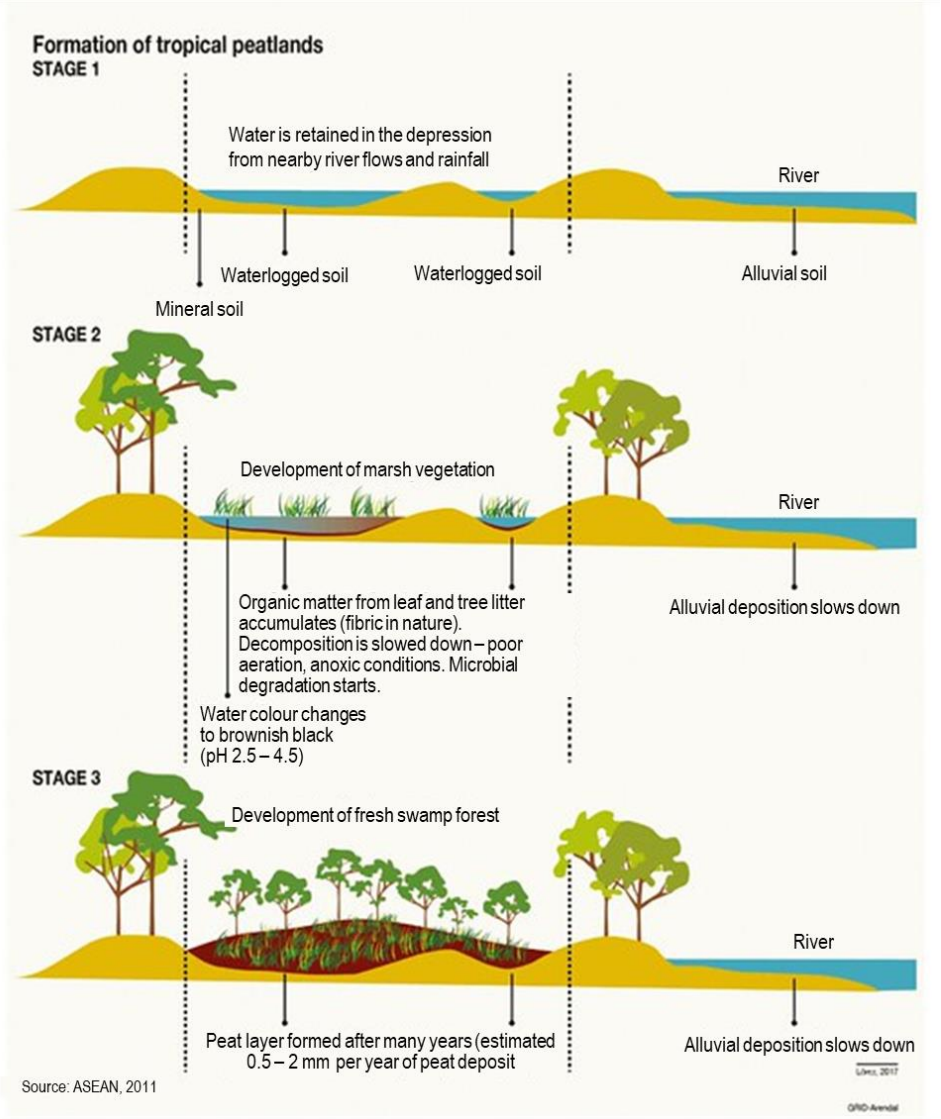

Figure 2-6 Formation of tropical peatlands. Note that Figure was created by Nieves Lopez Izquierdo and is taken with a permission from https://www.grida.no/resources/12531.

References

Afriyanti, D, Hein, L, Kroeze, C, Zuhdi, M, Saad, A (2019) Scenarios for withdrawal of oil palm plantations from peatlands in Jambi Province, Sumatra, Indonesia. *Regional Environmental Change* 19: 1201–1215. DOI: 10.1007/s10113-018-1452-1

Aldrian E, Susanto D (2003) Identification of three dominant rainfall regions within Indonesia and their relationship to sea surface temperature. *International Journal of Climatology* **23**: 1435–1452. DOI: 10.1002/joc.950.

Araki R (2019) Characteristics of Soil and Hillslope Runoff in Humid Tropical Forest in Sumatra, Indonesia. *Bachelor's Thesis*, Kyoto University, Kyoto, Japan: 27p.

Chang JH, Lau LS (1993) A definition of the humid tropics. In *Hydrology and Water Management in the Humid Tropics: Hydrological research issues and strategies for water management*, Bonell M, Hufschmidt MM, Gladwell JS (eds). UNESCO, Cambridge: Cambridge University Press; 571–574.

Drescher J, Rembold K, Allen K, Beckschäfer P, Buchori D, Clough Y, Faust H, Fauzi AM, Gunawan D, Hertel D, Irawan B, Jaya INS, Klarner B, Kleinn C, Knohl A, Kotowska MM, Krashevska V, Krishna V, Leuschner C, Lorenz W, Meijide A, Melati D, Nomura M, Pérez-Cruzado C, Qaim, M, Siregar IZ, Steinebach S, Tjoa A, Tscharntke T, Wick B, Wiegand K, Kreft H, Scheu (2016) Ecological and socio-economic functions across tropical land use systems after rainforest conversion. *Philosophical Transactions of the Royal Society B: Biological Sciences* 371: 20150275. DOI: 10.1098/rstb.2015.0275

Furukawa H, Supiandi S (1985) Agricultural Landscape in the Lower Batanghari, Sumatra. Part One: Statigraphy and Geomorphology of Coastal Swampy Lands. *Southeast Asian Studies* 23(1): 3-37. (In Japanese)

Huijnen V, Wooster MJ, Kaiser JW, Gaveau DLA, Flemming J, Parrington M, Inness A, Murdiyarso D, Main B, van Weele M (2016) Fire carbon emissions over maritime southeast Asia in 2015 largest since 1997. *Scientific Reports* 6: 26886. DOI: 10.1038/srep26886

Jambi Province Statistical Agency (2015) Jambi Province in Figures.

Ministry of Public Works (2003) Direction of Regional Spatial Planning in Batanghari River Basin. Ministry of Public Works, Indonesia

Sumawijaya, N (2006) Hydrology and peat-land development in Indonesia. Tropics 15(3):279-284. DOI: 10.3759/tropics.15.279

Katsura S, Kosugi K, Yamakawa Y, Mizuyama T (2014) Field evidence of groundwater ridging in a slope of a granite watershed without the capillary fringe effect. *Journal of Hydrology* 511: 703-718. DOI: 10.1016/j.jhydrol.2014.02.021

Katsuyama M, Ohte N, and Kosugi K (2004) Hydrological control of the streamwater NO_3 concentrations in a weathered granitic headwater catchment (in Japanese with English abstract), *J. Jpn. For. Soc.*:86, 27–36, 2004

NASA and METI (National Aeronautics and Space Administration, Ministry of Economy Trade and Industry of Japan) (2017) ASTER GDEM 2

Pribadi A, Kurata G (2017) Greenhouse gas and air pollutant emissions from land and forest fire in Indonesia during 2015 based on satellite data. *IOP Conf. Series: Earth and Environmental Science* 54:012060. DOI: 10.1088/1755-1315/54/1/012060

Supiandi S (1988) Studies on Peat in the Coastal Plains of Sumatra and Borneo: Part I Physiography and Geomorphology of the Coastal Plains. *Southeast Asian Studies* 26: 308-335 (in Japanese). DOI: 10.20495/tak.26.3_308.

Susiwidiyaliza (2015) Study the impact of oil palm expansion on the hydrological functions of Batang Tabir watershed using SWAT model. Master's Thesis, Bogor Agricultural University, Bogor, Indonesia. (in Indonesian).

Tarigan. SD (2016) Land Cover Change and its Impact on Flooding Frequency of Batanghari Watershed, Jambi Province, Indonesia. Procedia Environmental Sciences 33(2016):386-392. DOI: 10.1016/j.proenv.2016.03.089

Taufik M, Veldhuizen AA, Wösten JHM, van Lanen HAJ (2019) Exploration of the importance of physical properties of Indonesian peatlands to assess critical groundwater table depths, associated drought and fire hazard. *Geoderma* 347 160–9. DOI: 10.1016/j.geoderma.2019.04.001

Utami N, Sapei A, Apip (2017) Land use change assessment and its demand projection in Batanghari River Basin, Sumatera, Indonesia. *LIMNOTEK Perairan Darat Tropis di Indonesia* **24**: 52-60

Wahyunto, Ritung S, Subagjo H (2003) Maps of area of peatland distribution and carbon content in Sumatra, 1990–2002. Wetlands International—Indonesia Programme & Wildlife Habitat Canada (WHC), Bogor.

Yamamoto EMS, Sayama T, Yamamoto K, Apip (2020) Comparison of runoff generation methods for land use impact assessment using the SWAT model in humid tropics. *Hydrological Research Letters* 14(2): 81–88. DOI: 10.3178/hrl.14.81

Chapter 3 Applicability of the Rainfall-Runoff-Inundation Model in a Humid Tropical River Basin

3.1 Background

Rainfall-Runoff models have been applied to analyze the impact of land use change on hydrological cycle at basin scale and runoff. Most of hydrological models are developed for simulating river discharge with assumption of rainfall-runoff process such as quick subsurface flow in a shallow soil layer in a temperate region. For example, typical flood prediction model in Japan assumes that major source of runoff is saturated flow in the shallow soil layer on the bedrock (Tachikawa *et al.*, 2004). Recent flood models are capable of simulating river discharge with consideration of groundwater flow which recharge from a bedrock in a mountainous area in a temperate region (Sayama *et al.*, 2015a). On the other hand, there is a finding that rainfall can infiltrate and move to deep soil layer and runoff generates from the deep soil layer (Kumagai *et al.*, 2016). However, the current Rainfall-Runoff Model does not explicitly consider the runoff process in a deep soil layer. In addition, taking account into the high energy flux and tropical forest, it is important to consider the effect of evapotranspiration for both short or long-term Rainfall-Runoff simulation.

This study investigates the applicability of Rainfall-Runoff-Inundation (RRI) model, as an example of distributed rainfall runoff model, to a humid tropical river basin. The RRI is a two-dimensional model that is capable of simulating rainfall-runoff process and flood inundation at the same time (Sayama *et al.*, 2012). In the previous research (Sayama *et al.*, 2015b), there is not sufficient consideration of a deep soil layer for long-term rainfall runoff process in a humid tropical region. This research discusses the capacity of the RRI for simulating long-term rainfall runoff and flood inundation in a tropical peatland area at the downstream. Specifically, this study clarifies the reasonable model structure for a humid tropical area and potential use for analyzing long-term rainfall runoff process and inundation process with

satellite rainfall and potential evapotranspiration estimated by global data in data-scarce region in Sumatra island.

3.2 Methods

3.2.1 Overview of runoff process on RRI model

This section describes important structures for runoff process of RRI model, i.e. lateral subsurface flow, vertical infiltration flow and mountainous groundwater (Figure 3-1). In this study, applicability of the model was tested with several combinations of different runoff model structure and parameter sets.

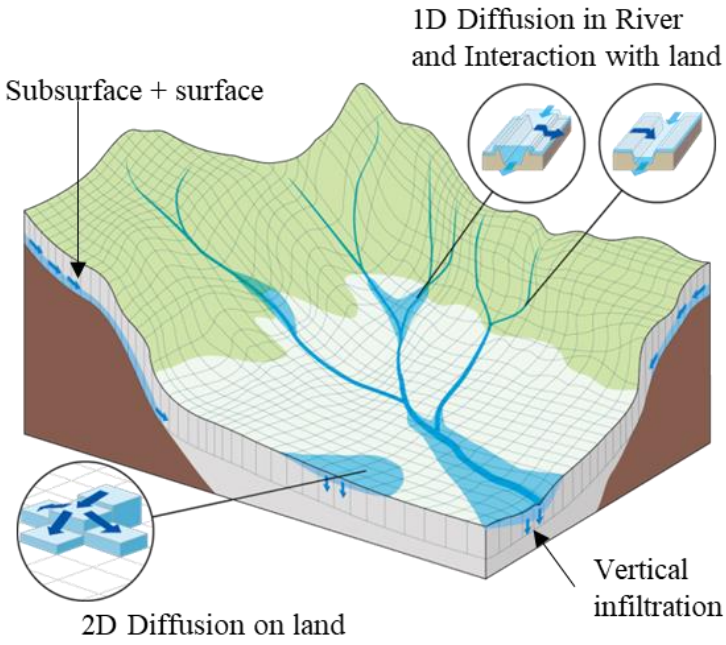

Figure 3-1 Schematic diagram of RRI model.

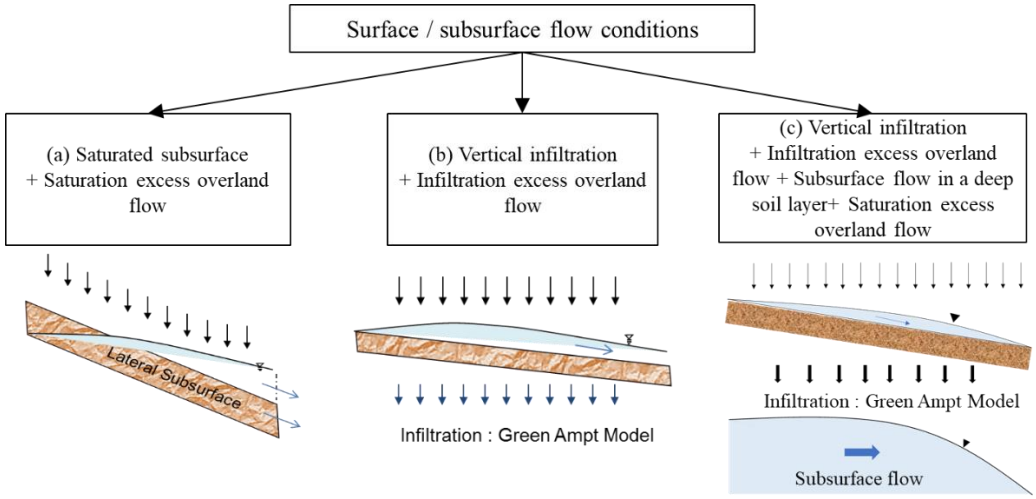

Figure 3-2 *Schematic diagram of runoff process in RRI model. (a) Lateral saturated subsurface flow that can generate saturation excess overland flow, (b) vertical infiltration flow that can generate infiltration excess overland flow and (c) the combined vertical infiltration flow and lateral subsurface flow in a deep soil layer.*

3.2.1.1 Lateral subsurface flow in a mountainous area

In mountainous area, lateral subsurface flow can be a dominant runoff process and can generate saturation excess overland flow (Figure 3-2a). A stage-discharge relationship equation was applied to saturated-unsaturated flow. In the RRI model, rainfall increases water depth (h) directly without explicit analysis of vertical infiltration. When $h<d_m$, unsaturated flow generates. When $d_m<h\leq d_a$, saturated flow generates based on Darcy's law. When $h>d_a$, surface flow generates based on Manning's law in addition to subsurface flow. The equations in x direction are shown as below.

$$q_x = \begin{cases} -k_m d_m \left(\frac{h}{d_m}\right)^{\beta} \frac{\partial H}{\partial x} & (h \leq d_m) \\ -k_a (h - d_m) \frac{\partial H}{\partial x} - k_m d_m \frac{\partial H}{\partial x} & (d_m < h \leq d_a) \\ -k_a (h - d_m) \frac{\partial H}{\partial x} - k_m d_m \frac{\partial H}{\partial x} & (d_a < h) \\ -\frac{1}{n} (h - d_a)^{\frac{5}{3}} \sqrt{\left|\frac{\partial H}{\partial x}\right|}\ sgn\left(\frac{\partial H}{\partial x}\right) & \end{cases} \quad \textit{(eq. 3-1)}$$

$$d_a = D \times \gamma_a \quad \textit{(eq. 3-2)}$$

$$d_m = D \times \gamma_m \quad \textit{(eq. 3-3)}$$

$$k_m = \frac{k_a}{\beta} \quad \textit{(eq. 3-4)}$$

where q_x is unit width discharge in x direction, k_a is lateral saturated hydraulic conductivity, d_a is soil depth (D) times effective porosity for saturated soil layer (γ_a), d_m is soil depth times effective porosity for unsaturated soil layer (γ_m), $k_m$is the lateral hydraulic conductivity in unsaturated zone , β is a constant, h is depth from a bedrock, *H* is water level and n is the Manning's coefficient for a slope.

3.2.1.2 Vertical infiltration flow in a flat area

In a flat area, infiltration amount is estimated by Green-Ampt model (Figure 3-2b) and the excess of infiltration will be surface flow. Once water infiltrates, it will evaporate or store in the soil layer.

$$f = k_v \left[1 + \frac{(\Phi - \theta_i) S_f}{F}\right] \quad \textit{(eq. 3-5)}$$

where k_v is vertical saturated conductivity, Φ is porosity, θ_i is initial water volume content, S_f is suction at the vertical wetting front, and f is cumulative infiltration depth.

3.2.1.3 Mountainous groundwater flow

The groundwater model assumes that the hydraulic conductivity in the bedrock reduces exponentially with depth. Therefore, subsurface flow can be calculated without any bottom of soil layer by accumulating groundwater flow. When water is available in the soil layer, it will recharge at constant rate. When groundwater is saturated, a excess water recharges to soil layer.

$$\gamma_g \frac{\partial z_g}{\partial t} + \frac{\partial q_g}{\partial x} = r_{sg} - r_{gl} \quad \textit{(eq. 3-6)}$$

$$q_g = -\frac{k_{g0}}{f_g} I_g \, exp\left(-f_g z_g\right) \quad \textit{(eq. 3-7)}$$

$$r_{sg} = \begin{cases} k_{sg} & (h_s > 0, z_g > 0) \\ 0 & (h_s = 0) \end{cases} \quad \textit{(eq. 3-8)}$$

where, q_g is unit width lateral flow of mountainous groundwater, k_{sg} is a vertical hydraulic conductivity, k_{g0} is a lateral hydraulic conductivity on a bedrock

surface, f_g is a constant that determines reduction rate of saturated hydraulic conductivity in a vertical axis, γ_g is effective porosity in a deep soil layer, z_g is depth to groundwater surface in a vertical direction, I_g is hydraulic gradient of mountainous groundwater, r_{gl} is a parameter which represent a discharge from groundwater system to outside of the system.

3.2.2 Dataset

This study uses Global Satellite Mapping of Precipitation (GSMaP) Reanalysis ver. 6 (Shimada *et al.*, 2017) from 2001 to 2013 (13 years) with a resolution of 0.1 degrees. The GSMaP Reanalysis product is satellite rainfall data that were calibrated using Japanese 55-year Reanalysis (JRA-55) data. In data-scarce regions such as the river basins of Sumatra Island, rain gauge data are typically too limited to accurately represent spatial patterns in rainfall data. Consequently, the availability of GSMaP data with a temporal resolution of 1 hour on any grid is well suited for hydrologic modeling. In this study, the quality of the GSMaP rainfall data is assessed based on gauged rainfall at 23 locations in the Batanghari river basin.

The climatic data used for estimating evapotranspiration, such as wind speed, temperature, surface pressure, specific humidity, downward long- and shortwave radiation fluxes, were obtained from WATCH Forcing Data based on ERA-Interim (Weedon *et al.*, 2014) with a 0.5-degree resolution at daily timesteps. Land surface variables, such as the Leaf Area Index, surface roughness and albedo were obtained from ECOCLIMAP (Champeaux *et al.*, 2005) at monthly timesteps. Based on the data, potential evapotranspiration was estimated by using the Penman-Monteith equation to reference present climate conditions. The actual evapotranspiration is estimated by the RRI model and the details are described in section 3.2.4 below (see description of Case 2).

3.2.3 Simulation condition of RRI model

Topographic data used in this study were obtained from HydroSHEDS (30-s resolution). The resolution corresponds approximately to 761 m × 924 m in this region. The model also requires information on river channel locations and cross-

sections. I used flow accumulation data sets included in HydroSHEDS. Grid cells with more than twenty flow accumulations were confirmed to have a river channel. For the river cross-sections, I used the following simple regression equations: width (m) = $1.22A^{0.566}$, depth (m) = $1.5A^{0.113}$, where A (km^2) is the flow accumulation area. The regression parameters for the river width were estimated at eight locations and the depth parameters were estimated at eleven locations based on measurements of river cross section. The levee height was set to be zero, as no apparent levee was found in the region, except for Jambi city. At Ancol water level station (see Figure 2-1), arbitrary cross section was used.

The simulation was conducted for the period 1 March 2000 to 28 February 2014. The simulation time steps were initially set to be 600 s for the slope grid cells and 60 s for the river grid cells. In this study, observed water level at three gauged stations was used to validate RRI model. Discharge was estimated using rating curves. The model is validated for a period of 2011 and 2013 because data quality was satisfactory.

3.2.4 Selection of model structure that is suitable for humid tropics and parameter setting

This study used three conditions that is combinations of the RRI model structure and parameter setting to investigate applicable settings for the RRI model. The impacts of four simulation conditions (Case1, Case2, Case3 and Case4) on river discharge and inundation were analyzed. In addition, this study compares results of simulation conditions for humid tropical region (Case2, Case3 and Case4) and for temperate region (Case1).

Table 3-1 Model structure and parameter sets for Case1, Case2, Case3 and Case4.

	Case1, Case2 and Case3		Case 4	
Precipitation	GSMaP reanalysis v6		GSMaP reanalysis v6	
ET	No consideration (Case1) Potential evapotranspiration (Case2 and 3)		Potential evapotranspiration	
Lower boundary	Water level=0		Water level=0	
Cross section	Estimated by empirical equation		Estimated by empirical equation	
Runoff process (Figure 3-2)	(a)	(b)	(c)	
Parameter	Mountain	Flatland	All land use types	
n_s ($m^{-1/3}s$)	0.3	0.3	n_s ($m^{-1/3}s$)	0.3
D (m)	1 (Case1 and 2) 3 (Case3)	1 (Case1 and 2) 3 (Case3)	D (m)	3
γ_a* (m)	0.39	-	k_{sg} (cm/s)	1.5×10^{-3}
γ_m*	0.07	-	k_{g0} (cm/s)	1.425×10^{-3}
k_a (m/s)	0.2	-	f_g	5.0×10^{-1}
k_m (m/s)	0.05	-	γ_g	3.7×10^{-2}
			r_{g0}	0
k_v*(m/s)	-	8.33×10-7	k_v*(m/s)	8.33×10-7
φ*	-	0.33	φ*	0.33
S_f*(m)	-	0.219	S_f*(m)	0.219
F_{limit}* (m)	-	0.39 (Case1 and 2) 1.17 (Case3)	F_{limit}* (m)	1.17
n_r ($m^{-1/3}s$)	0.03	0.03	n_r ($m^{-1/3}s$)	0.03

Case1 includes subsurface flow in a mountainous area and vertical infiltration flow in a flat area. The land uses at global scale from Global Land Cover by National Mapping Organizations are classified into two land uses. i.e., a mountainous area and flat area. The model parameters were suggested from previous model applications (Sayama *et al.*, 2012) and determined after a trial-and-error approach, owing to the lack of past hydrological records in the region. The Green-Ampt parameters are spatially distributed based on FAO soil map and the parameters are utilized based on “sandy clay loam”, “clay loam” and “clay” (Rawls *et al.*, 1993). The model structure and parameters are summarized in Table 3-1.

Case2 considers potential evapotranspiration data as an input to RRI model and used the same condition as Case 1 for other setting as shown in Table 3-1. The actual evapotranspiration is calculated by first subtracting surface water, before subtracting additional water from a cumulative infiltration amount estimated by the Green-Ampt model until it meets the potential evapotranspiration. When the value approaches 0, there is no water to evaporate and actual evapotranspiration at that time is less than the potential evapotranspiration.

Case3 used 3-m soil depth for saturated lateral subsurface flow model and the Green-Ampt model. The other simulation condition is identical to Case 2 (Table 3-1).

Case4 applied Green-Ampt model for vertical infiltration process and ground water model to whole river basin (Figure 3-2c). I assume that there is no bedrock on a slope and use the groundwater model to runoff process in deep soil layer that represents field measurements at Sekancing site (see Figure 2-4 in Chapter 2 for location). The soil depth is 3m and Green-Ampt parameters are based on "sandy clay loam", "clay loam" and "clay" (Rawls *et al.*, 1993). The soil depth is 3 m for whole river basin. The Green-Ampt parameters settings are identical to other Cases. The parameters for groundwater model are based on previous research (Syama *et al.*, 2015a). The other parameters are same as other Cases. The parameter sets are summarized in Table 3-1.

3.3 Results

3.3.1 Comparison of annual and monthly rainfall estimated using GSMaP reanalysis data with gauged rainfall data

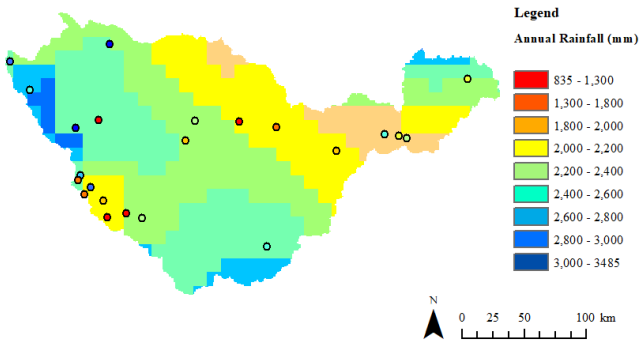

Figure 3-3 Comparison of annual rainfall estimated using GSMaP and gauged stations.

Figure 3-3 compares spatial distribution of GSMaP reanalysis data with that of gauged rainfall data. The GSMaP data indicate high annual rainfall in the northern mountainous ranges of the basin, which corresponds with the gauged rainfall data. I also compared basin-averaged GSMaP annual rainfall and gauged annual rainfall. The average annual rainfall over the basin was estimated to be 2,321 mm by GSMaP and 2,021 mm by the rain gauges (Yamamoto *et al.*, 2019). In addition, Figure 3-4 shows temporal pattern of average monthly rainfall estimated using GSMaP data is similar to that of gauged rainfall data. On the other hands, it should be noted that monthly rainfall in December is particularly higher than observed one.

3.3.2 Estimated potential evapotranspiration

Average annual potential evapotranspiration is 1,495 mm that is within a range of actual evapotranspiration, estimated using annual rainfall and annual total discharge in the previous study (Kuraji, 1996). Average monthly actual evapotranspiration varies from 106 mm to 145 mm and its standard deviation is small (Figure 3-4). Previous case study on tropical forest in Malaysia (Lion *et al.*, 2017) shows that evapotranspiration rate does not change depending on dry season.

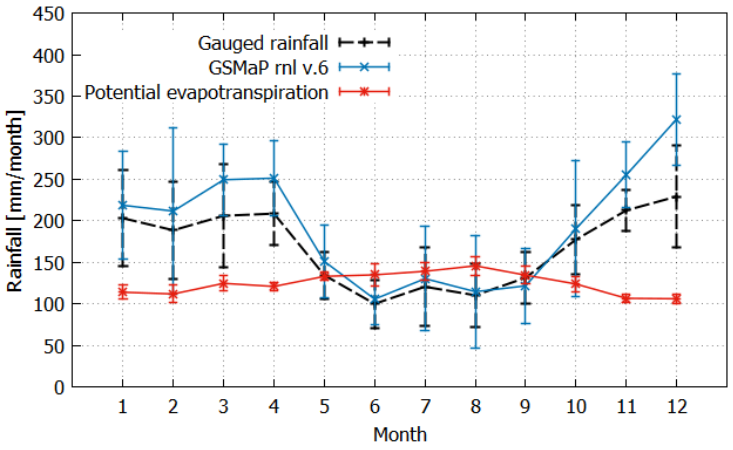

Figure 3-4 Average monthly potential evapotranspiration and average monthly rainfall estimated using GSMaP data and gauged stations. The bar indicates standard deviation based on data from 2001 to 2013.

3.3.3 Comparison between simulated river discharge and observation

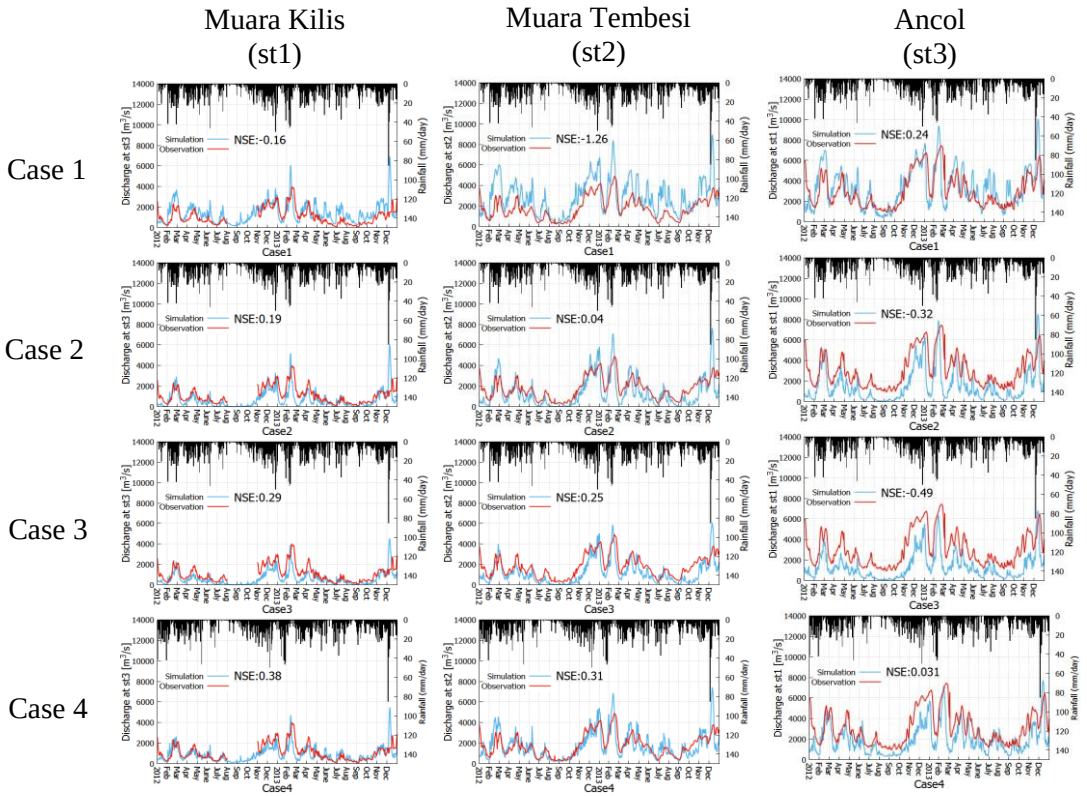

Figure 3-5 Comparison between simulated and observed discharge under 4 simulation conditions. First row is under Case 1, Second row is under Case 2, Third row is under Case 3, Fourth row is under Case 4. Left, middle and right column shows results at st1, st2 and st3 respectively.

Figure 3-5 shows a comparison between simulated daily river discharge and observation at three gauged stations (please refer to Figure 2-1 in chapter 2 for location of water level stations (WLS)), i.e., Muara Kilis WLS (st1), Muara Tembesi WLS (st2) and Ancol WLS (st3). The simulated discharge in Case 1 is overestimated at any gauged stations. In Case 2, volume of simulated discharge is reduced and the simulated results becomes closer to observation at st1 and st2. Case 3 shows that peak of simulated river discharge is closer to observation, compared with results of Case 2. The Nash coefficient in Case 3 (0.29 at st1 and 0.25 at st2) is improved, compared with that of Case 2 (0.19 at st1 and 0.04 at st2). However, Case 3 shows that simulated discharge is underestimated for a period of continuous small rainfall. Case 4 shows that the simulated discharge during little rainfall is closer to

observation and its Nash coefficient is improved from that of Case 3. It is noted that Case 4 shows that the simulated discharge at st3 is underestimated.

3.3.4 Estimated inundation depth distribution

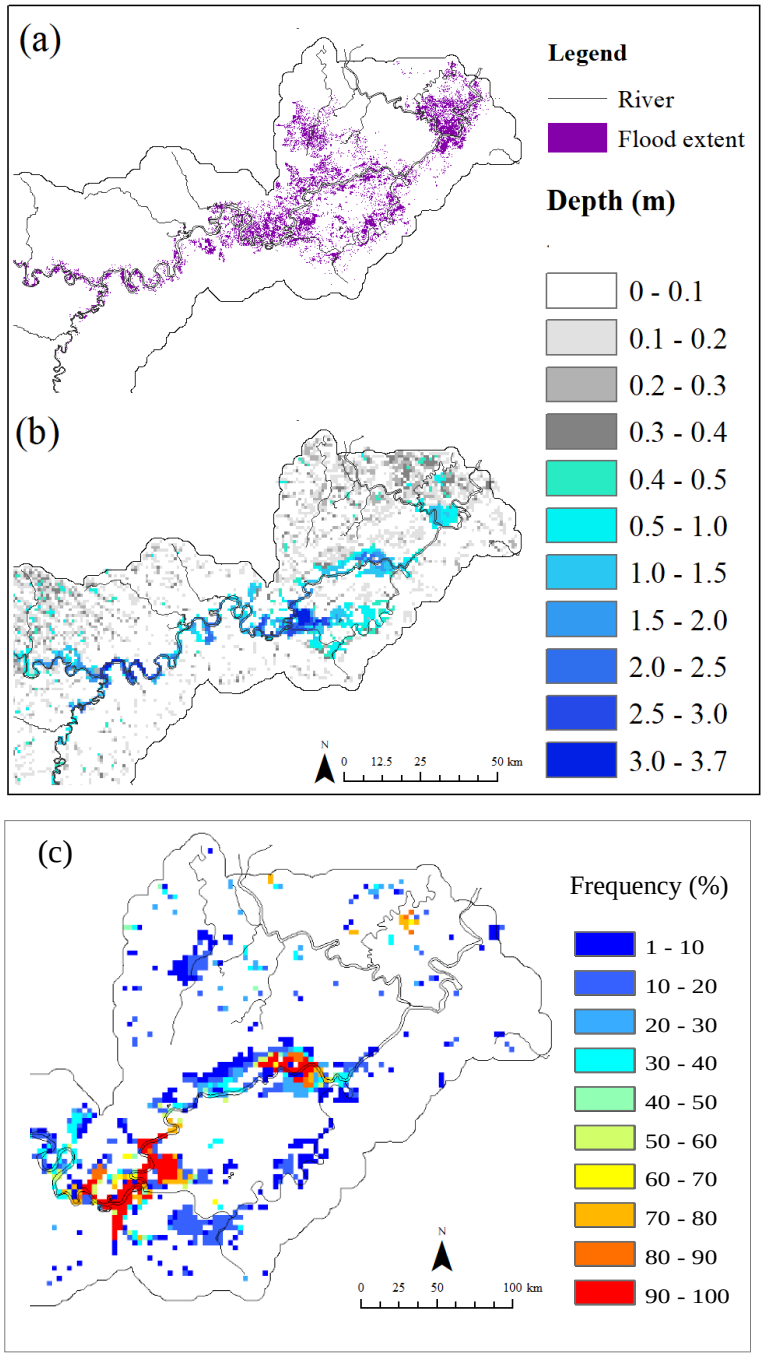

Figure 3-6 *Observation based and simulated flood inundation maps for downstream area (a) flood extent captured by sentinel satellite, (b) simulated maximum inundation depth distribution (Dec. 2016 – Mar. 2017) with GSMaP Reanalysis, and (c) flood (>0.5m) frequency (2001-2017).*

I compared performances of RRI under different simulation conditions and selected Case 4 that shows better performance for simulating river discharge. Under Case 4 condition, the simulation was conducted from 2001 to 2017. To validate the simulated inundation patterns, I compared the maximum inundation distribution from December 2016 to March 2017 using the maximum flood extent inferred by sentinel satellite imagery (Indonesian Local Government Community (MLI), 2017) (Figure 3-6). The simulated inundation pattern agrees well with the satellite image of the Batanghari River and its tributaries. In addition, I obtained frequency of inundation occurrence at downstream area. I consider that a grid cell is inundated if inundation depth exceeds 0.5 m. Then I count the number of inundated events for a period between 2001 and 2013 and divide the total by 13. Figure 3-6 shows the frequency of inundation exceeds 80 % at some parts of downstream area.

3.4 Discussion

Case 2 shows better peaks of river discharge than Case 1. This suggests that evapotranspiration is a factor to improve simulated river discharge. However, Case 2 shows that simulated river discharge is underestimated for a period of little rainfall or dry season. Monthly evapotranspiration rate from June to September is high that evaporates water on land in the model. Compared with Case 2, Case 3 shows the simulated peak discharge is smaller and closer to observed one and shows better Nash coefficients at st1 and st2. Thicker soil layer plays a role to generate more subsurface flow in mountainous area and store more water in flat area. Consequently, surface flow reduces and temporal water storage increases at the basin that increases actual evapotranspiration that improves performance of RRI model. Case 4 considers groundwater flow pathway in deep soil layer and shows model performance improved i.e., in particular, simulated low discharge is larger and closer to observed one. I compare annual actual evapotranspiration of Case 3 to that of Case 4. Case 4 shows smaller actual annual evapotranspiration compared with Case 3. In the RRI model, groundwater is not evaporated and the reduction of actual evapotranspiration explains that more water recharge groundwater. The improvement of low discharge attributes to groundwater flow that discharge water to river in dry season. However, model was not able to perform at st3. I consider two possible causes. The first

problem is the model estimate larger inundation volume in area between st2 and st3 that leads to underestimation of discharge at st3. The second problem is that rating curve has a problem and observed discharge is estimated largely than actual discharge. I discuss the issues by comparing between observed discharge at st2 and st3. Topography consists of flat area and small tributaries. Considering the factors, the river discharge at st3 does not increase more than that at st2. However, observed discharge at st3 increase by 1.5 times compared with that at st2. From the above, underestimated discharge at st3 is more likely to be caused by rating curve used for discharge at st3.

3.5 Conclusion

The spatial pattern and basin-averaged rainfall estimated using GSMaP reanalysis ver. 6 is similar to that of gauged stations. In addition, average annual rainfall estimated using GSMaP and average annual potential evapotranspiration estimated is within the range of values in a previous study. The findings show that GSMaP and Penman-Monteith equation are able to estimate rainfall and evapotranspiration in humid tropics.

The aim of our study is to clarify a model structure that is suitable for humid tropics. I investigated combinations of runoff process and parameter setting and discussed the suitable simulation condition of RRI model. The simulated discharge was improved when an evapotranspiration was used as an input for RRI model. In addition to this, parameter of soil was changed from 1 m to 3 m. The 3 m soil layer decreases surface flow and increases temporal storage. Consequently, the condition improved peaks of simulated discharge but could not reproduce discharge in dry season. Furthermore, the model is capable of reproducing discharge for long term including dry season by adding groundwater model to the updated simulation conditions. These results and discussions indicate that a model is capable of performing for long-term discharge, given that a simulation considers characteristic of hydrology in humid tropics such as evapotranspiration input, thicker soil layer and groundwater process in a deep soil layer. In addition, I conduct a simulation for flood inundation using the above model. I found out that the frequency of inundation exceeds 80 % at some parts of downstream area.

References

Champeaux, J, Masson, V, Chauvin, F (2005) ECOCLIMAP: A global database of land surface parameters at 1 km resolution. *Meteorological Applications* 12(1): 29-32. DOI:10.1017/S1350482705001519

FAO/UNESCO (2003) Digital Soil Map of the World and derived soil properties. FAO, Rome, Italy.

Indonesian Local Government Community (MLI) (2017) the role of communities towards healthy aquatic ecosystems, *Proceeding of General Assembly and Annual Scientific Conference III*:316-324

Kumagai, T, Kanamori H, and Chappell NA (2016) Tropical Forest Hydrology, *Forest Hydrology: Processes, Management and Assessment*, CAB Internationa and USDA

Kuraji, K (1996) Water balance studies on moist tropical forested catchments, *Journal of the Japanese Forestry Society* 78(1):89-99. DOI: 10.11519/jjfs1953.78.1_89. (In Japanese)

Koji K (1996) Water balance studies on moist tropical forested catchments, *Journal of the Japanese Forestry Society* 78(1), 89-99 (In Japanese).

Lion M., Kosugi Y, Takahashi S, Noguchi S, Itoh M, Katsuyama M, Matsuo N, Shamsuddin S-A (2017) Evapotranspiration and water source of a tropical rainforest in peninsular Malaysia, *Hydrological Processes* 31:4338-4353

Masson V, Champeaux J-L, Chauvin F, Meriguet C, and Lacaze R (2003) A Global Database of Land Surface Parameters at 1-km Resolution in Meteorological and Climate Models, *J. Clim.* 16:1261-1282

Rawls WJ, Ahuja LR, Brakensiek DL, and Shirmohammadi A (1993) Infiltration and soil water movement. In: D.R. Maidment (ed). *Handbook of Hydrology*. McGraw-Hill, Inc. New York.

Sayama T, Ozawa G, Kawakami T, Nabesaka S, Fukami K (2012) Rainfall–runoff–inundation analysis of the 2010 Pakistan flood in the Kabul River basin. *Hydrological Sciences Journal*, 57(2):298-312

Sayama T, Kosugi K, Iwami Y (2015a) Development of a distributed rainfall-runoff model simulating for mountainous groundwater, *JSCE B1 (Hydraulic Engineering)* 71(4):331-336

Sayama T, Tatebe Y, Tanaka S (2015b) An emergency response-type rainfall-runoff-inundation simulation for 2011 Thailand floods, *Journal of Flood Risk Management* 1-8. DOI:10.1111/jfr3.12147

Shimada, U, Aonashi K (2017) Tropical cyclone intensity change and axisymmetricity deduced fron GSMaP, *American Meteorological Society* 145: 1003-1017

Tachikawa Y, Nagatani G, Takara K (2004) Development of stage discharge relationship equation incorporating saturated-unsaturated flow mechanism, *JSCE Annual Hydraulic Engineering* 48:7 – 12 (in Japanese with English Abstract)

Weedon GP, Balsamo G, Bellouin N, Gomes S, Best MJ, Viterbo P (2014) The WFDEI meteorologicalforcing data set: WATCH Forcing Datamethodology applied to ERA-Interimreanalysis data, *Water Resour. Res.*50:7505–7514. DOI:10.1002/2014WR015638

Yamamoto K, Sayama T, Apip, Takara K. 2019. Applicability of Rainfall-Runoff-Inundation Model in a Humid Tropical River Basin. *Journal of Japan Society of Civil Engineering* **75**: I_253-I_258 (in Japanese).

Chapter 4 Climate Change Impact on Flood and Inundation in a Tropical River Basin in Indonesia

4.1 Introduction

Climate change will have significant impact on water-related disasters and environmental problems in Indonesia. The country is one of the regions in which extreme monsoon-related rainfall is projected to increase (Hijioka *et al.*, 2014), and such increases are expected to expose a larger proportion of the population to floods (Hirabayashi *et al.*, 2013). In Sumatra and the Kalimantan Islands of Indonesia, coastal lowland areas are mostly comprised of peatland. Peatland is a wetland environment that is initially maintained by flooding from rivers and which has, in recent years, been extensively developed for oil palm and other plantations. Changes in the frequency and magnitude of flood inundation due to climate change may disturb the peatland environment and its carbon stores, as well as cause damage to the agricultural plantations in the region.

The use of General Circulation Models (GCMs) is indispensable for projecting future climate change. However, GCMs have limitations in reproducing reasonable rainfall patterns in humid tropics, especially in areas with many islands such as those in the so-called Indonesian Maritime Continent (MC), which is surrounded by the Indian and Pacific oceans (Neale and Slingo 2003). These limitations can be attributed to the imperfect parameterization of physical processes (e.g., convection, cloud generation, local land sea breeze circulation and regional variations in the diurnal cycle) (Gianotti *et al.*, 2012; Ulate *et al.*, 2014), as well as the coarse resolution of topography (Neale and Slingo 2003; Schiemann *et al.*, 2014; Hertwig *et al.*, 2015). Given the high levels of uncertainty associated with GCMs, they are considered to be poorly suited for projecting future climate signals in and around the MC (Hijioka *et al.*, 2014). On the other hand, Regional Climate Models (RCMs) are capable of representing local climate systems and therefore have potential for realistically reproducing rainfall events. Several studies have shown that RCMs can

successfully reproduce local rainfall patterns in space and time in the MC (Juneng *et al.*, 2016; Cruz *et al.*, 2017; Rashid and Hirst 2017; Ratna *et al.*, 2017; Kang 2018).

Despite an abundance of studies on rainfall projections, studies on the impact of rainfall projections on river discharge are still limited in Indonesia (Emam *et al.*, 2016; Marhaento *et al.*, 2018). Moreover, very few studies have focused on flood inundation due to climate change at a river-basin scale, which is important for assessing the impacts on flood damage (Iwami *et al.*, 2017) and wetland environmental conditions.

Even though RCMs are potentially better for hydrologic impact assessment in the MC, there is still a need to correct the bias associated with RCMs (Christensen *et al.*, 2008). Among the various bias correction methods (Teutschbein *et al.*, 2012), the Quantile Mapping (QM) method has been widely applied to correct rainfall inputs for hydrologic models (Huang *et al.*, 2014; Marhaento *et al.*, 2018; Lee *et al.*, 2019). However, the applicability of the QM method to correct for bias in the MC region, particularly to assess flood inundation at the river-basin scale, has not been thoroughly investigated. Our previous study showed that inundation is more sensitive to rainfall than it is to runoff (Sayama *et al.*, 2015). Therefore, it is important to investigate appropriate bias correction methods to assess the impact of flood inundation in a humid tropical river basin. Specifically, this study focuses on the effects of spatial variations of rainfall on flood inundation. The Variance Scaling (VS) method (Teutschbein *et al.*, 2012) applied in this study is one of the potential approaches that can be used to match both the mean and the spatial variance of a data series with observed data.

The objective of this study was to assess the impact of climate change on flood inundation in a river basin on Sumatra Island. This study applied dynamically downscaled RCM rainfall data as the input for the RRI model, and identified appropriate bias correction methods for flood simulations. The specific objectives are:

1. What is the impact of non-/bias corrected rainfall output of the RCM on river discharge and flood inundation?
2. What is the most suitable method to correct rainfall bias when using the RCM to perform river discharge and inundation simulations?

3. What are the projected future changes in rainfall, streamflow and flood inundation in the studied region on Sumatra Island?

4.2 Methods

4.2.1 Dataset

This study uses climate data produced by the Non-Hydrostatic Regional Climate Model (NHRCM) that was developed by the Japan Meteorological Research Institute (MRI). The NHRCM is based on the Non-hydrostatic Model (Saito *et al.*, 2006), and the Kain and Fritsch scheme is used to parameterize cumulus convection (Kain *et al.*, 1993). The MRI-JMA Simple Biosphere Model is used to describe land surface processes (Hirai *et al.*, 2004). The NHRCM uses a boundary condition of the Atmospheric General Circulation Model developed in ver. 3.2S (AGCM) at a 20 km resolution for downscaling to a 5 km resolution (Sasaki *et al.*, 2008; Cruz *et al.*, 2017). The future boundary condition is based on changes of the CMIP3 ensemble mean Sea Surface Temperature (SST) under the Representative Concentration Pathways 8.5 scenario (RCP8.5) (Endo *et al.*, 2012). Downscaling was performed for our study area in Sumatra Island (-3.32°S – 0.41°S; 99.65°E – 105.25°E). The model is run for 21 years of present climate (1980 – 2000) and for 20 years of future climate (2079 – 2098) under the RCP8.5 scenario.

As reference rainfall data, this study uses Global Satellite Mapping of Precipitation (GSMaP) Reanalysis ver. 6 (Shimada *et al.*, 2017) from 2001 to 2013 (13 years) with a resolution of 0.1 degrees. The GSMaP Reanalysis product is satellite rainfall data that were calibrated using Japanese 55-year Reanalysis (JRA-55) data. In data-scarce regions such as the river basins of Sumatra Island, rain gauge data are typically too limited to accurately represent spatial patterns in rainfall data. Consequently, the availability of GSMaP data with a temporal resolution of 1 hour on any grid is well suited for hydrologic modeling. However, it should be noted that the reference data also contain uncertainty. For example, compared with other reanalysis datasets, some issues have been identified in JRA-55 data over tropical regions, such as weaker equatorial waves and Madden-Julian oscillation due to the characteristics of the forecasting model used for JRA-55 with resolution of 60 km

(Harada *et al.*, 2016). In this study, the quality of the GSMaP rainfall data is assessed based on gauged rainfall at 23 locations in the Batanghari River Basin.

The climatic data used for estimating evapotranspiration, such as wind speed, temperature, surface pressure, specific humidity, downward long- and shortwave radiation fluxes, were obtained from WATCH Forcing Data based on ERA-Interim (Weedon *et al.*, 2014) with a 0.5-degree resolution. Land surface variables, such as the Leaf Area Index, surface roughness and albedo were obtained from ECOCLIMAP (Champeaux *et al.*, 2005). Based on the data, potential evapotranspiration was estimated by using the Penman-Monteith equation to reference present climate conditions. The actual evapotranspiration is estimated by the RRI model and the details are described in the Rainfall-Runoff-Inundation Model section.

4.2.2 Bias correction and validation

This study compares two methods to correct for bias in NHRCM rainfall data, i.e., the QM method and a combination of QM and VS methods (hereafter, the QM-VS method). The QM method used in this study employs equiratio cumulative distribution function (CDF) matching developed by Wang and Chen (2014). The method assumes that a ratio between the observed and modeled values at the same percentile is preserved in the projection period. Specifically, the bias between modeled and observed values in the reference period is quantified by the ratio of the observed quantile value (F_{o-c}^{-1}) to the modeled quantile value (F_{m-c}^{-1}) at the same percentile in a future projection period ($F_{m-p}(\overline{x_{m-p}})$). The statistical transformation of bias correction is shown in equation (4-1),

$$x_{m-p.QM.}^{i} = x_{m-p}^{i} \cdot \frac{F_{o-c}^{-1}(F_{m-p}(\overline{x_{m-p}}))}{F_{m-c}^{-1}(F_{m-p}(\overline{x_{m-p}}))} \qquad \textit{(eq. 4-1)}$$

where, F_{m-p} is a CDF of RCM outputs in a future projection, F_{o-c}^{-1} is an inverse CDF corresponding to the observations, F_{m-c}^{-1} is an inverse CDF of RCM variables in the reference period and, x_{m-p}^{i} is a quantile of a variable in a future projection at a grid i. $\overline{x_{m-p}}$ represents the spatial average over the basin of x_{m-p}^{i}. In this study, CDF is constructed based on basin-averaged daily rainfall estimated using entire daily rainfall obtained from observation and NHRCM data. The quantiles of the

observation or model during the reference period at a given percentile of future rainfall are estimated by linear interpolation to compensate for differences in the size of the of the model and observation datasets.

The second method is a combination of the QM method and the VS method, which was described by Teutschbein *et al.* (2012). In this study, the QM-VS corrects spatial pattern of QM-corrected daily rainfall in following steps. After calculating the differences in $x^i_{m-p.QM.2}$ from the spatial mean $\overline{x_{m-p.QM.}}$ as shown in Eq. (4-2) on a daily basis, the VS method calculates the standard deviations of the spatial pattern $\sigma_{m-c.QM.|j}$ depending on the average rainfall categories represented as *j* (*j* = 1, ..., 21). Specifically, the categories include basin-averaged rainfall at a percentile ($\overline{x^{per}_{m-p.QM.}}$) in an interval of five percentiles between 2.3 and 99. Note that when *j* equals 21, the category includes rainfall exceeding $\overline{x^{99}_{m-p.QM.}}$. The spatial standard deviation is then adjusted according to Eq. (4-3), based on the spatial standard deviation of the observed rainfall ($\sigma_{o-c|j}$) for each category. Finally, the corrected quantiles $x^i_{m-p.QM.3}$ are shifted back to estimate the bias-corrected results $x^i_{m-p.QM-VS.}$ using Eq. (4-4).

$$x^i_{m-p.QM.2} = x^i_{m-p.QM.} - \overline{x_{m-p.QM.}} \qquad \textit{(eq. 4-2)}$$

$$x^i_{m-p.QM.3} = x^i_{m-p.QM.2} \cdot \frac{\sigma_{o-c|j}}{\sigma_{m-c.QM.|j}} \quad (j = 1, \dots, 21) \qquad \textit{(eq. 4-3)}$$

$$x^i_{m-p.QM-VS.} = x^i_{m-p.QM.3} + \overline{x_{m-p.QM.}} \qquad \textit{(eq. 4-4)}$$

4.2.3 Rainfall-Runoff-Inundation model

The RRI model is a two-dimensional, distributed hydraulic and hydrological model that is capable of simulating rainfall-runoff and flood inundation simultaneously. The river channel is expressed as a single vector on a single grid cell, which also has a slope. Interaction between a river and the slope is calculated based on different overflowing formulae that vary according to levee height, river and slope water depth. On a slope grid cell, the model can deal flexibly with rainfall-runoff processes and runoff-generation mechanisms; subsurface flow and saturated excess overland flow; vertical infiltration and excess overland flow; and complete surface flow. In addition, groundwater flow can be combined with subsurface flow and

vertical infiltration processes (Sayama *et al.*, 2012). In the RRI model, actual evapotranspiration is calculated by first subtracting surface water, before subtracting additional water from a cumulative infiltration amount estimated by the Green-Ampt model until it meets the potential evapotranspiration. When the value approaches 0, there is no water to evaporate and actual evapotranspiration at that time is less than the potential evapotranspiration.

4.2.4 Application of the RRI model

For application of the RRI model, the Manning's roughness for river and land were set to 0.03 $m^{-1/3}s$ and 0.3 $m^{-1/3}s$, respectively, based on a previous study (Sayama *et al.*, 2012). The soil depth and parameters of the groundwater model, which affect discharge, were adjusted for the calibration period (2001-2006) and used for the validation period (2007-2013). The details of the model parameters and model set up were the same as those of used in the Chapter 3. The performance of the RRI model with GSMaP Reanalysis rainfall input was evaluated based on observed river discharge for the calibration period and the validation period. In addition, the maximum inundation distribution was estimated for four months (December 2016 to March 2017) using the RRI model. The estimates were compared with sentinel satellite images from four flood events (December 6, 2016, and January 23, February 27 and March 24, 2017). The sentinel images were developed using the radar reflection intensity before and after flooding, and the maximum extent of flood inundation during these periods was estimated for comparison with our simulations.

4.3 Results

4.3.1 Comparison of annual and 15-day rainfall patterns and basin-averaged values estimated using the NHRCM with GSMaP data and gauged data

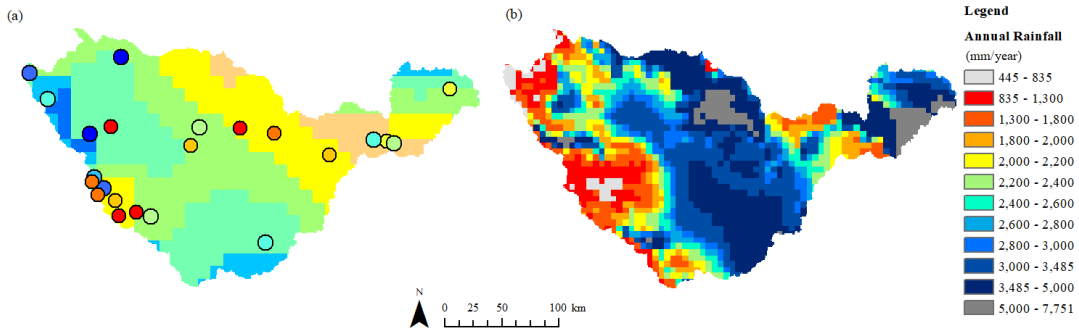

Figure 4-1 Comparison of average annual rainfall maps. (a) GSMaP with gauged rainfall (2001-2013) and (b) NHRCM (1980-2000).

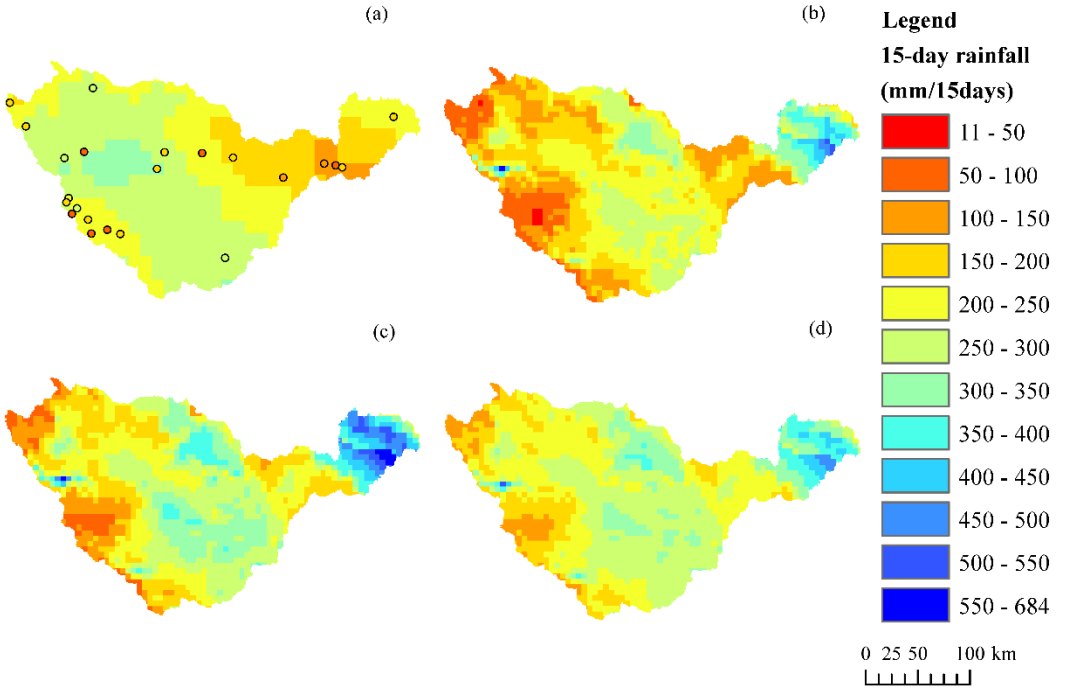

Figure 4-2 Comparison of average annual maximum 15-day rainfall maps. (a) GSMaP with gauged rainfall data (2001-2013), (b) original data, (c) QM bias-corrected data, and (d) QM and VS-corrected NHRCM data. Note that the 15-day gauged rainfall data are estimated at the same time as the annual maximum of the GSMaP data.

I compared the spatial distribution patterns of annual rainfall (Figure 4-1) and annual maximum 15-day rainfall (Figure 4-2) estimated using the NHRCM with reference rainfall data (i.e., GSMaP and gauged data). According to analysis of

cumulative basin-averaged rainfall prior to annual maximum water level (not shown in this dissertation), annual maximum 15-day rainfall is strongly correlated to observed annual maximum water level at Ancol station, shown in Figure 2-1 in Chapter 2. Figure 4-1(a) shows that the GSMaP data indicate high annual rainfall in the northern mountainous ranges of the basin, which corresponds with the gauged rainfall data. The detailed values for the gauged rainfall data and the gridded GSMaP rainfall data are shown in the supplemental materials (at the end of this chapter) as Figure S1 and Table S1. Figure 4-1 (a) also shows that the rainfall patterns in the basin have a diagonal pattern that is parallel with the mountain ranges in the western part of the basin. I can visually distinguish that the rainfall in the basin is divided into several parts, i.e., the mountainous region, the central region, the area next to Jambi city (narrowest part of the basin) and the coastal region. The NHRCM data shown in Figure 4-1 (b), in general, also show a similar division of rainfall patterns. Based on reference rainfall data, rainfall was high in the northern part of the mountain ranges and low in the central part of the mountain ranges. The NHRCM data show consistently lower rainfall in the mountainous areas. The rainfall of the reference data is relatively high in the center of the basin, decreasing towards the west. The rainfall decreases near Jambi city before increasing towards the coastal region. These rainfall patterns can also be observed in the NHRCM data, although the rainfall is higher in the central and eastern parts of the basin (approximately 3500 mm to 7500 mm) compared to the reference data, as shown by the dark grey areas in Figure 4-1 (b). Moreover, the NHRCM data show higher spatial variability in annual rainfall compared to the reference data. Figure 4-2 (a) shows a comparison of the annual maximum 15-day rainfall GSMaP data with gauged data. On the one hand, the GSMaP data have a similar 15-day rainfall pattern as the gauged data in the mountainous regions, the southwestern part of the basin, and downstream areas, such as the area around Jambi city and the coastal area. On the other hand, the GSMaP data tend to show higher rainfall in some parts of mountainous regions in the western part of the basin. The detailed values of gauged rainfall and the gridded rainfall of the GSMaP are shown in the supplemental materials as Figure S2 and Table S2. Figure 4-2 (b) shows that NHRCM data also have higher spatial variability in terms of annual maximum 15-day rainfall compared to reference data (Figure 4-2 (a)), and

it also has higher rainfall amounts (about 350 mm to 552 mm) in areas such as the lowland areas.

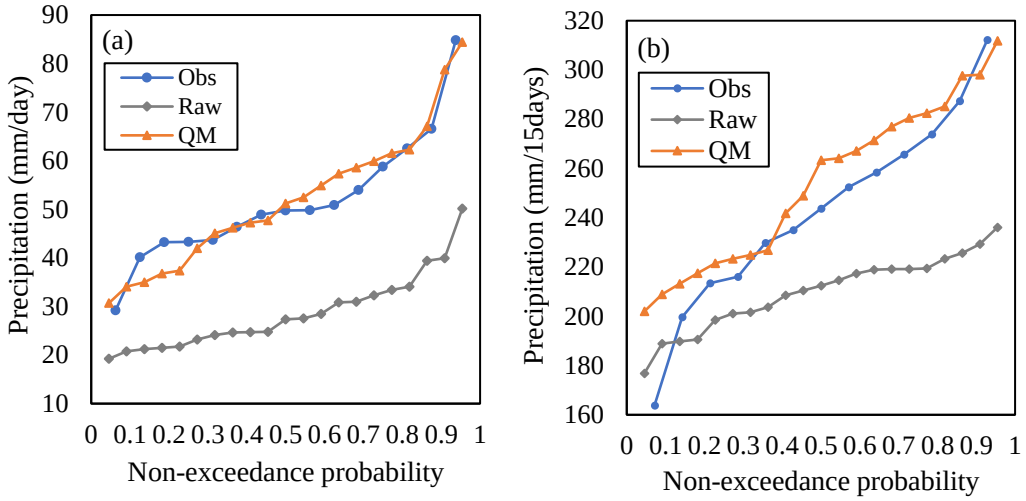

Figure 4-3 Comparison of CDFs of annual maximum cumulative rainfall for different durations. (a) Daily and (b) 15-day rainfall of raw data, QM bias-corrected NHRCM and GSMaP data.

I also compared basin-averaged values of the NHRCM and the reference rainfall data with the gauged data. The average annual rainfall over the basin was estimated to be 2321 mm by GSMaP and 2021 mm by the rain gauges (Yamamoto *et al.*, 2019). The basin-averaged annual rainfall values of the NHRCM are higher than the reference rainfall data, which was 2913 mm. Figure 4-3 shows a comparison of the CDFs of annual maximum daily and 15-day rainfall of raw and QM bias-corrected NHRCM and GSMaP data. The annual maximum basin-averaged daily rainfall of NHRCM data (average 29 mm) is lower than that of GSMaP data (average 51 mm). Figure 4-3 also compares the annual maximum 15-day rainfall (basin average) - cumulative rainfall which is strongly correlated with peak discharge. NHRCM data generally have a lower annual maximum 15-day rainfall (average 206 mm) compared to GSMaP data (average 242 mm).

4.3.2 Effects of bias corrections (QM and QM-VS) on rainfall

In this study, two bias correction methods were compared, i.e., the QM method and the QM-VS method. The annual basin average rainfall was improved from 2,913 mm to 2,316 mm by using the QM method and to 2,328 mm by using QM-VS method, which is closer to the GSMaP value (2,321 mm). Since QM-VS preserves

basin-averaged daily rainfall estimated by QM, both bias correction methods result in similar CDFs for the annual maximum daily and 15-day rainfall.

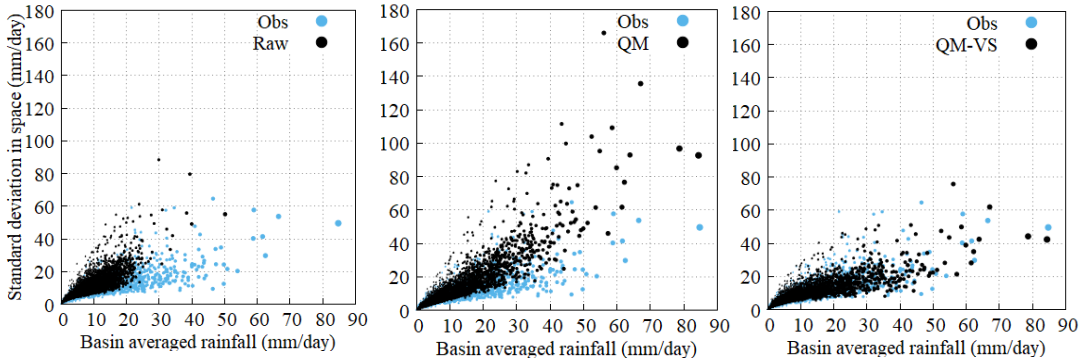

Figure 4-4 Scatter diagram of basin-averaged daily rainfall and corresponding standard deviations in space of (a1) raw NHRCM data, QM bias-corrected (a2) NHRCM data, and QM and VS bias-corrected (a3) NHRCM data.

Despite the similar results in the corrected basin average values, the application of both methods gives different results in the spatial variability of annual rainfall and annual maximum 15-day rainfall. The application of the QM method lowers the spatial variability of annual rainfall, but does not improve the variability for the annual maximum 15-day rainfall. Figure 4-2 (c) shows the results of the QM method after it was applied to the spatial variability observed in the annual maximum 15-day rainfall data. Some areas, including the central parts of the basin and the mountainous areas, showed that rainfall is corrected within the range of 250 mm to 400 mm, which more closely reflects the reference data (about 150 mm to 333 mm). However, the rainfall values obtained in the lowland areas showed much higher values, ranging from 350 mm to 600 mm compared with the reference data (about 140 mm to 250 mm). On the other hand, the application of the QM-VS method results in a lower spatial variability for both annual rainfall and annual maximum 15-day rainfall. Figure 4-2(d) shows the bias correction results obtained using the QM-VS method, which typically has lower spatial variability than the corrections obtained using the QM method. Unlike the results obtained using the QM method, the rainfall values observed in the lowland areas are closer to those of GSMaP. The improvement in spatial variability due to bias correction is confirmed by Figure 4-4, which shows the relationship between spatially averaged daily rainfall and the corresponding spatial standard deviations over the basin. The original NHRCM data have higher spatial

standard deviations compared with the GSMaP data. The application of the QM method results in higher standard deviations, particularly at high rainfall rates; conversely, the application of the QM-VS method successfully improved the standard deviations, making them comparable with the standard deviations obtained using GSMaP.

4.3.3 Effects of bias corrections on the RRI simulation

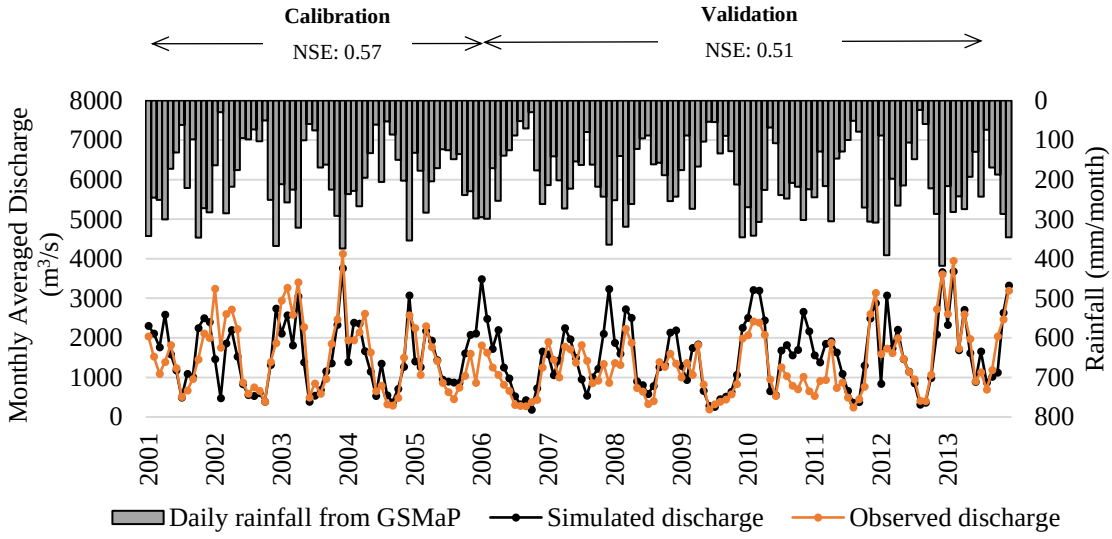

Figure 4-5 Comparison of simulated monthly discharge with observations at Muara Tembesi with basin-averaged daily rainfall from GSMaP.

This study uses the findings in Chapter 3 to run the hydrological model, however, this study uses different calibration and validation periods as shown in Figure 4-5. The model performance is considered satisfactory (Moriasi *et al.*, 2007) in that the Nash-Sutcliffe efficiency (NSE) is 0.57 in the calibration period (2001-2006) and 0.51 in the validation period (2007-2013). The simulated annual maximum inundation extent was compared using composites of inundation extent from Sentinel-1 imageries (from December 2016 to March 2017) (see Chapter 3 Figure 3-6). The simulated inundation pattern agrees well with the satellite image of the Batanghari River and its tributaries.

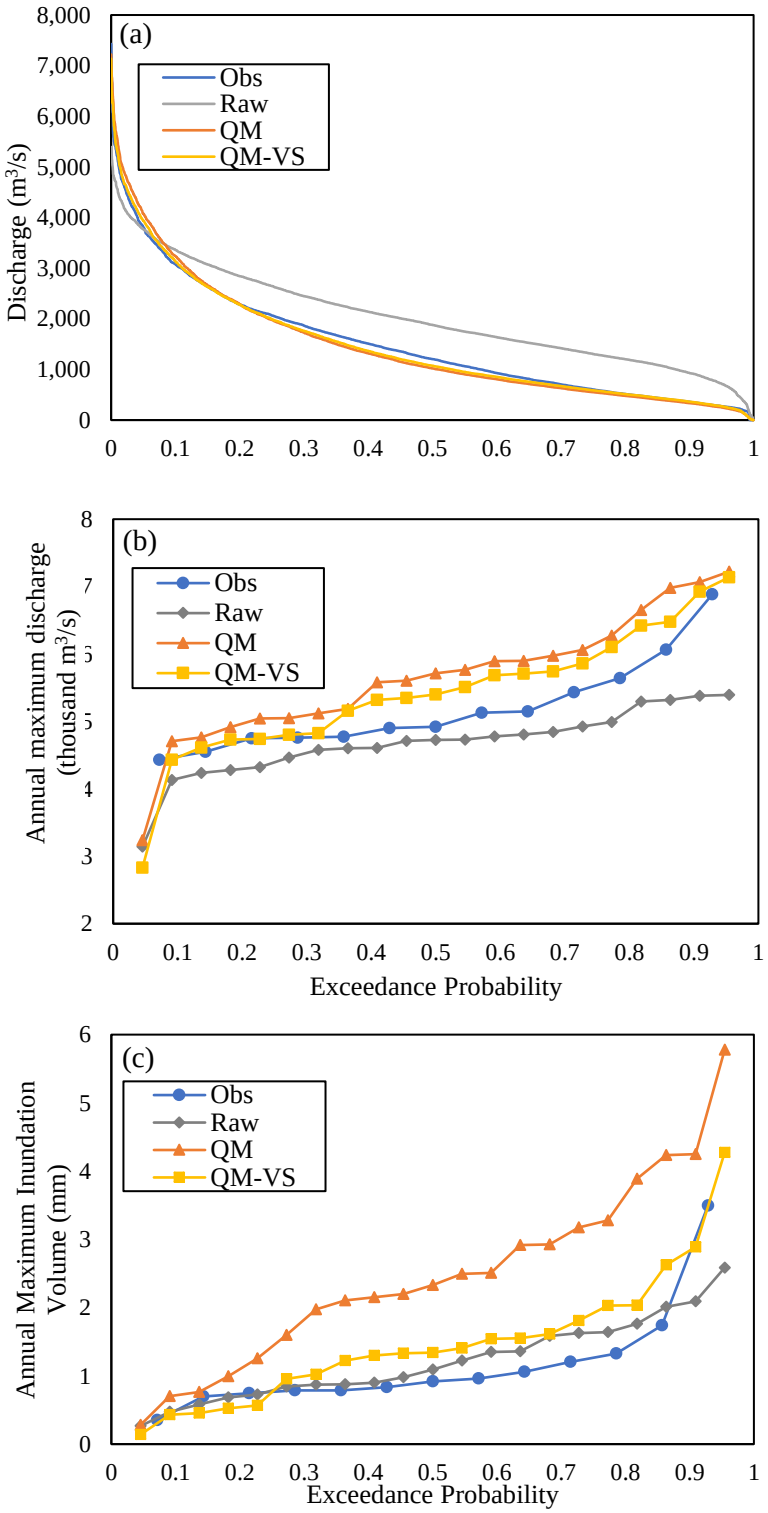

Figure 4-6 *Effects of bias corrections on hydrological variables. Comparison of (a) FDCs, (b) CDFs of annual maximum discharge and (c) CDFs of annual maximum inundation volume of raw data, QM and QM-VS bias-corrected NHRCM data and GSMaP data.*

Figure 4-6 shows the simulated flow duration curves (FDCs), annual maximum discharge, and inundation volume estimated using the original NHRCM, GSMaP, and bias-corrected rainfall data. For the reference discharge and inundation volume (referred to as observed (Obs) in Figure 4-6), this study uses the GSMaP rainfall data as the input for the simulation. The simulated FDC obtained using the original NHRCM data shows that medium flows (Q_{20} to Q_{60}) and low flows (Q_{70} to Q_{99}) are overestimated, and high flows ($Q_{0.1}$ to Q_{10}) are underestimated (Figure 4-6a) ; the ranges of high, medium and low flows are defined based on Mohamoud (2009).

Table 4-1 Evaluation of annual peak discharges and annual maximum inundation volume with a raw/bias corrected NHRCM against those with GSMaP. The notations of bias corrections are "Raw" for non-bias correction, "QM" for quantile mapping and "QM-VS" for quantile mapping and variance scaling. The table show relative root mean square error (RMSE) and relative mean error (RME).

Bias Correction Method	Annual Peak Discharge	Annual Maximum Inundation Volume
Raw	RRMSE: 0.11 RME: -0.094	RRMSE: 0.35 RME: 0.048
QM	RRMSE: 0.11 RME: 0.093	RRMSE: 1.06 RME: 1.13
QM - VS	RRMSE: 0.079 RME: 0.047	RRMSE: 0.39 RME: 0.37

Table 4-1 summarizes the evaluation scores obtained for the annual maximum discharge (Fig 4-6b) and inundation volume (Fig 4-6c) simulated by raw/bias-corrected NHRCM rainfall data, compared with reference data. The score is estimated based on relative root mean square error (RRMSE) and relative mean error (RME). For annual maximum discharges, Table 1 shows that the QM method had nearly the same accuracy, in terms of the RRMSE (0.11), as the original NHRCM. However, compared to the raw data, the accuracy of the QM method was lower for estimating annual maximum inundation volumes. I confirmed that the application of the QM and VS bias correction method improved the RRMSE (0.39) and RME (0.37) compared to the RRMSE (1.06) and RME (1.13) obtained using the QM method alone.

4.3.4 Projection of rainfall, discharge and inundation under future climate conditions

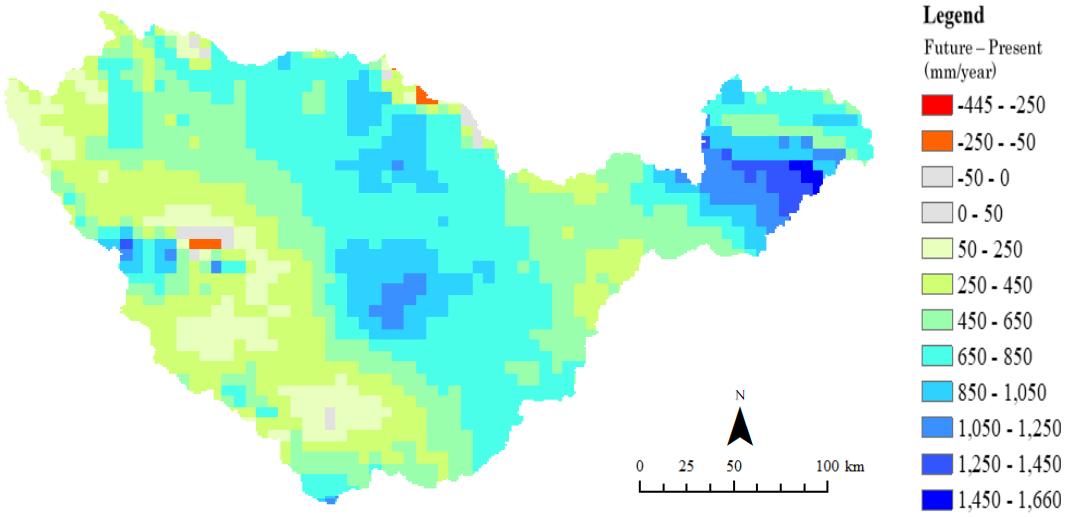

Figure 4-7 *Change of past (1980-2000) and future (2079-2098) bias-corrected NHRCM annual rainfall data.*

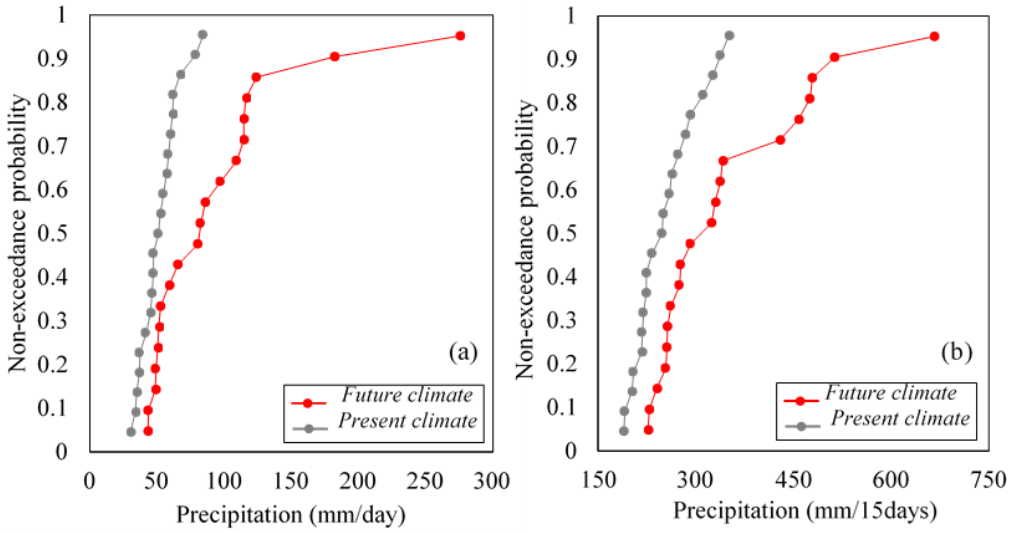

Figure 4-8 *Projected CDF of present and future NHRCM annual maximum (a) daily and (b) 15-day rainfall data.*

Figure 4-7 shows the change in annual rainfall patterns between the present and future climate conditions. In general, annual rainfall will increase throughout the basin. In some areas, including the central or lower parts of the basin, the projected increase in annual rainfall is more than 650 mm. Figure 4-8 shows that the basin-

averaged annual maximum daily and 15-day rainfall will also increase for all return periods. For example, annual maximum daily rainfall corresponding to a 20-year return period (i.e., non-exceedance probability equals 0.95) will increase from 84 mm to 276 mm, and the corresponding increase in annual maximum 15-day rainfall will be from 350 mm to 666 mm.

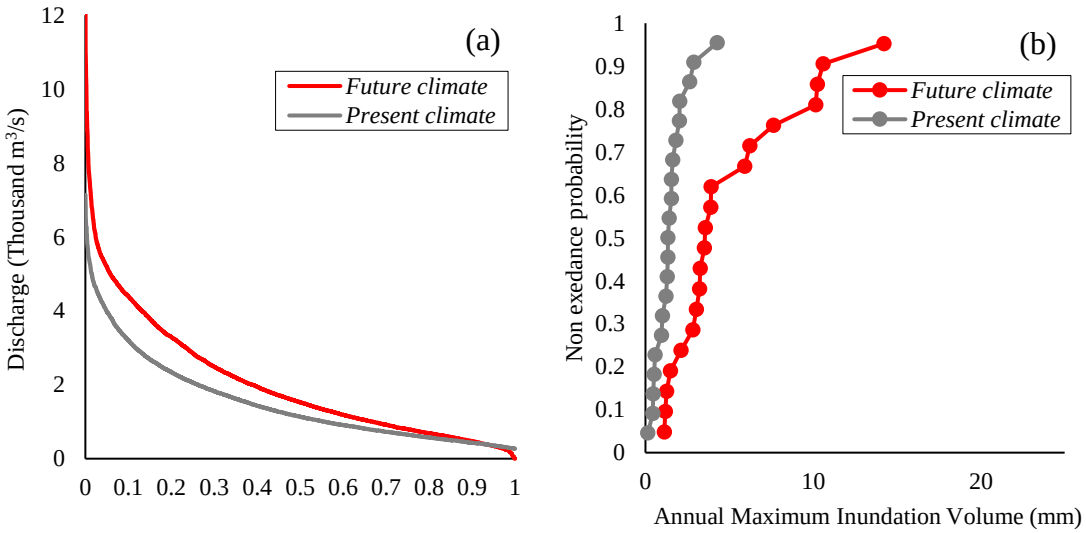

Figure 4-9 Hydrological variables of bias-corrected present and future data. (a) Flow duration curve and (b) CDFs of annual maximum inundation volume.

Figure 4-9 shows the FDC and basin-averaged annual maximum inundation volume under present and future climate conditions. The range of the FDC will increase under the future climate conditions (Figure 4-9 (a)). In particular, the medium flow in the future climate is 2035 m^3/s, which is a 42% increase compared to the present climate. Future flood inundation volume will increase for all return periods (Figure 4-9 (b)). For example, flood inundation volume in the future climate corresponding to a 20-year return period is 14.2 mm, which is an increase of 3.3 times compared to the present (4.3 mm). Annual maximum inundation distributions under future climate conditions (Figure 4-10 (b)) show that flood depth reaches a maximum of 4.8 m, and the total inundated area increases by 2.3 times, compared to that of the present climate. Most of the lowland areas are exposed to flooding and flood depth ranges within 0.4 m and 4.8 m.

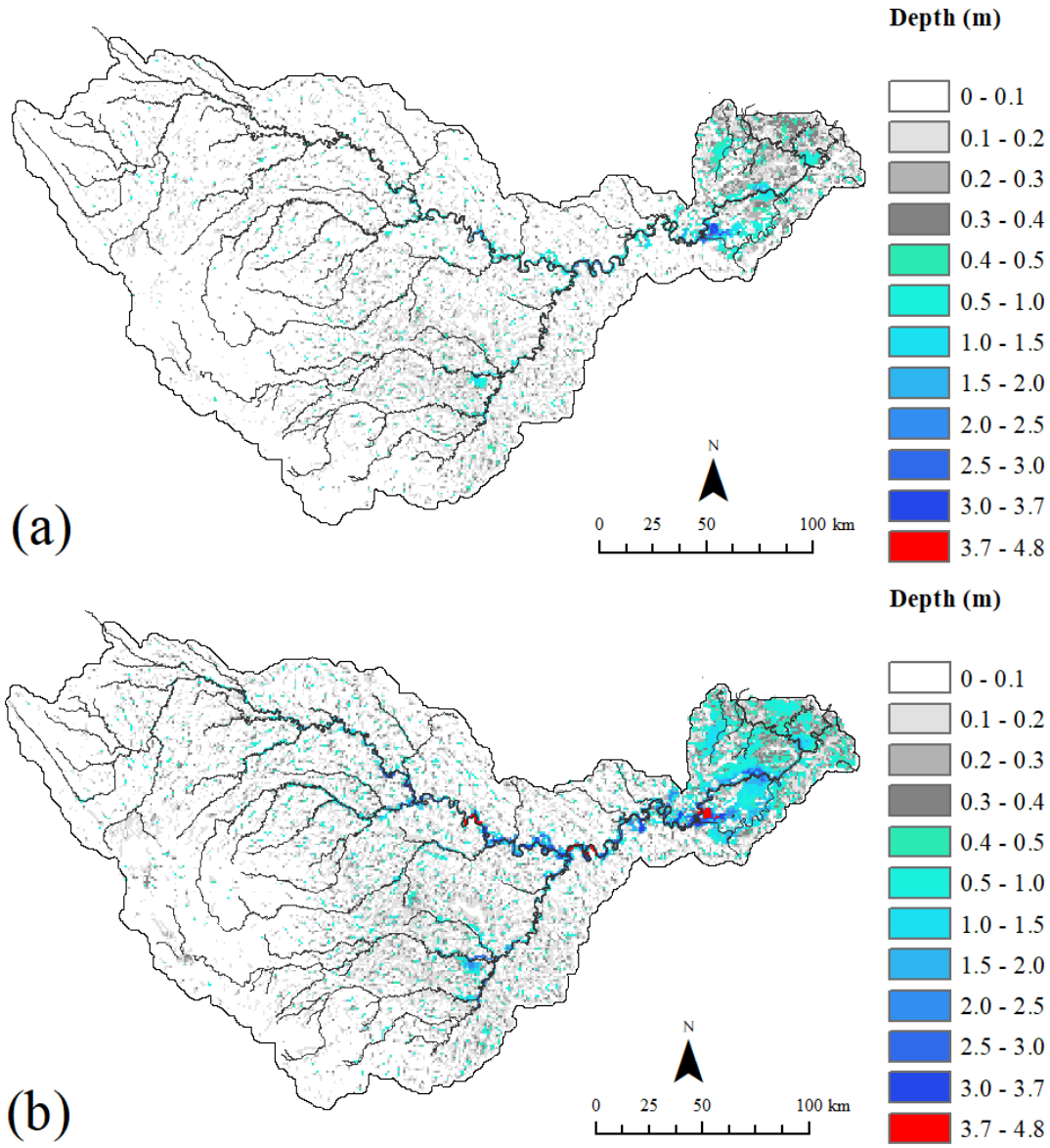

Figure 4-10 Projection of NHRCM annual maximum inundation depth distribution in (a) under present and (b) future climate conditions.

4.4 Discussion

4.4.1 Effects of bias corrections on precipitation, river discharge and inundation volume

In terms of annual rainfall, the NHRCM rainfall data for the Batanghari River Basin are higher than the reference rainfall data (GSMaP and gauged data). In the same target river basin, three RCMs from BMKG also overestimated annual rainfall

(Handoko *et al.*, 2019). This wet bias may be caused by the boundary conditions associated with dynamical downscaling (Gianotti *et al.*, 2012; Cruz *et al.*, 2016).

As in the reference data, the NHRCM (Figure 4-1 (b)) shows similar differences in the rainfall patterns that developed parallel to the mountain range (Figure 4-1 (a)). I find that this is also true for the annual maximum 15-day rainfall of the NHRCM (Figure 4-2 (b)). However, differences between the NHRCM and reference rainfall data were also observed. In the reference rainfall data, rainfall was high only in the northern parts of the mountain ranges, but it was low in the central parts of the mountains. On the other hand, the NHRCM rainfall data showed that rainfall was consistently lower in the mountainous areas. In addition, NHRCM rainfall data showed that rainfall in the central and eastern parts of the basin was higher than that measured using the reference data. Compared to early GCM outputs, the representation of topography and dynamical downscaling have improved the spatial and temporal resolution of rainfall maps in recent years (Schiemann *et al.*, 2014; Johnson *et al.*, 2015). However, our analysis shows that NHRCM exhibits high spatial variability in both annual rainfall and extreme rainfall data. This variability may be attributed to the rain-shadow effect, i.e., rainfall is reduced on the leeward side of a mountain and increased on the windward side (Chang *et al.*, 2005). Previous studies on the NHRCM also reported that this effect may explain some of the rainfall variability observed in the NHRCM data (Kieu-Thi *et al.*, 2016; Cruz *et al.*, 2017). The high variability of NHRCM data may also be one of the reasons for the slightly higher annual maximum inundation volume, which can be affected by spatially and temporally concentrated rainfall (Sayama *et al.*, 2015).

Both of the bias correction methods resulted in similar improvements for basin-averaged rainfall values (annual, annual maximum daily, and annual maximum 15-day), which is expected because the additional VS method does not change the average values, only the variance over space. While the two methods reduced the spatial variability of annual rainfall, they differed in the spatial variability of annual maximum 15-day rainfall; the QM method increased the spatial variability, while the QM-VS method decreased it. The use of equiratio cumulative distribution function matching, as described in the Methods section, may explain why the spatial variability increases after the application of the QM method. Unlike the typical use

case of the QM method, which matches the CDF at a grid scale, this study matches the CDF of basin-averaged daily rainfall values to preserve the spatial pattern of the NHRCM. Nevertheless, the variability observed in the raw NHRCM data changes after the multiplying the ratio uniformly by all rainfall values in the basin; when the ratio <1 the variability is reduced, and when it is >1 the variability is increased. When the basin-averaged value is more than about 12 mm, the ratio is more than 1. The annual 15-day rainfall data are mostly a series of high rainfall values with a ratio >1, which causes the high variability. The additional variance-scaling step in the QM-VS method matches the variance with the reference data, reducing the high variability through application of the equiratio CDF matching.

I also investigated the impact of the bias correction methods on hydrologic simulations. The simulation using the QM bias-corrected rainfall data improved the FDC, as has been demonstrated by several hydrological impact studies that used QM bias-corrected GCM or RCM rainfall as an input for their hydrologic models (Teutschbein *et al.*, 2012; Huang *et al.*, 2014; Lee *et al.*, 2019). However, the simulation using QM bias-corrected rainfall leads to overestimation of extreme variables (annual maximum discharge and annual maximum inundation volume). This may be caused by the higher spatial variability of rainfall, which is attributed to NHRCM rainfall data before bias corrections. On the other hand, QM-VS bias correction improved basin average and spatial variabilities of annual maximum 15-day rainfall, producing reasonable extreme variables over the target river basin.

Although correction of basin-averaged rainfall is not typical, it is considered rational for river discharge simulations. According to Beven and Hornberger (1982), assessing the correct volume of rainfall input from a highly spatially variable pattern is considerably more important than rainfall spatial pattern in predicting storm flow hydrographs. However, bias correction methods that match the CDF of basin-averaged rainfall with equiratio CDF matching may lead to higher spatial variability, particularly for extreme values; therefore, correcting the variance over the space improves the results.

4.4.2 Projection of rainfall, discharge and inundation under future climate conditions

The strongest and most consistent increase in seasonal rainfall broadly follows the Inter Tropical Convergence Zone, which lies above southern Indonesia in December, January and February and northern Indonesia in June, July and August (Christensen *et al.*, 2007). A recent study showed that RCMs, dynamically downscaled from three GCMs over the Western Maritime Continent, consistently projected an increase in rainfall in December, January and February under RCP4.5 and RCP8.5 scenarios in parts of Sumatra Island, and a significant decrease in rainfall during inter-monsoon seasons (Kang *et al.*, 2018).

In this study, annual maximum 15-day rainfall intensity was projected to increase in the Batanghari River Basin under RCP8.5 in the late 21st century. This agrees with IPCC AR5, which reports that the frequency and intensity of extreme rainfall will likely increase over wet tropical regions in the late 21st century (Stocker *et al.*, 2013). Collins *et al.* (2013) also showed that in most parts of Sumatra Island, annual maximum 5-day rainfall increased by more than 20% in the late 21st century under RCP8.5 scenarios. In addition, extreme events, such as 100-year annual maximum daily rainfall, will occur more frequently in the late 21st century under RCP8.5 scenarios (Stocker *et al.*, 2013). The findings of this and previous study (Muis *et al.*, 2015) show that the annual maximum inundation volume is projected to increase in the Batanghari River Basin under RCP8.5 in the late 21st century. Based on Muis (2015), using the global flood model combined with scenarios of 5 GCMs with 4 RCPs also projects an increase in inundation volumes with a 100-year return period in parts of Sumatra Island; however, there is considerable uncertainty across the projections for the Indonesian region. Our results suggested that frequent expansion of the flood inundation area in the downstream area of the basin will damage agricultural crops. According to a global data projection by Fujimori *et al.* (2018), in one of the Shared Socioeconomic Pathways (SSP) (Popp *et al.*, 2017), particularly SSP3, cropland area in the Batanghari River Basin will increase continuously until 2100. Without implementing any adaptation measures, the lowland areas of Sumatra Island are likely to become more agriculturally developed

due to the large potential of unused areas, such as peatlands. The findings suggest that the river basin should be managed by implementing adaptation measures, such as land use regulation of plantations, promoting wetland conservation in order to prevent damage due to flooding under future climate conditions, and protecting the unique environments of tropical peatland areas.

4.4.3 Limitations of the research

In some regions of Asia, shallow orographic rainfall occurs by low-level orographic lifting of maritime air leading to heavy rainfall (Shige *et al.*, 2013, 2016). In humid areas that experience tropical rainfall caused by these shallow orographic rain systems, original satellite rainfall products tend to perform poorly because they employ microwave radar algorithms (Kubota *et al.*, 2007, Shige *et al.*, 2013). To overcome the issue, the ability to distinguish between orographic and non-orographic rainfall systems has been developed and implemented in the GSMaP algorithm ver. 6 (Shige *et al.*, 2013, Yamamoto and Shige 2015). Furthermore, for the GSMaP reanalysis data, the wind dataset from JRA-55 is used to detect orographic rainfall. Nevertheless, according to Nodzu *et al.* (2019), who assessed rainfall in areas with very complex topography (including several mountainous ranges) in northern Vietnam, some bias remains in GSMaP reanalysis ver. 6; specifically, they observed higher (lower) rainfall on the leeward (windward) side of mountains in their case study. In our study, the coverage of the gauged data is still not sufficient to accurately assess the characteristics and potential biases of the GSMaP product. With the limited data, the annual rainfall and 15-day rainfall were overestimated, particularly in the leeward side of the Barisan Mountains. These uncertainties in the reference data may affect the model calibration and other parts of our study.

Our studies shows that the application of QM-VS method to NHRCM basin-averaged daily rainfall data can improve river discharge and flood inundation. However, we also recognized there is still biases of river discharge and flood inundation because there are still biases associated with higher spatial rainfall of NHRCM data. This study suggests future task to improve hydrological simulations by reducing biases related to higher spatial variability of NHRCM data.

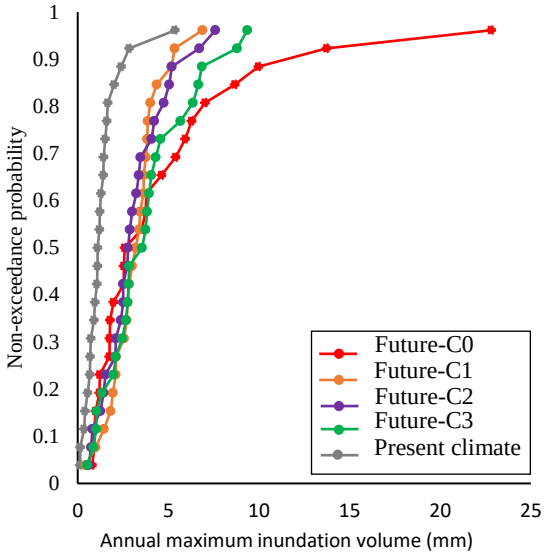

Figure 4-11 Projected CDFs of annual maximum inundation volume based on present and future AGCM data with four SST clusters (C0, C1, C2 and C3).

It is essential that climate change impact studies evaluate the uncertainty of future climate change impacts by comparing results with/without dynamical downscaling using different RCP/SST scenarios and GCMs/RCMs. In this study, a dynamically downscaled product of AGCM under one SST scenario was used due to limitations imposed by computational resources and to retain the focus of this paper on bias correction methods. As for the effects of different SST scenarios, I ran the RRI model based on the original AGCM outputs without dynamical downscaling. Figure 4-11 shows that the increasing rates of flood inundation volume range from 1.9 to 4.8 times without downscaling. Although the result of 3.3 times based on the downscaling was within the range, I realize that there are large uncertainties and that these are dependent upon on SST patterns. In a future study, it will be necessary to conduct more downscaling experiments with different SST patterns.

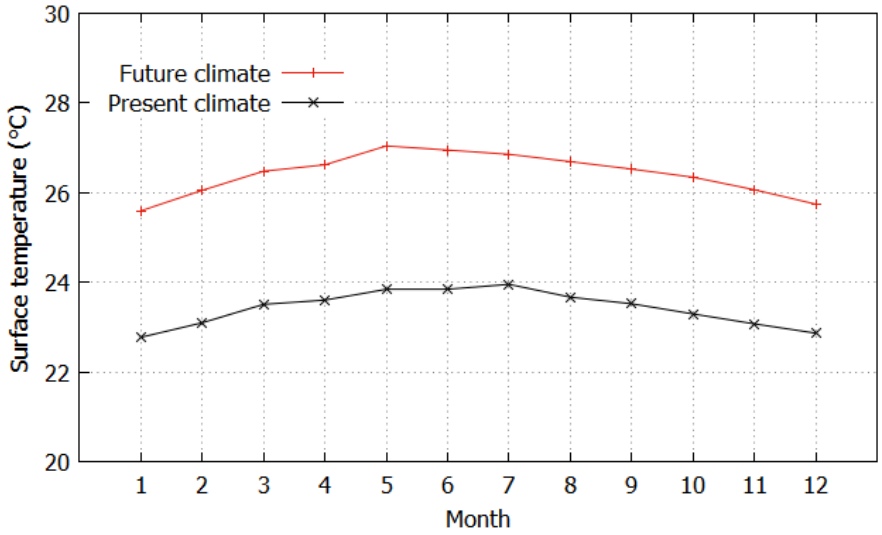

Figure 4-12 Monthly average surface temperatures (basin average) under present climate (1980-2000) and future climate (2079-2098) conditions projected by NHRCM.

To focus on the flood analysis, this study did not consider future temperature changes in the Batanghari River Basin. However, changes in temperature can increase evapotranspiration, which can dry the land and promote fires. According to the NHRCM, average monthly surface temperature (basin average) increases by 3°C in any season in the Batanghari River Basin (see Figure 4-12 showing the basin-averaged monthly temperature for present and future simulations using the original NHRCM). In order to assess the impact on the tropical peatland environment, it is necessary to use future temperature as an input for the hydrologic model.

4.5 Conclusions

This study compared the two bias correction methods, i.e., the QM method and a combination of the QM and VS methods, to examine how each method improves estimates of rainfall patterns, and subsequently, the simulated flood inundation by the RRI model in the Batanghari River Basin, Indonesia. Originally, the dynamically downscaled NHRCM rainfall data showed higher spatial variation in the 15-day rainfall and annual rainfall compared to the reference data. While this does not markedly influence the simulated FDC, it largely overestimated the extreme values, such as the annual maximum flood inundation volume. The combination of QM and

VS methods successfully decreased the rainfall spatial variability and improved the estimations of the FDCs and the extreme values.

Our analysis showed that the projected change of flood inundation is significant, particularly in the lowland areas of Sumatra Island. Annual maximum flood inundation volume corresponding to a 20-year return period would increase by 3.3 times. The annual maximum inundation map under a future climate scenario showed that the inundation depths would increase and the inundated area would expand in tropical peatland areas. These results suggest the need to consider future climate change scenarios for river basin management, particularly to reduce the risk of flood damage and to sustainably maintain the unique ecosystem of tropical peatlands.

4.6 Supplemental material

Table S1 *Comparison between annual rainfall values of gauged rainfall and gridded rainfall from GSMaP.*

ID	Gauge	GSMaP
1	2827.05	2493.4
2	2436	2797.14
3	3309.49	2594.31
4	1634.07	2431.5
5	2673.16	2431.5
6	1364.49	2049.78
7	2826.69	2085.4
8	1179.72	2594.1
9	1840.27	2048.03
10	834.66	2159.17
11	3484.96	2414.97
12	1088.97	2232.81
13	2218.7	2324.82
14	1905.16	2383.85
15	2238.35	2318.16
16	1142.25	2188.25
17	2402.12	2525.63
18	1404.38	2101.55
19	1885.49	2063.28
20	2509.59	1929.23
21	2047.38	1910.44
22	2392.44	1916.55
23	2160.41	2377.85

Table S2 *Comparison between 15-day rainfall values of gauged rainfall and annual maximum 15-day rainfall of gridded rainfall from GSMaP.*

ID	Gauge	GSMaP
1	190.23	211.05
2	178.63	268.3
3	311.71	287.02
4	156.62	252.2
5	219.34	252.2
6	99.88	-9999
7	277.07	224.7
8	97.95	319.57
9	180	211.61
10	93.42	207.8
11	411.33	269.56
12	93.62	226.91
13	176.1	235.07
14	195.92	300.81
15	179.35	271.96
16	75.72	213.99
17	254.32	272.7
18	158.04	186.7
19	149.32	191.71
20	112.4	147.77
21	87.01	139.66
22	169.92	140.36
23	165.46	213.73

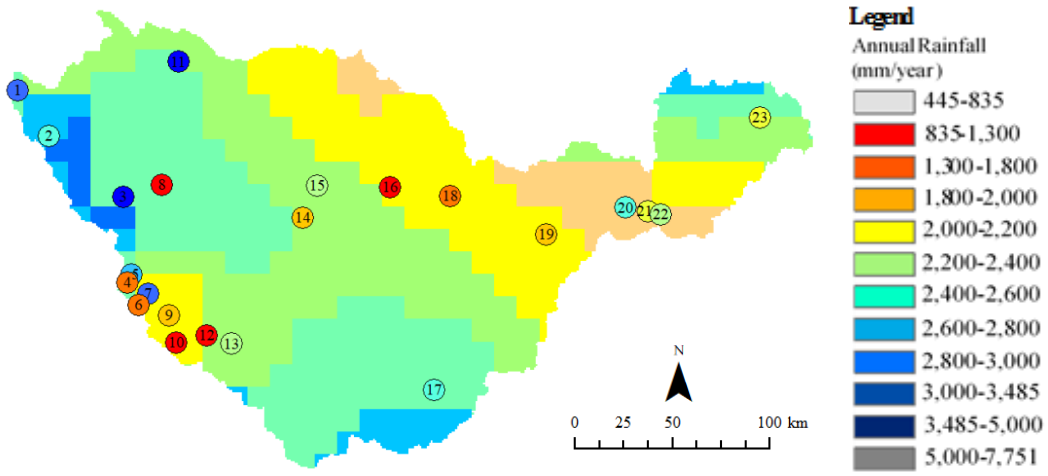

Figure S1 Identical image and legend as for Figure 2a, but the station numbers are shown.

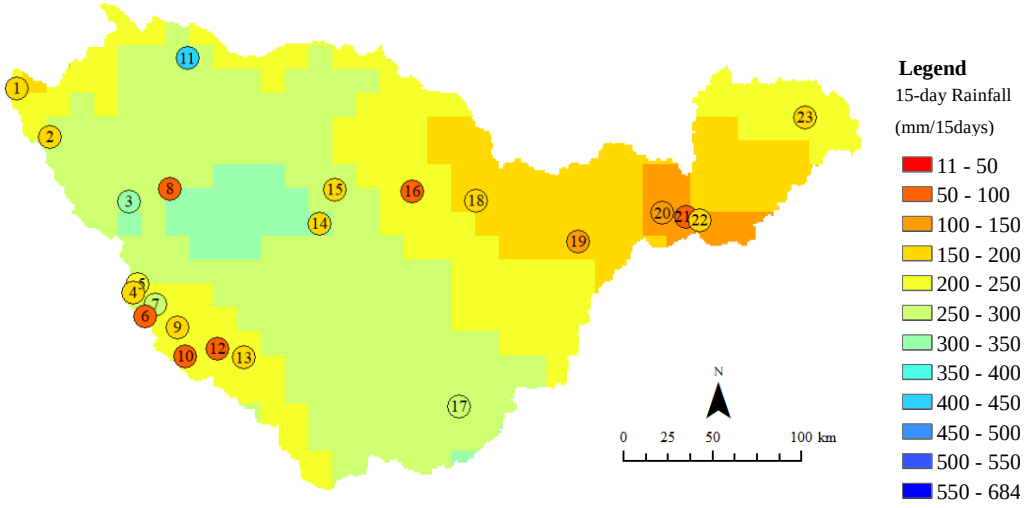

Figure S2 Identical image and legend as for Figure 3a, but the station numbers are shown.

References

Beven KJ, Hornberger GM (1982) Assessing the effect of spatial pattern of precipitation in modeling stream flow hydrographs. *J Am Water Resour Assoc* 18(5):823-829

Champeaux JL, Masson V, Chauvin F (2005) ECOCLIMAP: a global database of land surface parameters at 1 km resolution. *Meteorol Appl* 12(1):29-32. DOI:10.1017/S1350482705001519

Chang CP, Wang Z, Mcbride J, Liu CH (2005) Annual cycle of Southeast Asia—Maritime Continent rainfall and the asymmetric monsoon transition. *J Climate* 18:287-301. DOI:10.1175/JCLI-3257.1.

Chang JH, Lau LS (1993) A definition of the humid tropics. In: Bonell M, Hufschmidt MM, Gladwell JS (eds) *Hydrology and Water Management in the Humid Tropics: Hydrological research issues and strategies for water management*, Cambridge University Press, UNESCO, Cambridge, pp 571-574.

Christensen JH, Hewitson B, Busuioc A, Chen A, Gao X, Held I, Jones R, Kolli RK, Kwon W-T, Laprise R, Magaña Rueda V, Mearns L, Menéndez CG, Räisänen J, Rinke A, Sarr A, Whetton P (2007): Regional Climate Projections. Solomon S, Qin D, Manning M, Chen Z, Marquis M, Averyt KB, Tignor M and Miller HL (eds.) In: *Climate Change 2007: The Physical Science Basis. Contribution of Working Group I to the Fourth Assessment Report of the Intergovernmental Panel on Climate Change.* Cambridge University Press, Cambridge, United Kingdom and New York, NY, USA.

Christensen JH, Boberg F, Christensen OB, Lucas-Picher P (2008) On the need for bias correction of regional climate change projections of temperature and precipitation. *Geophys Res Lett* 35 (20):L20709. DOI:10.1029/2008GL035694

Collins M, Knutti R, Arblaster J, Dufresne JL, Fichefet T, Friedlingstein P, Gao X, Gutowski WJ, Johns T, Krinner G, Shongwe M, Tebaldi C, Weaver AJ, Wehner M (2013) Long-term Climate Change: Projections, Commitments and Irreversibility. In: Stocker TF, Qin D, Plattner G-K, Tignor MMB, Allen SK, Boschung J, Nauels A, Xia Y, Bex V and Midgley PM (eds.) *Climate Change 2013: The Physical Science Basis. Contribution of Working Group I to the Fifth Assessment Report of the Intergovernmental Panel on Climate Change.* Cambridge University Press, Cambridge, United Kingdom and New York, NY, USA

Cruz FT, Sasaki H, Narisma GT (2016) Assessing the sensitivity of the Non-Hydrostatic Regional Climate Model to Boundary Conditions and Convective Schemes over the Philippines. *J Meteorol Soc Jpn* 94(A):165-179. DOI:10.2151/jmsj.2015-059

Cruz FT, Sasaki H (2017) Simulation of present climate over Southeast Asia using the non-hydrostatic regional climate model. *SOLA* 13:13-18. DOI:10.2151/sola.2017-003

Emam AR, Mishra BK, Kumar P, Masago Y, Fukushi K (2016) Impact assessment of climate and land-use changes on flooding behavior in the upper Ciliwung River, Jakarta, Indonesia. *MDPI Water* 8(12):559. DOI:10.3390/w8120559

Endo H, Kitoh A, Ose T, Mizuta R, Kusunoki S (2012) Future changes and uncertainties in Asian precipitation simulated by multiphysics and multi–sea surface temperature ensemble experiments with high-resolution Meteorological Research Institute atmospheric general circulation models (MRI-AGCMs). *J Geophys Res* 117:D16118. DOI:10.1029/2012JD017874

Fujimori S, Hasegawa T, Ito A, Takahashi K, Masui T (2018) Gridded emissions and land-use data for 2005-2100 under diverse socioeconomic and

climate mitigation scenarios. *Sci Data* 5:13. DOI:10.1038/sdata.2018.210

Gianotti RL, Zhang D, Eltahir EAB (2012) Assessment of the regional climate model version 3 over the maritime continent using different cumulus parameterization and land surface schemes. *J Climate* 25:638-656. DOI:10.1175/JCLI-D-11-00025.1

Handoko U, Boer R, Aldrian E, Latifah AL, Dasanto BD, Apip A, Misnawati M (2019) Comparison performance of the multi-Regional Climate Model (RCM) in simulating rainfall and air temperature in Batanghari watershed. *Aceh Int J Sci Technol* 8(2):52-67. DOI: 10.13170/aijst.8.2.12340

Harada Y, Kamahori H, Kobayashi C, Endo H, Kobayashi S, Ota Y, Onda H, Onogi K, Miyaoka K, Takahashi K (2016) The JRA-55 reanalysis: representation of atmospheric circulation and climate variability. *J Meteor Soc Japan* 94:269-302. DOI:10.2151/jmsj.2016-015

Hijioka Y, Lin E, Pereira JJ, Corlett RT, Cui X, Insarov GE, Lasco R, Lindgren E, Surjan A (2014) Asia. In: Barros VR, Field CB, Dokken DJ, Mastrandrea MD, Mach KJ, Bilir TE, Chatterjee M, Ebi KL, Estrada YO, Genova RC, Girma B, Kissel ES, Levy AN, MacCracken S, Mastrandrea PR, White LL (eds.) *Climate Change 2014: Impacts, Adaptation, and Vulnerability. Part B: Regional Aspects. Contribution of Working Group II to the Fifth Assessment Report of the Intergovernmental Panel on Climate Change.* Cambridge University Press, Cambridge, United Kingdom and New York, NY, USA, pp 1327-1370

Hirabayashi Y, Mahendran R, Koirala S, Konoshima L, Yamazaki D, Watanabe S, Kim H, Kanae S (2013) Global flood risk under climate change. *Nature Clim Change* 3:816-821. DOI:10.1038/nclimate1911

Hirai M, Sakashita T, Kitagawa H, Tsuyuki T (2007) Development and validation of a new land surface model for JMA's operational global model using the CEOP observation dataset. *J Meteor Soc Japan* 85:1-24. DOI:10.2151/jmsj.85A.1

Hertwig E, Storch JSV, Handorf D, Dethloff K, Fast I, Krismer T (2015) Effect of horizontal resolution on ECHAM6-AMIP performance. *Clim Dyn* 45:185-211. DOI:10.1007/s00382-014-2396-x

Hirano T, Segah H, Kusin K, Limin S, Takahashi H, Osaki M (2012) Effects of disturbances on the carbon balance of tropical peat swamp forests. *Glob Chang Biol* 18(11):3410-3422. DOI: 10.1111/j.1365-2486.2012.02793.x

Huang S, Krysanova V, Hattermann FF (2014) Does bias correction increase reliability of flood projections under climate change? A case study of large rivers in Germany. *Int J Climatol* 34:3780-3800. DOI: 10.1002/joc.3945

Iwami Y, Hasegawa A, Miyamoto M, Kudo S, Yamazaki Y, Ushiyama T, Koike T (2017) Comparative study on climate change impact on precipitation and floods in the Asian river basins. *Hydrol Res Lett* 11(1):24-30. DOI:10.3178/hrl.11.24

Johnson SJ, Levine RC, Turner AG, Martin GM, Woolnough SJ, Schiemann R, Mizielinski MS, Roberts MJ, Vidale PL, Demory ME, Strachan J (2015) The resolution sensitivity of the South Asian monsoon and Indo-Pacific in a global 0.35°AGCM. *Clim Dyn* 46:807-831. DOI:10.1007/s00382-015-2614-1

Juneng L, Tangan F, Chung JX, Ngai ST, Tay TW, Narisma G, Cruz F, Phan-Van T, Ngo-Duc T, Santisirisomboon J, Singhruck P, Gunawan D, Aldrian E (2016) Sensitivity of Southeast Asia rainfall simulations to cumulus and

air-sea flux parameterizations in RegCM4. *Clim Res* 69:59-77. DOI:10.3354/cr01386

Kain JS, Fritsch JM (1993) Convective parameterization for mesoscale models: The Kain–Fritsch scheme. In: Emanuel KA, Raymond DJ (eds.) *The Representation of Cumulus Convection in Numerical Models. Meteorological Monographs.* American Meteorological Society, Boston, MA, pp 165-170. DOI:10.1007/978-1-935704-13-3_16

Kang S, Im ES, Eltahir EAB (2018) Future climate change enhances rainfall seasonality in a regional model of western Maritime Continent. *Clim Dyn* 52:747-764. DOI:10.1007/s00382-018-4164-9

Kieu-Thi X, Vu-Thanh H, Nguyen-Minh T, LE D, Nguyen-Manh Linh, Takayanu I, Sasaki H, Kitoh A (2016) Rainfall and tropical cyclone activity over Vietnam simulated and projected by the Non-Hydrostatic Regional Climate Model – NHRCM. *J Meteor Soc Japan* 94:135-150. DOI:10.2151/jmsj.2015-057

Kubota T, Shige S, Hashizume H, Aonashi K, Takahashi N, Seto S, Hirose M, Takayabu YN, Nakagawa K, Iwanami K, Ushio T, Kachi M, Okamoto K (2007) Global precipitation map using satellite-borne microwave radiometers by the GSMaP Project: Production and validation. *IEEE Trans Geosci Remote Sens* 45(7):2259-2275. DOI:10.1109/tgrs.2007.895337

Lee MH, Im ES, Bae DH (2019) Impact of the spatial variability of daily precipitation on hydrological projections: A comparison of GCM- and RCM- driven cases in the Han River basin, Korea. *Hydrological Processes* 33(16):2240-2257. DOI:10.1002/hyp.13469

Marhaento H, Booij MJ, Hoekstra AY (2018) Hydrological response to future land-use change and climate change in a tropical catchment. *Hydrol Sci J* 63(9):1368-1385. DOI:10.1080/02626667.2018.1511054

Mizuta R, Yoshimura H, Murakami H, Matsueda M, Endo H, Ose T, Kamiguchi K, Hosaka M, Sugi M, Yukimoto S, Kusunoki S, Kitoh A (2012) Climate simulations using MRI-AGCM3.2 with 20-km grid. *J Meteor Soc Japan* 90:233-258. DOI:10.2151/jmsj.2012-A12

Mohamoud YM (2008) Prediction of daily flow duration curves and streamflow for ungauged catchments using regional flow duration curves. *Hydrol Sci J* 53(4):706-724. DOI:10.1623/hysj.53.4.706

Moriasi DN, Arnold JG, Van Liew MW, Bingner RL, Harmel RD, Veith TL (2007) Model evaluation guidelines for systematic quantification of accuracy in watershed simulations. *Trans ASABE* 50(3):885-900. DOI:10.13031/2013.23153

Muis S, Güneralp B, Jongman B, Aerts JCJH, Ward PJ (2015) Flood risk and adaptation strategies under climate change and urban expansion: a probabilistic analysis using global data *Sci. Total Environ* 538:445-457. DOI:10.1016/j.scitotenv.2015.08.068

Neale R, Slingo J (2003) The maritime continent and its role in the global climate: a GCM study. *J Climate* 16:834-848. DOI:10.1175/1520-0442(2003)016<0834:TMCAIR>2.0.CO;2

Nodzu MI, Matsumoto J, Trinh-Tuan L, Ngo-Duc T (2019) Precipitation estimation performance by Global Satellite Mapping and its dependence on wind over northern Vietnam. *Prog Earth Planet Sci* 6:58 DOI:10.1186/s40645-019-0296-8

Popp A, Calvin K, Fujimori S, Havlik P, Humpenöder F, Stehfest E, Bodirsky BL, Dietrich JP, Doelmann JC, Gusti M, Hasegawa T, Kyle P, Obersteiner M, Tabeau A, Takahashi K, Valin H, Waldhoff S, Weindl I, Wise M, Kriegler E, Lotze-Campen H, Fricko O, Riahi K, Vuuren Dv (2017). Land-use futures in the shared socio-economic pathways. *Global Environ Change* 42:331-345DOI:10.1016/j.gloenvcha.2016.10.002

Ramage CS (1968) Role of a tropical “maritime continent” in the atmospheric circulation. *Mon Wea Rev* 96(6):365-370. DOI:10.1175/1520-0493(1968)096<0365:ROATMC>2.0.CO;2

Rashid HA, Hirst AC (2017) Mechanisms of improved rainfall simulation over the Maritime Continent due to increased horizontal resolution in an AGCM. *Clim Dyn* 49:1747-1764. DOI: 10.1007/s00382-016-3413-z

Ratna SB, Ratnam JV, Behera SK, Tangang FT, Yamagata T (2017) Validation of the WRF regional climate model over the subregions of Southeast Asia: climatology and interannual variability. *Clim Res* 71:263-280. DOI:10.3354/cr-1445

Saito K, Fujita T, Yamada Y, Ishida J, Kumagai Y, Aranami K, Ohmori S, Nagasawa R, Kumagai S, Muroi C, Kato T, Eito H, Yamazaki Y (2006) The operational JMA nonhydrostatic mesoscale model. *Mon Wea Rev* 134:1266-1298. DOI:10.1175/MWR3120.1

Sayama T, Ozawa G, Kawakami T, Nabesaka S, Fukami K (2012) Rainfall-Runoff-Inundation analysis of the 2010 Pakistan flood in the Kabul River Basin. *Hydrol Sci J* 57(2):298-312. DOI:10.1080/02626667.2011.644245

Sayama T, Tatebe Y, Iwami Y, Tanaka S (2015) Hydrologic sensitivity of flood runoff and inundation: 2011 Thailand floods in the Chao Phraya River basin. *Nat. Hazards Earth Syst Sci* 15:1617-1630. DOI:10.5194/nhess-15-1617-2015

Sasaki H, Kurihara K, Takayabu I, Uchiyama T (2008) Preliminary experiments of reproducing the present climate using the Non-hydrostatic Regional Climate Model. *SOLA* 4:25-28. DOI:10.2151/sola.2011-044

Schiemann R, Demory ME, Mizielinski MS, Roberts MJ, Shaffrey LC, Strachan J, Vidale PL (2014) The sensitivity of the tropical circulation and maritime continent rainfall to climate model resolution. *Clim Dyn* 42:2455-2468. DOI:10.1007/s00382-013-1997-0

Shige S, Kida S, Ashiwake H, Kubota T, Aonashi K (2013) Improvement of TMI rain retrievals in mountainous areas. *J Appl Meteor Climatol* 52:242-254. DOI:10.1175/jamc-d-12-074.1

Shige S, Kummerow CD (2016) Precipitation-top heights of heavy orographic rainfall in the Asian monsoon region. *J Atmos Sci* 73:3009-3024. DOI:10.1175/JAS-D-15-0271.1

Shimada U, Kazumasa A (2017) Tropical cyclone intensity change and axisymmetricity deduced from GSMaP. *Mon Wea Rev* 145:1003-1017. DOI:10.1175/MWR-D-16-0244.1

Stocker TF, Qin D, Plattner GK, Alexander LV, Allen SK, Bindoff NL, Bréon FM, Church JA, Cubasch U, Emori S, Forster P, Friedlingstein P, Gillett N, Gregory JM, Hartmann DL, Jansen E, Kirtman B, Knutti R, Krishna KK, Lemke P, Marotzke J, Masson-Delmotte V, Meehl GA, Mokhov II, Piao S, Ramaswamy V, Randall D, Rhein M, Rojas M, Sabine C, Shindell D, Talley LD, Vaughan DG and Xie S-P (2013) Technical Summary. In: Stocker TF, Qin D, Plattner G-K, Tignor MMB, Allen SK, Boschung J, Nauels A, Xia Y, Bex V and Midgley PM (eds.*) Climate Change 2013: The Physical Science Basis. Contribution of Working Group I to the Fifth Assessment Report of the Intergovernmental Panel on Climate Change*. Cambridge University Press, Cambridge, United Kingdom and New York, NY, USA

Takahashi H, Usup A, Hayasaka H, Limin SH (2003) Estimation of ground water level in a peat swamp forest as an Index of peat/forest fire. In: Osaki M, Iwakuma T, Kohyama T, Hatano R, Yonebayashi K, Tachibana H, Takahashi H, Shinano T, Higashi S, Simbolon H, Tuah SJ, Wijaya H, Limin SH (eds) *Proceeding of the International Symposium of Land Management and Biodiversity in Southeast Asia, Bali, 2002*

Teutschbein C, Seibert J (2012) Bias correction of regional climate model simulations for hydrological climate-change impact studies: Review and

evaluation of different methods. *J Hydrol* 456-457:12-29. DOI:10.1016/j.jhydrol.2012.05.052

Ulate M, Dudhia J, Zhang C (2014) Sensitivity of the water cycle over the Indian Ocean and Maritime Continent to parameterized physics in a regional model. *J Adv Model Earth Syst* 6(4):1095-1120. DOI:10.1002/2014MS000313

Wang L, Chen W (2014) Equiratio cumulative distribution function matching as an improvement to the equidistant approach in bias correction of rainfall. *Atmos Sci Let* 15:1-6. DOI:10.1002/asl2.454

Weedon GP, Balsamo G, Bellouin N, Gomes S, Best MJ, Viterbo P (2014) The WFDEI meteorological forcing data set: WATCH Forcing Data methodology applied to ERA-Interim reanalysis data. *Water Resour Res* 50:7505-7514. DOIi:10.1002/2014WR015638

Yamamoto MK, Shige S (2015) Implementation of an orographic/nonorographic rainfall classification scheme in the GSMaP algorithm for microwave radiometers. *Atmos Res* 163:36-47. https://doi.org/10.1016/j.atmosres.2014.07.024

Yamamoto K, Sayama T, Apip, Takara K (2019) Applicability of Rainfall-Runoff-Inundation model in a humid tropical river basin. *J Japan Soc Civil Eng* 75(2):I_253-I_258. (in Japanese)

Yamamoto EMS, Sayama T, Yamamoto K, Apip (2020) Comparison of runoff generation methods for land use impact assessment using the SWAT model in humid tropics. *Hydrol Res Lett* 14(2):81-88

Chapter 5 Comparison between Climate Change and Land Use Change Impacts on Flood Inundation

5.1 Introduction

Tropical forests have been cleared and utilized for human activity. Indonesia experienced fastest deforestation rate in two decades (Hensen *et al.*, 2013) and Sumatra island is evident due to intensive forest clearing that shows 70 % of 1990 forest area has been converted between 1990 and 2010 (Margono *et al.*, 2012). Large scale commercial logging and agro-industrial development are main drivers of forest loss between 1990 and 2010 (Margono *et al.*, 2012). The global demand of the oil palm is projected to increase constantly up to 2050 following the historical expansion of 1990 to 2010 (Harris *et al.*, 2013). Unless there is an improvement in oil palm production (yield/area), to meet the demand, deforestation will continue in Indonesia that is currently largest palm oil producer in the world.

Land use and climate change are key factors that affect hydrological cycle, causing flood hazard. Observations in tropical watershed revealed that the forests clearing decreases annual evapotranspiration and increases amount of river flows (Kuraji *et al.*, 1996). The rapid expansion of oil palm plantation requires forests clearing and use of machine, leading to change in local hydrological cycle. In particular, the soil compaction in oil palm plantation degrades surface soil and leads to reducing storage and soil infiltrability (Comte *et al.*, 2012; Jennifer *et al.*, 2016). The large-scale land conversion such as oil palm plantation can affect the hydrological cycle at catchment scale and increase flood risks (Tarigan *et al.*, 2016). Climate change increases the frequency and intensity of rainfall in wet tropics including humid tropical regions. The increase of rainfall can increase frequency and magnitude of flood hazard.

The distributed hydrological model is a useful tool to understand the response of future land use and climate change. Soil Water Assessment Tool (SWAT) model (Arnold *et al.*, 1998; 2012), HEC-HMS (Feldman *et al.*, 2000) and MIKE-SHE model (Farjad *et al.*, 2017) were widely used to assess the land use change impact

on hydrology. These models also assess the effect of climate change on hydrology. Among those models, there are many applications of SWAT model in Indonesia. However, the application of these models did not consider inundation phenomena explicitly extent, particularly, for land use impact assessment.

Rainfall-Runoff-Inundation model is one of integrated physical models of rainfall-runoff process and inundation process at basin scale. The model has been used for assessing single effect of climate change on flood inundation in a large river basin in Asia (Kudo *et al.*, 2015; Ushiyama *et al.*, 2016; Iwami *et al.*, 2017). To date, the model has not yet used for land use impact assessment.

The objective of this study is to understand the response of climate and land use change and compared the effects on flood inundation. Batanghari river basin in Sumatra island is selected. This study applies RRI model under future land use and climate scenario. To discuss response of land use and climate change among different models, this study compares the results of SWAT model with the RRI under the same future scenarios.

5.2 Methods

5.2.1 Dataset

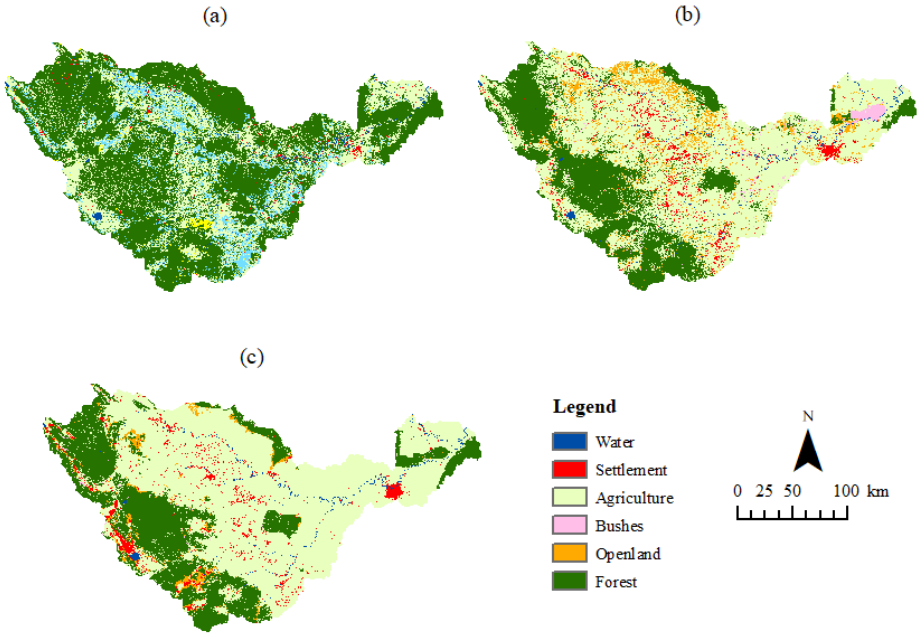

Figure 5-1 Historical, present and future land use map. The year of the map is (a) 1990, (b) 2015 and (c) 2040.

Past and present land use maps were classified from four landsat images from 1990, 1997. 2005 and 2015 with resolution of 30 m (Utami *et al.*, 2017). Future land use map in 2040 was estimated using dynamic Conversion of Land Use and its Effect (CLUE) model (Utami *et al.*, 2017). The dynamic CLUE model was capable of predicting future land use based on past demands of land use data. The future demand in 2040 was obtained by linearly extrapolating land areas estimated using 4 historical landsat imagery (1990, 1999, 2005 and 2015). Figure 5-1 shows 1990, 2015 and 2040 land use maps. The agricultural expansion is a main change of land uses from 1990 to 2015. The agricultural area is estimated to increase from 28 % in 1990 to 59 % in 2015 and will continuously increase to 65 % by 2040. Settlement area has increased by three times from 1990 to 2015 and will continue to increase by 4 times compared to 1990 in 2040. The expansion of agricultural is mainly offset by loss of forests and bushes between 1990 and 2040.

This study uses rainfall data downscaled by the Non-Hydrostatic Regional Climate Model (NHRCM) with a spatial resolution of 5 km (Sasaki *et al.*, 2008; Cruz *et al.*, 2017). Downscaling was performed for the Batanghari river basin in Sumatra Island (-3.32°S – 0.41°S; 99.65°E – 105.25°E). Climate change effects were projected by adding changes of ensemble mean Sea Surface Temperature (SST) under the Representative Concentration Pathways 8.5 scenario (RCP8.5) to present SST patterns (Endo *et al.*, 2012). The simulation period is 21 years of present climate (1980 – 2000) and for 20 years of future climate (2079 – 2098). The NHRCM does not take account into a feedback of deforestation to climate system in the study area.

5.2.2 Simulation condition for future land use and climate impact assessment

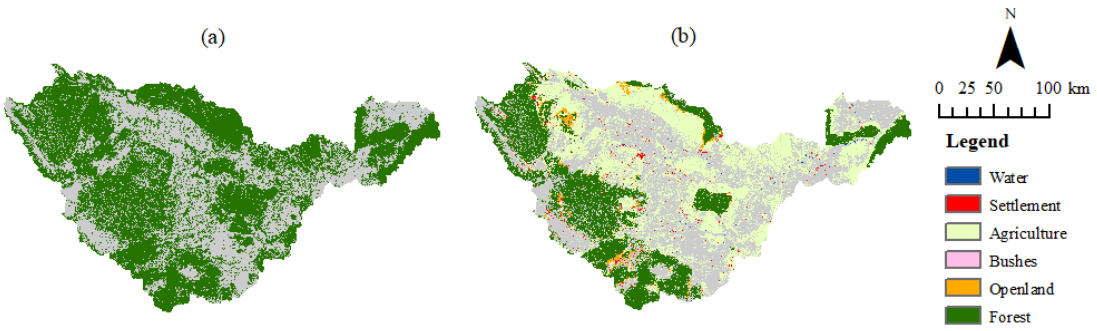

Figure 5-2 *1990 and 2040 land use map. (a) 1990 forest area and (b) Converted area from 1990 forest to other land uses in 2040 and the remaining forests. The gray color in (a) and (b) shows non-forest area in 1990.*

The model parameters and model structures were selected based on performance of discharge under different settings. In this study, the combination of Green-Ampt model and groundwater model were selected because they are the most suitable simulation condition to represent a runoff process in humid tropical region (Yamamoto *et al.*, 2019). Green-Ampt parameters for "sandy clay loam", "clay loam" and "clay" (Rawls *et al.,* 1993) were used and allocated spatially for each soil based on a FAO soil map. This study considers the Green-Ampt parameters and FAO soil map as natural soil conditions.

Future land use impacts on infiltration rates are estimated by obtaining converted area in 2040 within 1990 forest extent and estimate infiltration change from forest to other land uses. This study overlaid 2040 land use map (Figure 5-1c) on 1990 forestry area (Figure 5-2a) and obtained an area map that was converted from 1990 forest to 2040 other land uses (Figure 5-2b). To represent impact of land use on soil, I used vertical infiltration results in forest, urban, agriculture (oil palm and rubber tree), bushes and openland in upper part of Batanghari river basin (Tarigan *et al.*, 2018) and estimated the ratio of the hydraulic conductivity of other land use to that of forest hydraulic conductivity (Table 5-1). Table 5-1 shows that land conversion from forests to agriculture (urban area) reduces hydraulic conductivity by one tenth (one hundredth). Finally, I multiply the ratio with the Green Ampt vertical hydraulic conductivity in the converted area of 1990 forest.

Table 5-1 RRI model setting for vertical hydraulic conductivity to reflect land use change.

1990	2040	Change of vertical hydraulic conductivity (ratios)
Forest	Urban	0.01
	Agriculture	0.1
	Bush	0.01
	Open land	0.1
	Forest	1

In this study, RRI model projects future changes of flood inundation under RCP 8.5. Prior to impact assessment, bias correction is conducted for NHRCM daily rainfall by quantile mapping for basin averaged rainfall and variance scaling for

spatial variation of rainfall. The NHRCM does not include feedback effect of deforestation to climate systems. Considering that climate The detail of RRI model setting and the bias correction method and are mentioned in Chapter 3 and 4.

5.2.3 Comparison with another hydrological model

In this study I compared the simulation results using the RRI model with another hydrological model. I selected the SWAT model as it is widely use in the tropical river basin for both land use and climate change assessments. The setting of SWAT model –originally developed for temperate region – was adjusted to fit with the humid tropical river basin based on Yamamoto *et al.* (2020). A distinct adjustment to the typical application of SWAT model is the use of the Green-Ampt as runoff generation model, instead of the SCS Curve Number model. Another adjustment is to adjust soil parameters i.e. soil depth and saturated conductivity to fit with the conditions in humid tropics as well as biological parameters such as LAI to fit in the vegetation growth under tropical conditions.

Based on the earlier studies and findings from the Sekancing site, the conversion of land use from forest to agriculture affect the infiltration rate due to the compaction of surface soil layer. However, the hydraulic conductivity of deeper soil remains high. Yamamoto *et al.* (2020) optimized the value of saturated hydraulic conductivity of the surface layer (30 mm) at one order of magnitude lower in the agricultural site than in forested site. The optimized parameters can be viewed in Table 5-2.

Table 5-2 Soil parameters setting in SWAT model (Yamamoto *et al.*, 2020).

Parameters	Parameter definition (unit)	Value
v_SOL_K(1).sol_AGRL*)	Saturated hydraulic conductivity of 1st soil layer in agriculture fields (mm/h)	57.80
v_SOL_K(1).sol_FRSE	Saturated hydraulic conductivity of 1st soil layer in evergreen forests (mm/h)	479
v_SOL_K(1).sol_BARR	Saturated hydraulic conductivity of 1st soil layer in barren lands (mm/h)	60
v_SOL_K(1).sol_URBN	Saturated hydraulic conductivity of 1st soil layer in settlements (mm/h)	30
v_SOL_K(1).sol_RNGB	Saturated hydraulic conductivity of 1st soil layer in bushes (mm/h)	18

v_SOL_K(2).sol	Saturated hydraulic conductivity of 2nd soil layer in all types of land uses (mm/h)	500
v_SOL_Z(1).sol	Depth from soil surface to bottom of 1st layer (mm)	30
v_SOL_Z(2).sol	Depth from soil surface to bottom of 2nd layer (mm)	1506
r_SOL_AWC().sol *)	Available water capacity of both soil layers	1.016

[1] Lower range is infiltration rate of oil palm and upper range is infiltration rate of rubber plantations (Tarigan *et al.*, 2018)

[2] Tarigan *et al.* (2018)

[3] Soil depth from cone penetration test in Batanghari catchment is 1.5-4.5 m from soil surface (Yamamoto *et al.*, 2019)

I compared three simulations using SWAT model similar to the RRI model i.e. (1) land use map of 1990 and present climate; (2) land use map of 1990 and future climate; and (3) land use map of 2040 and future climate.

5.3 Results

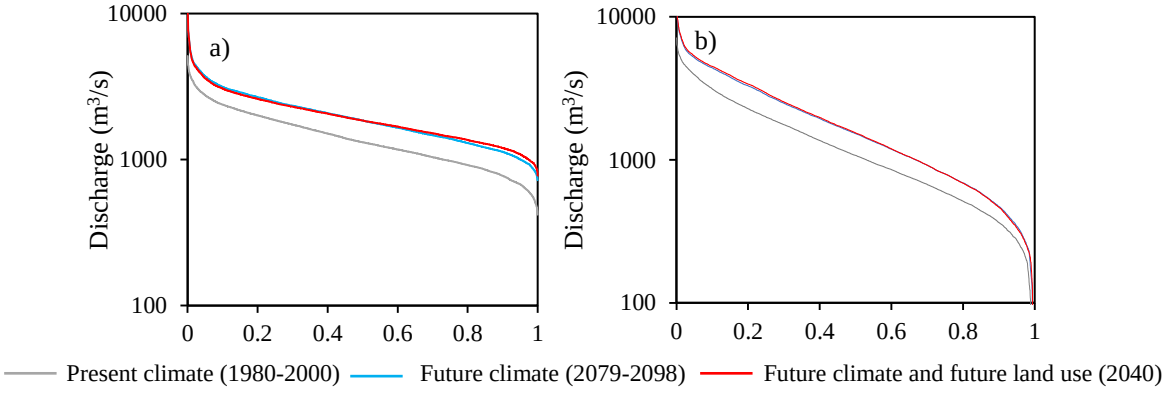

Figure 5-3 *Flow duration curves estimated using (a) SWAT model and (b) RRI model under three conditions. Gray line shows present climate condition, blue line shows future climate scenario, red line shows combined scenario of future climate and future land use.*

Figure 5-3 shows flow duration curves (FDC) under present climate condition, future climate condition and combined climate change and land use change condition. FDC is constructed based on simulated daily discharge for an entire simulation period. The consistent change of FDC was obtained for SWAT model (Figure 5-3a) and RRI model (Figure 5-3b). The FDC under future climate scenario shows that entire flow rate will increase significantly compared with that under present climate scenario. Under the combined effect of climate change and land use change scenario, flow rate slightly increases compared with that under a single climate change effect. Thus, the land use change impact is not so significant.

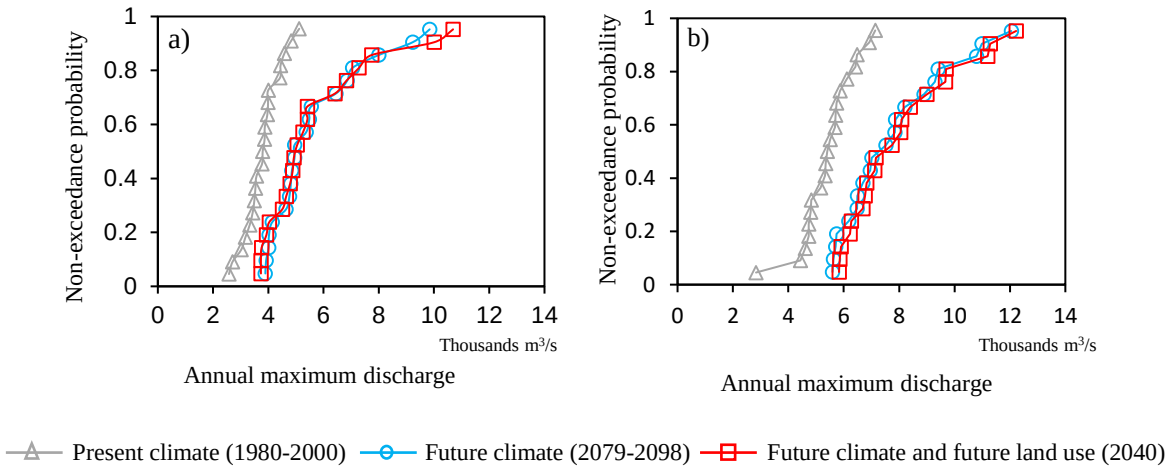

Figure 5-4 *Cumulative distribution functions of annual maximum daily discharge estimated using (a) SWAT model and (b) RRI model under three scenarios. Gray line shows present climate condition, blue line shows future climate scenario, red line shows combined scenario of future climate and future land use.*

Figure 5-4 shows cumulative distribution function (CDF) of annual maximum discharge under the respective condition. The consistent change of annual maximum discharge was obtained for SWAT model (Figure 5-4a) and RRI model (Figure 5-4b). The future annual maximum discharge will increase by maximum 1.7 times compared with present climate condition. Annual maximum discharge under the combined land use and climate change effect is not different from that under only climate change scenario.

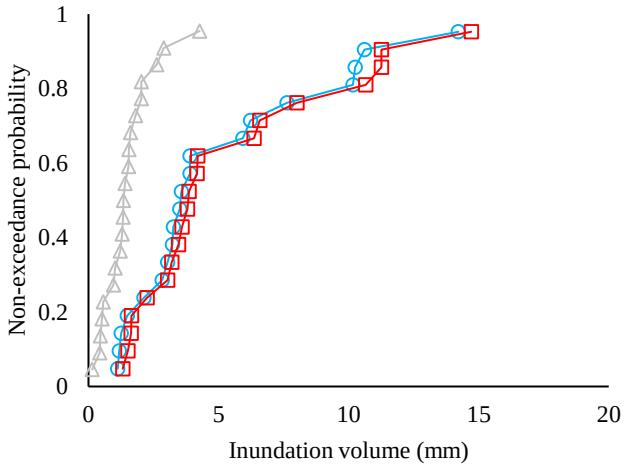

Figure 5-5 *Cumulative density functions of inundation volume estimated using RRI model under three conditions. Gray line shows present climate condition, blue line shows future*

climate scenario, red line shows combined scenario of future climate and future land use.

Figure 5-5 shows CDF of annual maximum inundation volume. In this study, the inundation volume was obtained by multiplying annual maximum inundation depth more than 50 cm with grid area, and averaging it by total basin area. Under the future climate scenario, inundation volume increases largely compared with that under present climate scenario. On the other hands, there is a little change in inundation volume, comparing between a single climate change scenario and the combined climate change and land use change scenario.

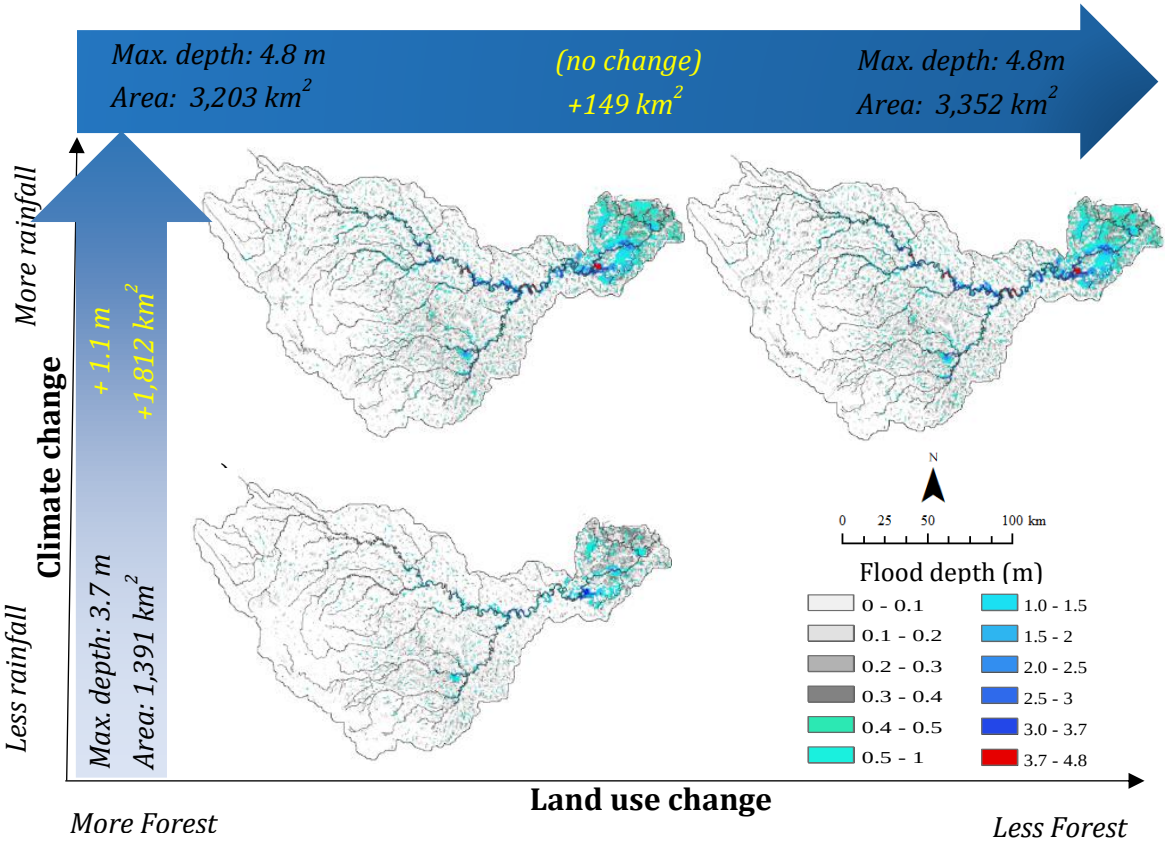

Figure 5-6 Inundation maps under three conditions. a) Present climate condition, b) Future climate scenario, c) combined scenario of future climate and future land use.

Figure 5-6 compares annual maximum inundation depth maps under the different scenarios. Under climate change effect, inundation area increases by 1.812 km^2 and maximum inundation depth increases by 1.1 m (Figure 5-6a and Figure 5-6b). On the other hands, under the combined effect of land use change, inundation area increases by 149 km^2 and maximum inundation depth does not change (Figure 5-6b

and Figure5-6c). The two future scenarios (Figure 5-6b and Figure 5-6c) show that inundation area increases significantly at downstream area of Batanghari river basin.

5.4 Discussion

For land use impacts assessments, this study considers infiltration change from forest to other land uses. Despite that infiltration reduces by more than one tenth in a large part of study area, the land use change impacts on high flows are estimated to be much less than climate change impacts by both RRI and SWAT models. Prior to this study, the application of SWAT model in the study area shows the infiltration reduction by one order of magnitude did not change high flow because infiltration in converted area still has high capacity and little surface flow generates (Yamamoto *et al.*, 2020). The recent field observation in natural forest in the study area (Araki *et al.*, 2019) show that even though forest conversion lowers the infiltration rates by one order of magnitude, surface runoff remains negligible after forest conversion. In addition, the effect of soil compaction on the top soil structure are very clear at the plot scale but less clear at catchment scale. Especially the land use change impacts on floods are inconsistent for larger catchment (> 100km^2) (Beck *et al.*, 2013).

The increase of flood inundation area and depth potentially increase the risk of flood damage on agriculture and urban area. Furthermore, more agricultural area and settlement can be exposed by flooding in the future because the agricultural area will continuously expand and settlement increases until 2040. In addition, the demand of oil palm is projected to be increasing until 2050 (Harris *et al.*, 2013) and more oil palm can be expected in lowland area of Indonesia due to potential land resources (Mietten *et al.*, 2012). Proper land use management is necessary, in particular for lowland agricultural area and settlement to mitigates the future flood risks and adapt the increasing flood.

5.5 Conclusion

This study compares climate change and land use change impacts on flood inundation in a humid tropical river basin. I found out that the effect of climate change on floods is larger than the effect of land use change. The land use impacts are associated with characteristic of humid tropical soil that is resilient against land

conversion and maintains high infiltration rates even though land conversion from forest area reduces infiltration reduction by one order of magnitude. Moreover, in a large river basin, spatial variability of rainfall masked out land use change effects. In conclusion, climate change gives a more significant impact on floods in a large humid tropical river basin.

References

Araki R. 2019. Characteristics of Soil and Hillslope Runoff in Humid Tropical Forest in Sumatra, Indonesia. *Bachelor's Thesis*, Kyoto University, Kyoto, Japan: 27p.

Arnold JG, Srinivasan R, Muttiah RS, Williams JR. 1998. Large area hydrologic modeling and assessment Part 1: Model development. *Journal of the American Water Resources Association* 34: 73–89. DOI: 10.1111/j.1752-1688.1998.tb05961.x.

Arnold J, Moriasi D, Gassman P, Abbaspour K, White M, Srinivasan R, Santhi C, Harmel R, van Griensven A, Van Liew M, Kannan, N, Jha M. 2012. SWAT: Model use, calibration, and validation. *Transaction of ASABE* 55: 1491–1508. DOI: 10.13031/2013.42256.

Beck, H.E., *et al.*, 2013. The impact of forest regeneration on streamflow in 12 mesoscale humid tropical catchments. Hydrology and Earth System Sciences, 17 (7), 2613–2635. DOI:10.5194/hess-17-2613-2013

Comte, I, Colin, F, Whalen, JK, Grünberger, O, Caliman, J-PP. 2012. Agricultural Practices in Oil Palm Plantations and Their Impact on Hydrological Changes, Nutrient Fluxes and Water Quality in Indonesia. *A Review., 1st ed, Advances in Agronom*y. DOI: 10.1016/B978-0-12-394277-7.00003-8

Cruz FT, Sasaki H, Narisma GT (2016) Assessing the sensitivity of the Non-Hydrostatic Regional Climate Model to Boundary Conditions and

Convective Schemes over the Philippines. *J Meteorol Soc Jpn* 94(A):165-179. DOI:10.2151/jmsj.2015-059

Farjad, B, Gupta, A, Razavi, S, Faramarzi, M, Marceau, DJ. 2017. An Integrated Modelling System to Predict Hydrological Processes under Climate and Land-Use/Cover Change Scenarios. *MDPI Water* 9(767):1-23. DOI：10.3390/w9100767

Feldman, A.D., 2000. Hydrologic Modeling System HEC-HMS technical reference manual. Davis, CA: US Army Corps of Engineers Hydrologic Engineering Center, CPD-74B.

Hansen MC, Potapov PV, Moore R, Hancher M, Turubanova SA, Tyukavina A, Thau D, Stehman SV, Goetz SJ, Loveland TR. 2013. High-resolution global maps of 21st-century forest cover change. *Science* 342: 850–853

floods in Asian river basins. *Hydrological Research Letters* 11(1):24–30. DOI : 10.3178/hrl.11.24

Harris NL, Brown K, Netzer M, Gunarso P, Killeen TJ. 2013. Projections of oil palm expansion in Indonesia, Malaysia and Papua New Guinea from 2010 to 2050. In: Kileen, TJ, Goon, J (eds.) *Reports from the Technical Panels of the 2nd Greenhouse Gas Working Group of the Roundtable on Sustainable Palm Oil (RSPO)*: 89-112.

Iwami, Y, Hasegawa, A, Miyamoto, M, Kudo, S, Yamazaki, Y, Ushiyama, T, Koike, T. 2017. Comparative study on climate change impact on precipitation and

Jennifer Merten, Alexander Roll, Thomas Guillaume, Ana Mejide, Suria Tarigan, Herdhata Agusta, Claudia Dislich, Chiristoph Dittrich, Heiko Faust, Dodo Gunawan, Jonas Hein, Hendrayanto, Alexander Knohl, Yokov Kuzyakov, Kerstin Wiegand and Dirk Holscher: Water scarcity and oil

palm expansion: social views and environmental processes, *Ecology and Society* 21(2), 2016.

Miettinen, J, Hooijer,A, Tollenaar,D, Page, S, Malins, C, Vernimmen, R, Shi, C, Liew, SC. 2012. Historical Analysis and Projection of Oil Palm Plantation Expansion on Peatland in Southeast Asia. *White Paper Number 17*.

Kudo, S, Sayama, T, Hasegawa,A, Iwami, Y. 2015. Assessment of climate change impact on flood discharge and inundation in the Solo river basin, Indonesia. *Journal of Japan Society of Civil Engineers Ser B1* 71(4): I_1321-6. DOI: 10.2208/jscejhe.71.I_1321

Kuraji, K. 1996. Water balance studies on moist tropical forested catchments, Journal of the Japanese Forestry Society 78(1):89-99. DOI: 10.11519/jjfs1953.78.1_89. (In Japanese)

Margono BA, Turubanova S, Zhuravlena I, Potapov P, Tyukavina A, Baccini A, Goetz S, and Hansen MC. 2012. Mapping and monitoring deforestation and forest degradation in Sumatra (Indonesia) using Landsat time series data sets from 1990 to 2010. *Environmental Research Letters* 7: 034010

Rawls, W.J., L.R. Ahuja, D.L. Brakensiek, and A. Shirmohammadi. 1993. Infiltration and soil water movement. In: D.R. Maidment (ed). *Handbook of Hydrology*. McGraw-Hill, Inc. New York.

Sasaki H, Kurihara K, Takayabu I, Uchiyama T (2008) Preliminary experiments of reproducing the present climate using the Non-hydrostatic Regional Climate Model. *SOLA* 4:25-28. DOI:10.2151/sola.2011-044

Tarigan. SD. 2016. Land Cover Change and its Impact on Flooding Frequency of Batanghari Watershed, Jambi Province, Indonesia. *Procedia Environmental Sciences* 33(2016):386-392. DOI: 10.1016/j.proenv.2016.03.089

Tarigan S, Wiegand K, Sunarti, Slamet B. 2018. Minimum forest cover required for sustainable water flow regulation of a watershed: a case study in Jambi Province, Indonesia. *Hydrology and Earth System Sciences* 22: 581–594. DOI: 10.5194/hess-22-581-2018.

Ushiyama, T, Hasegawa, A, Miyamoto, M, Iwami, Y. 2016. Dynamic downscaling and bias correction of rainfall in the Pampanga River Basin, Philippines, for investigating flood risk changes due to global warming. *Hydrological Research Letters* 10(3), 106–112 (2016). DOI: 10.3178/hrl.10.106

Utami N, Sapei A, Apip. 2017. Land use change assessment and its demand projection in Batanghari River Basin, Sumatera, Indonesia. *LIMNOTEK Perairan Darat Tropis di Indonesia* 24: 52-60

Yamamoto EMS, Sayama T, Yamamoto, K Apip. 2020. Comparison of runoff generation methods for land use impact assessment using the SWAT model in humid tropics. *Hydrological Research Letters* 14(2):81–88. DOI: 10.3178/hrl.14.81

Yamamoto K, Sayama T, Apip, Takara K. 2019. Applicability of Rainfall-Runoff-Inundation Model in a Humid Tropical River Basin. *Journal of Japan Society of Civil Engineering* **75**: I_253-I_258 (in Japanese).

Yulianti, M. (2018), Preliminary study of soil permeability properties using principal component analysis, *Earth Environ. Sci*. 118, 012029

Chapter 6 Flood Inundation Impact Assessment on Oil Palm Plantation

6.1 Introduction

There is a global awareness that climate change will threaten a development of lowland area in a tropical region. IPCC AR5 reported that an extreme rainfall is more likely to increase in a humid tropical region and consequently increase floods. The increase of rainfall at upstream catchment can affect inundation regime in lowland area. Tropical lowland area is originally swamp forests and a habitat for diverse species of animals and vegetation (Sodhi *et al.*, 2004). Due to potential land resources, lowland tropical forests have been intensively logged and converted into agricultural areas (Miettinen *et al.*, 2012). Over the past two decades, the main driver of land conversion in a tropical lowland is Acacia and oil palm plantation (Miettinen *et al.*, 2016). Due to increase of global demand of oil palm (Harris *et al.*, 2013), the oil palm establishment will continue in lowland areas of Indonesia (Miettinen *et al.*, 2012) that is the largest producing countries of oil palm in the world. The change in inundation regime due to climate change will give an impact on oil palm plantation in lowland of Indonesia and further affects development of economic and society.

The floods impact on oil palm is different for different growing stages. The young oil palm under three years old is more likely to die when floods are prolonged (JICA, 1982). After an oil palm gets matured, the oil palm becomes more resilient against prolonged floods. However, long-term floods can topple the tree (Sumarga *et al.*, 2016) or reduce fruits under poor drainage condition (Hensen *et al.*, 2008). Moreover, flooding prevents accessing plantation sites and impacts on the amount of harvested fruits. After 25 years of planting, the oil palm has to be replaced and young oil palm has to be replanted because revenue from the fruits is less than costs. To meet global demand of palm oil, oil palm needs to produce sustainably in the future. In order to adapt the increasing floods due to climate change, it is important to discuss oil palm suitability in lowland area based on vulnerability of young oil palm and future flood hazard.

In Indonesia, a large oil palm plantation is established on peatlands. Peats are characterized by poor nutrient, poor drainage and 90 % of water (Sumawijaya, 2006). Thus, the plantation introduced drainage system to lower water levels in peatlands. The main concern of the land conversion to plantation is that drainage system dries and oxidized, leading to peat subsidence, high CO_2 emissions and peatland fire. The impacts of drainage on peatlands raised debates on appropriate use of peatlands for recent agriculture such as oil palm and acacia plantation.

The objective of this study is to assess the impacts of future floods on oil palm plantation in a lowland area of a tropical river basin. In particular, focuses are on effect of future floods on oil palm plantation in peatlands. This study will make use of flood model outputs under future climate scenario and estimate mortality of oil palm due to flooding.

6.2 Method

6.2.1 Dataset

This study uses dynamically downscaled rainfall data produced by the Non-Hydrostatic Regional Climate Model (NHRCM) with resolution of 5 km (Sasaki *et al.*, 2008; Cruz *et al.*, 2017). Downscaling was performed for our study area in Sumatra Island (-3.32°S – 0.41°S; 99.65°E – 105.25°E). The model is run for 21 years of present climate (1980 – 2000) and for 20 years of future climate (2079 – 2098) under the Representative Concentration Pathways 8.5 scenario (RCP8.5) (Endo *et al.*, 2012).

The oil palm distribution map was derived from composites of Sentinel-1 and 2 imageries (1-year (2015) composites for Sentinel-1 and 3-year (2015-2018) composites for Sentinel 2). The distribution map of oil palms was classified to young oil palms (less than 3 years old) and mature oil palms (more than 3 years old). The oil palms distribution map was classified using Machine Learning Classification (Random Forest) in the Google Earth Engine platform. The model was trained and

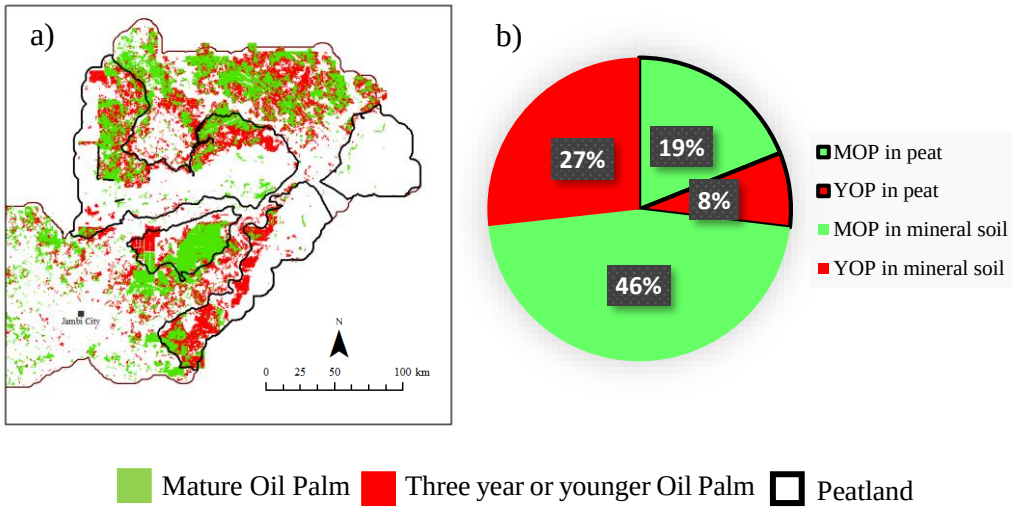

Figure 6-1 *a) Oil palm map and peatland map at the downstream of Batanghari river basin and b) overlapped area among peatland, mineral soils, young and mature oil palm. Green and red area in a) is mature and young oil palm. Young oil palm is defined as three years or younger* (Yamamoto *et al.*, accepted).

validated using 5,455 points which was collected using orthophotos in the Google Earth Pro. The young oil palms were identified from the orthophotos as oil palms with crown projected area (CPA) less than 16 m^2. In order to improve the classification, in addition to the standard bands of Sentinel 1 and 2, texture analysis (median filter and Gray-Level Co-Occurrence Matrix) was applied (Yamamoto *et al.*, accepted).

Peatland map is downloaded from the department of forestry in Indonesia. The map is a conservation target and includes deep peat that has depth of more than 0.50 m.

Figure 6-1 shows that large mature oil palm area is located in peatland area at the center of downstream. Among all the planted areas of oil palm in the lower part of the Batanghari River basin, the 27 % is positioned in the peatland area (19 % and 8 % are matured and young oil palm, respectively). As indicated the map in Figure 6-1, the peatland area is utilized as the production area of oil palm.

6.2.2 Future projection of mortality map

The RRI model was applied to the study area with resolution of 1km. The model parameters and model structures were selected based on performance of discharge under different settings. In this study, the combination of Green-Ampt model and

groundwater model were selected because they are the most suitable simulation condition to represent dominant subsurface flow and groundwater flow based on filed investigation in upstream natural forest in the study area. (Yamamoto *et al.*, 2019). Groundwater flow is recharged from cumulative infiltration amounts estimated by the Gree-Ampt model. The m uses HydroSHEDS (about 1km) as an elevation data and river flows, which does not represent microtopography of peatland surface and drainage system introduced in peatland. The detail of application of RRI model to study area is explained in Chapter 3.

RCP 8.5 is used as future climate scenario. Based on the future scenario, NHRCM estimated future rainfall between 2079 and 2098. The bias-corrected rainfall was used as an input of RRI model to estimate future inundation map. The detail of application of bias correction methods are explained in Chapter 4. Based on model outputs, inundation duration was obtained at each grid by counting continuous days when inundation depth exceeds 0.25 m.

Table 6-1 Mortality of young oil palm trees up to 3 years old depending on flood durations.

Flood Duration (Days)	Flood Depth (m)	Mortality (%)
7	0.25	10
14	0.25	20
21	0.25	70
28	0.25	100

The longest inundation duration was selected in a year for 20 years under present and future periods. As shown in equation (6-1), the annual inundation duration was transformed to annual mortality of young oil palm using flood duration-mortality curve based on a study that summarized flood damage estimation in rivers of Peninsular Malaysia (JICA, 1982). Specifically, this study uses flood damage factors on oil palm, taken from the Kelantan river basin studies in Malaysia (Government of Malaysia, 1977). The Table 6-1 summarized the mortality of young oil palm trees up to 3 years old depending on flood durations. To compensate the insufficient mortality data shown in Table 6-1, the data is linearly interpolated. Then, 20-year average of mortality rate is obtained as shown in equation (6-2). Finally, probability

of death within three years was calculated in equation (6-3) for each simulation grid-cell.

$$M_{i,y} = f(x_{i,y}) \qquad \textit{(eq. 6-1)}$$

$$\overline{M_i} = \frac{1}{N}\sum_1^N M_{i,y} \qquad \textit{(eq. 6-2)}$$

$$p_i = 1 - (1 - \overline{M_i})^3 \qquad \textit{(eq. 6-3)}$$

where $M_{i,y}$ is a mortality at a grid in a year, f is a function of flood duration-mortality curve, x_i is an annual maximum inundation duration at a grid, $\overline{M_i}$ is an average mortality at a grid, N is total year of simulation period, p_i is a mortality within three year

6.3 Results

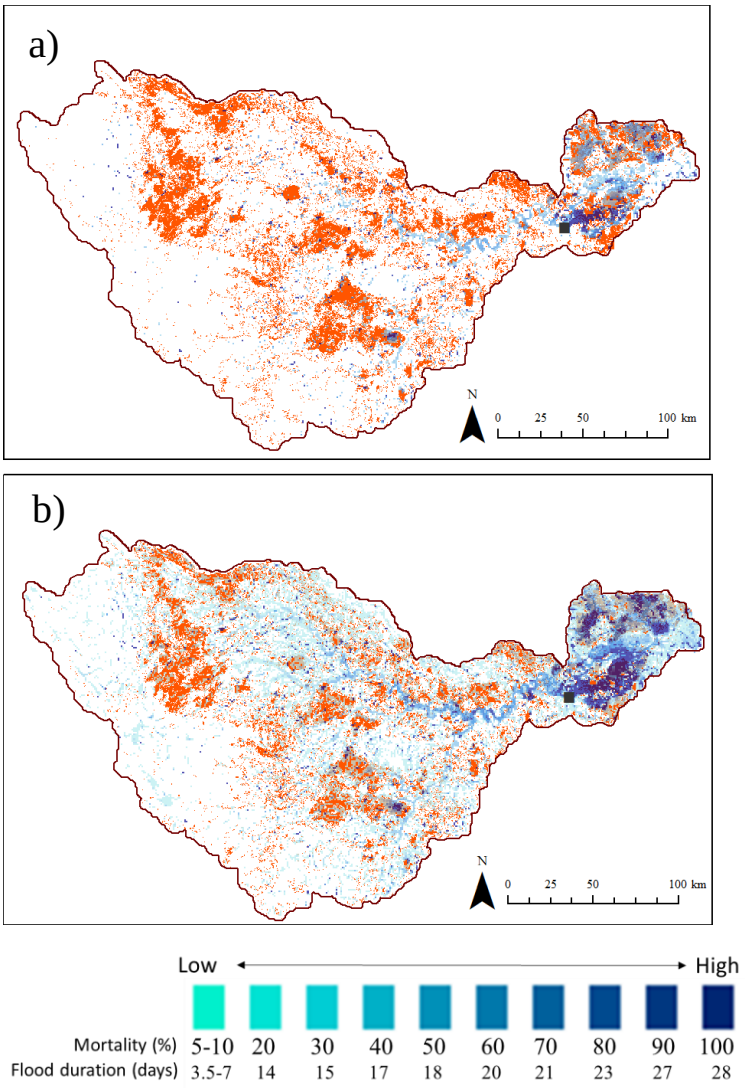

Figure 6-2 Mortality maps due to flood inundation under a) present climate and b) future climate conditions with a background map of oil palm (orange color) (Yamamoto *et al.*, accepted). *Note that a mortality is a death rate of oil palm within three years after planting.*

Figure 6-1 shows the mortality map of oil palm tree due to flooding in a present and future climate conditions and current oil palm extent. The mortality rate indicates the probability for a planted oil palm tree to be deadly affected by the flood inundation within three years. Under the present climate condition, a downstream area of Jambi city shows higher mortality than other areas (Figure 6-2a). Most of the downstream oil palm plantation area does not show high mortality area. Under future climate condition, inundation duration is projected to be longer and larger part of downstream area shows high mortality, compared with present climate. In particular, large part of current oil palm plantation area show high mortality under future climate condition (Figure 6-2b).

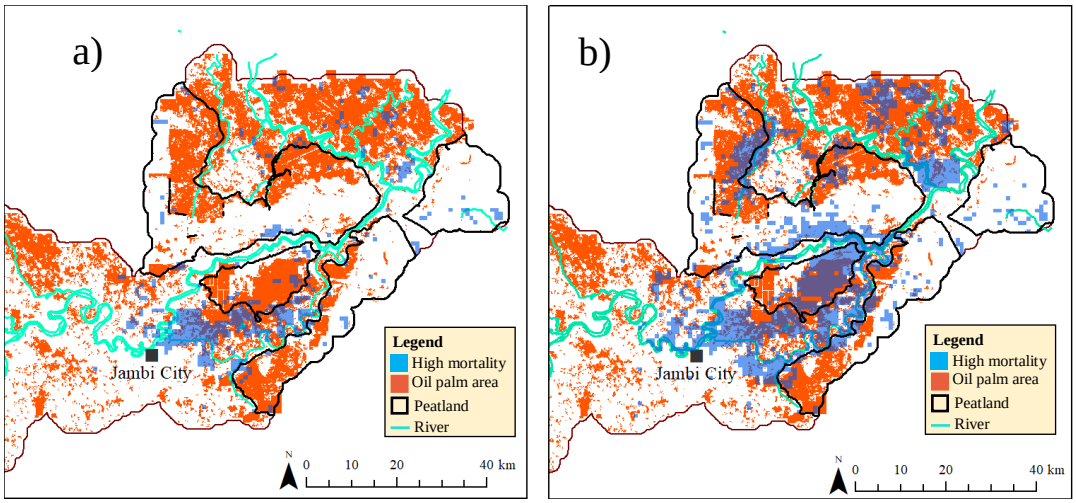

Figure 6-3 Downstream area of Figure 1. a) Present climate condition b) future climate condition.

Figure 6-3 focuses on the same comparison of Figure 6-2 at downstream with peatland map. Here, mortality more than 50 % is defined as high mortality. Peatland maps shows that peatland is not distributed along rivers but located at inner land. In a present climate, area outside of peatland shows high mortality (Figure 6-3a). In the future climate, larger area of peatland shows high mortality (Figure 6-3b).

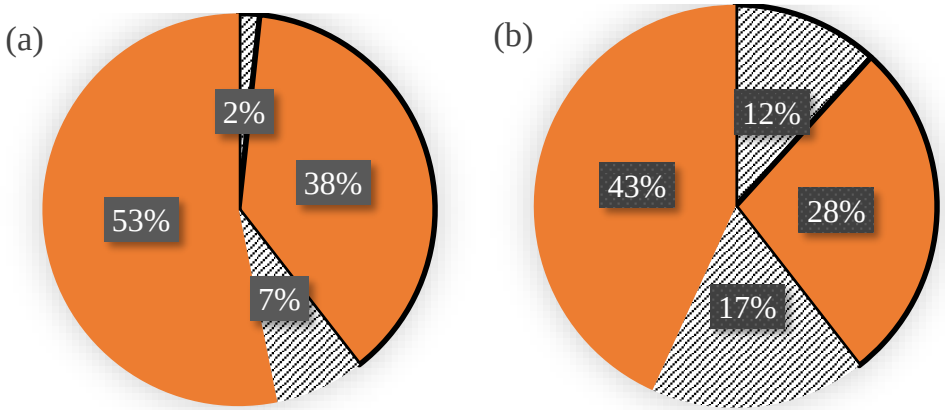

Figure 6-4 *Classification of oil palms based on mortality maps and a peatland map. (a) Present climate and (b) future climate. Area surrounded by blackline shows a peatland area, hatch shows a high mortality area and Orange color shows low mortality. Note that low mortality includes 0 %.*

Figure 6-4 is a pie chart summarizing the overlapped area of high mortality, peatland and current oil palm extent shown in Figure 6-3. Figure 6-4a shows condition in a present climate and Figure 6-4b in future climate condition. In present climate condition, 9 % of downstream area shows high mortality due to long-term flooding that is further classified as 2 % in peatland area and 7 % in mineral soil (Figure 6-4b). In future climate condition, 29 % of the downstream area shows high mortality that is further classified in to 12 % in peatland and 17 % in mineral soils. (Figure 6-4c. The projected change of downstream area which shows high mortality is 3.2 times that is further classified into 6 times in peatland and 2.4 times in mineral soil. The comparison between high mortality area in the present and future climate condition shows that peatland will be impacted more significantly. In particular, peatland between two rivers, where mature oil palm is shown in Figure 6-1, will have high mortality in the future climate condition.

6.4 Discussion

6.4.1 Why the high mortality area of peatland will increase significantly in a future climate?

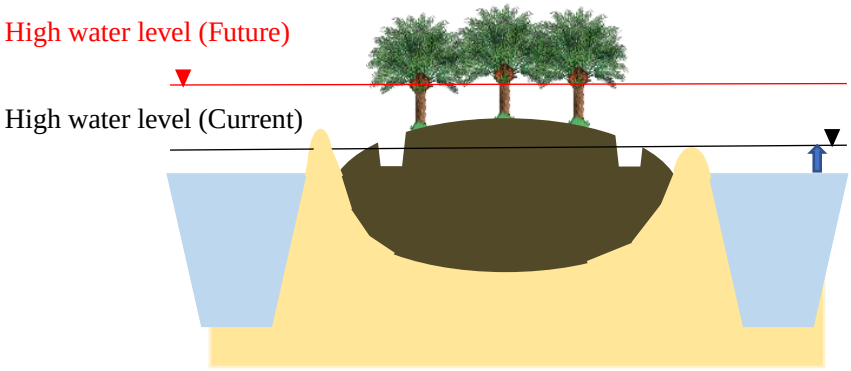

Figure 6-5 Conceptual diagram of inundated peat dome with typical surrounding environment.

In a present climate condition, only 2 % of peatland area shows mortality exceeding 50 % within three years after planting. In a future climate condition, the peatland area, which shows mortality exceeding 50 %, increases significantly by 6 times. The increased high mortality area is associated with a location of peatlands formation. Tropical peatland starts forming in a depression between rivers ten million years ago (Furukawa and Supiandi, 1985). Initially, a river inundates a depression zone and makes wetlands. In wetlands, freshwater swamp forests were developed and the dead body of trees are not decomposed because of waterlogged condition and accumulated. Floodwater has brought a mineral and peatlands at this stage has more or less nutrients from rivers. Flood water contributes to formation of peat until a peat forms flat surface. Due to relatively high rainfall, a peat accumulates further and peat dome developed, which consists of higher land than river water levels. Because of a higher land, inundation duration does not always stay long in a peatland in a present climate condition (Figure 6-5). However, a river water level increases due to climate change and inundation duration is prolonged in an area between rivers (Figure 6-5). In particular, this study shows that prolonged inundation area increases significantly where two rivers are diverging and meeting.

6.4.2 Implication of future flood impacts on peatlands

The inundation is projected to be prolonged in peatland area due to climate change. In addition, the projected future mortality within three years after planting increases significantly in peatland area. Prolonged inundation can increase groundwater level in peatland that gives a challenge to maintain oil palm production that requires drainage. Based on the online-interview to Indonesian Oil Palm Company Association, an industrial oil palm company will not continue oil palm plantation if flood duration is long. Thus, those peatland areas can be abandoned. In worst scenario, nobody will manage water level in the canal that can increase fire risk (Takahashi et al. 2003). The abandoned area might be used by small holder for oil palm. However, the small holder typically was not able to manage water level in the canal that can also lead to increase of fire risk. These results imply that increase of flood duration due to climate change potentially cause fire risk in the future, that will threaten the sustainability of oil palm production in downstream area of a basin in Sumatra island.

6.5 Conclusion

This study assesses the impact of future flood inundation on oil palm at the downstream of Batanghari river basin. Under RCP 8.5 scenario, inundation duration gets longer in downstream lowland area, leading to increasing area of high mortality for young oil palm. Particularly, peatland area shows significant increase of high mortality area by 6 times. This suggests that currently suitable peatland under drainage condition will not be suitable for replanting oil palm. In addition, prolonged inundation can increase groundwater level in peatland that gives a challenge to maintain oil palm production that requires drainage. According to an online interview, the company will not use a land for oil palm production if inundation is frequent and prolonged. Furthermore, abandoned peatland gives a public concern on peatland fire. These results suggest that current oil palm plantation is not be sustainable, particularly in peatland due to increase of flood inundation and potential fire risk under climate change condition and thereby, adaptation measures for climate change should be taken for sustainable oil palm management and environmental protection of peatland.

References

Endo H, Kitoh A, Ose T, Mizuta R, Kusunoki S (2012) Future changes and uncertainties in Asian precipitation simulated by multiphysics and multi–sea surface temperature ensemble experiments with high-resolution Meteorological Research Institute atmospheric general circulation models (MRI-AGCMs). J Geophys Res 117:D16118. DOI:10.1029/2012JD017874

Furukawa, H, Supiandi, S. 1985. Agricultural Landscape in the Lower Batanghari, Sumatra. Part One: Statigraphy and Geomorphology of Coastal Swampy Lands. *Southeast Asian Studies* 23(1): 3-37. (In Japanese)

Government of Malaysia 1977 The Kelantan River Basin study, Main Report (ENEX)

Henson IE, Harun MH, ChangKC (2008) Some observations on the effects of high water tables and flooding on oil palm, and a preliminary model of oil palm water balance and use in the presence of a high water table. *Oil Palm Bulletin* 56: 14-22.

JICA (1982) National water resources study, Malaysia sectoral report 5:10

Miettinen J, Hooijer A, Tollenaar D, Page S, Malins C, Vernimmen R, Shi C, Liew SC. 2012. Historical Analysis and Projection of Oil Palm Plantation Expansion on Peatland in Southeast Asia. *White Paper Number 17*.

Miettinen J, Shi C, Liew S. 2016. Land cover distribution in the peatlands of Peninsular Malaysia, Sumatra and Borneo in 2015 with changes since 1990 *Glob. Ecol. Conserv.* 6: 67–78. DOI: 10.1016/j.gecco.2016.02.004

Sodhi NS, Koh LP, Brook BW, Ng PKL (2004) Southeast Asian biodiversity: an impending disaster. Trends in Ecology & Evolution 19: 654–660.

Sumarga E, Hein L, Hooijer A, Vernimmen R. 2016. Hydrological and economic effects of oil palm cultivation in Indonesian peatlands. *Ecology and Society* 21(2):52. DOI: 10.5751/ES-08490-210252

Sumawijaya, N. 2006. Hydrology and peat-land development in Indonesia. Tropics 15(3):279-284. DOI: 10.3759/tropics.15.279

Takahashi H, Usup A, Hayasaka H, Limin SH (2003) Estimation of ground water level in a peat swamp forest as an Index of peat/forest fire. In: Osaki M, Iwakuma T, Kohyama T, Hatano R, Yonebayashi K, Tachibana H, Takahashi H, Shinano T, Higashi S, Simbolon H, Tuah SJ, Wijaya H, Limin SH (eds) *Proceeding of the International Symposium of Land Management and Biodiversity in Southeast Asia, Bali, 2002*

Yamamoto EMS, Sayama T, Yamamoto K, Apip. 2021. Mapping of Mature and Young Oil Palm Distributions in a Humid Tropical River Basin for Flood Vulnerability Assessment. IOP Conference Series. *Earth and Environmental Sciences*. (accepted)

Chapter 7 Conclusion

This study assesses the climate change and land use change impacts on flood inundation in a humid tropical river basin in Sumatra island in Indonesia. As a case study, this dissertation selected Batanghari river basin in Sumatra island in Indonesia, where a half of forest were lost and severe land use change took place. This study applied Rainfall-Runoff-Inundation model (RRI) to the study area using satellite data and datasets estimated using global hydrological model, owing to a lack of observed datasets. This study used some field data to discuss the suitability of the model in a river basin. Using the suitable model structure and parameter setts, the climate and land use change effects on flooding are projected by the RRI model. The future rainfall is estimated using NHRCM under RCP8.5 scenarios. Biases corrections for rainfall outputs are conducted to adjust a rainfall spatial pattern, a flow duration curve and flood inundation volume. Using basin corrected rainfall as an input of RRI model, the change of flood inundation is projected. This study also uses future land use data estimated using land use prediction model. Finally, this study compares climate and land use change impacts on flood inundation. To discuss the floods impact on downstream agriculture and peatland, this study estimates mortality of young oil palm trees and analyzed the relationship between flooding, oil palm and peatlands.

Chapter 3 investigated combinations of runoff process and parameter setting and discussed the suitable simulation condition of RRI model. This study compared the model structures and parameters with the default model structure and parameter setting that are based on subsurface dominated flow in a shallow soil layer without effect of evapotranspiration rate.

At the beginning, the accuracy of satellite rainfall and evapotranspiration input was validated. The spatial pattern and basin-averaged rainfall estimated using GSMaP reanalysis ver. 6 is similar to that of gauged stations. In addition, average annual rainfall estimated using GSMaP and average annual potential evapotranspiration estimated is within the range of values in a previous study. The findings show that GSMaP and Penman-monteith equation are able to estimate

rainfall and evapotranspiration in humid tropics. The default settings overestimated discharge.

The simulated discharge was improved under simulation condition including evapotranspiration rates, compared with default one. Another simulation condition, that includes evapotranspiration and deeper soil thickness, improved peaks of simulated discharge, compared with that includes only evapotranspiration rates. However, the RRI model was not able to produce discharge in dry season. The underestimation of river discharge during dry season is solved by adding groundwater model to the above-mentioned deep soil layer and evapotranspiration rates. These results and discussions indicate that the RRI model is capable of performing for long-term discharge, given that a simulation considers characteristic of hydrology in humid tropics such as evapotranspiration input, thicker soil layer and groundwater process in a deep soil layer. Using the suitable simulation condition, the RRI model estimated that the probability of inundation occurrence exceeds 80 % at downstream area. In conclusion, this study suggests that the RRI model is applicable for a humid tropical river basin by taking account into characteristic of hydrology in humid tropics for analyzing long-term river discharge and inundation.

Chapter 4 compared the two bias correction methods, i.e., the QM method and a combination of the QM and VS methods, to examine how each method improves estimates of rainfall patterns, and subsequently, the simulated flood inundation by the RRI model in the Batanghari River Basin, Indonesia. Originally, the dynamically downscaled NHRCM rainfall data showed higher spatial variation in the 15-day rainfall and annual rainfall compared to the reference data. While this does not markedly influence the simulated FDC, it largely overestimated the extreme values, such as the annual maximum flood inundation volume. The combination of QM and VS methods successfully decreased the rainfall spatial variability and improved the estimations of the FDCs and the extreme values.

Our analysis showed that annual maximum flood inundation volume corresponding to a 20-year return period would increase by 3.3 times in the future. In addition, the flood inundation extent would increase, particularly in the lowland areas of Sumatra Island. In conclusion, this study suggests the need to consider future

climate change scenarios for river basin management, particularly to reduce the flood damage and to sustainably maintain the unique ecosystem of tropical peatlands.

Chapter 5 compares the effect of climate change and land use change on river discharge and flood inundation. In addition, this study also compares these impacts estimated using the RRI model and the Soil Water Assessment Tools model that is widely used for land use impact assessment all over the world. According to estimated FDC and annual maximum discharge, both SWAT model and RRI models suggest that climate change has more impacts than land use change. In addition, RRI model suggests that climate change has more impacts on annual maximum inundation volume than land use change. Specifically, due to climate change, inundation area increases by 1,812 km^2 and the maximum inundation depth increases by 1.1 m, while inundation area increases by 149 km^2 and the maximum inundation depth does not change, due to land use change. The above-mentioned results show that the estimated change of river flows and flooding using the RRI model is similar to those of the SWAT model. In conclusion, this study suggests that the effect of climate change on river flows and flooding is more significant than that of land use change in the study area.

Chapter 6 assesses the impact of flood inundation on young oil palm in peatland to discuss sustainable adaptation measures for oil palm production. This study develops a basin-scale mortality map of oil palm within three years after planted in present climate and future climate conditions. Under future climate condition, inundation duration is projected to be longer and larger part of downstream area shows mortality exceeding 50%, compared with present climate. This study further analyzed the impact of future flood inundation on peatland area and oil palm area. In future climate condition, peatland area, which shows mortality exceeding 50 %, increases to 6 times, compared with present climate case. In particular, peatland area, which consists of higher elevation called a peat dome, shows high mortality of oil palm caused by prolonged inundation. Moreover, these results suggest that prolonged inundation would increase groundwater level in peatland that gives a challenge to maintain oil palm production that requires drainage. Furthermore, this study implies that prolonged inundated area due to climate change may not be used for oil palm production, which leads to poor management of drainage and fire

disaster during dry season. In conclusion, this study suggests that current oil palm plantation is not be sustainable, particularly in peatland under climate change condition and thereby, adaptation measures for climate change should be taken for sustainable oil palm management and environmental protection of peatland.

This study concluded that the RRI model is applicable to simulate discharge and inundation extent in the humid tropical river basin and can be used for land use and climate change impact studies. However, the application needs careful parameterization considering the deep soil layer in the region as well as effects of evapotranspiration (long-term simulation). Results of this study also showed that the use of RCM is better than GCM, particularly in the study area. Furthermore, the use of RCM should be bias corrected based on the needs of the study. In the case of this study, the combination of QM and VS was able to give better results in the simulation. After comparing the results of changes due to land use and climate change, this study concluded that the impact of climate change is much severe than land use change, particularly on the increase of inundation extent and maximum depth. Finally, this study suggested that the adaptation strategies to mitigate impacts of land use and climate change in the future should carefully consider the sensitive areas such as peatlands that are abundant in the region.